

UNCLASSIFIED

AD NUMBER
ADB084552
NEW LIMITATION CHANGE
TO Approved for public release, distribution unlimited
FROM Distribution authorized to U.S. Gov't. agencies and their contractors; Specific authority; 31 Aug 1987. Other requests must be referred to HQ Military Airlift Command, Attn: XPQT, Scott AFB, IL 62225.
AUTHORITY
AFRL/IFOIP ltr, 1 Jun 2004

THIS PAGE IS UNCLASSIFIED

UNCLASSIFIED

AD NUMBER
ADB084552
NEW LIMITATION CHANGE
TO Distribution authorized to U.S. Gov't. agencies and their contractors; Specific authority; 31 Aug 1987. Other requests must be referred to HQ Military Airlift Command, Attn: XPQT, Scott AFB, IL 62225.
FROM Distribution authorized to U.S. Gov't. agencies only; Test and Evaluation; May 1984. Other requests shall be referred to Hq. Military Airlift Command, Attn: XPQT, Scott AFB, IL 62225.
AUTHORITY
HQ MAC/XPQT, per DTIC Form 55, 31 Aug 1987

THIS PAGE IS UNCLASSIFIED

L
AD-B084 552

2

RADC-TR-84-7
In-House Report
May 1984



PROJECT BIRD WATCH AT DOVER AFB

William L. Simkins, Paul VanEtten and Michael C. Wicks

DISTRIBUTION LIMITED TO U.S. GOVERNMENT AGENCIES ONLY; TEST AND EVALUATION; May 84.
OTHER REQUESTS FOR THIS DOCUMENT SHALL BE REFERRED TO MAC/XPOT, SCOTT AFB, IL 62225.

HQ

SUBJECT TO EXPORT CONTROL LAWS

This document contains information for manufacturing or using munitions of war. Exporting this information or releasing it to foreign nationals living in the United States without first obtaining an export license violates the International Traffic in Arms Regulations. Under 22 USC 2778, such a violation is punishable by up to two years in prison and by a fine of \$100,000.

ROME AIR DEVELOPMENT CENTER
Air Force Systems Command
Griffiss Air Force Base, NY 13441

DTIC
ELECTE
JUL 30 1984
S B

DTIC FILE COPY

64 07 07 01

RADC-TR-84-7 has been reviewed and is approved for publication.

APPROVED:



FRED J. DEMMA
Chief, Surveillance Technology Branch
Surveillance Division

APPROVED:



FRANK J. REHM
Technical Director
Surveillance Division

FOR THE COMMANDER:



JOHN A. RITZ
Acting Chief, Plans Office

If your address has changed or if you wish to be removed from the RADC mailing list, or if the addressee is no longer employed by your organization, please notify RADC (OCTS) Griffiss AFB NY 13441. This will assist us in maintaining a current mailing list.

Do not return copies of this report unless contractual obligations or notices on a specific document require that it be returned.

UNCLASSIFIED

SECURITY CLASSIFICATION OF THIS PAGE

REPORT DOCUMENTATION PAGE				
1a. REPORT SECURITY CLASSIFICATION UNCLASSIFIED		1b. RESTRICTIVE MARKINGS N/A		
2a. SECURITY CLASSIFICATION AUTHORITY N/A		3. DISTRIBUTION/AVAILABILITY OF REPORT USGO agencies only; test and evaluation; May 84. Other requests Hq MAC/XPQT, Scott AFB IL 62225.		
2b. DECLASSIFICATION/DOWNGRADING SCHEDULE N/A		4. PERFORMING ORGANIZATION REPORT NUMBER(S) RADC-TR-84-7		
4. PERFORMING ORGANIZATION REPORT NUMBER(S) RADC-TR-84-7		5. MONITORING ORGANIZATION REPORT NUMBER(S) N/A		
6a. NAME OF PERFORMING ORGANIZATION Rome Air Development Center		6b. OFFICE SYMBOL (If applicable) OCTS	7a. NAME OF MONITORING ORGANIZATION N/A	
6c. ADDRESS (City, State and ZIP Code) Griffiss AFB NY 13441		7b. ADDRESS (City, State and ZIP Code)		
8a. NAME OF FUNDING/SPONSORING ORGANIZATION N/A		8b. OFFICE SYMBOL (If applicable)	9. PROCUREMENT INSTRUMENT IDENTIFICATION NUMBER N/A	
8c. ADDRESS (City, State and ZIP Code)		10. SOURCE OF FUNDING NOS		
		PROGRAM ELEMENT NO. 62702F	PROJECT NO. 4506PROJ	TASK NO.
				WORK UNIT NO.
11. TITLE (Include Security Classification) PROJECT BIRD WATCH AT DOVER AFB				
12. PERSONAL AUTHOR(S) William L. Simkins, Paul VanEtten and Michael C. Wicks				
13a. TYPE OF REPORT In-House		13b. TIME COVERED FROM Feb 83 TO Jan 84	14. DATE OF REPORT (Yr, Mo, Day) May 1984	15. PAGE COUNT 180
16. SUPPLEMENTARY NOTATION None				
17. COSATI CODES		18. SUBJECT TERMS (Continue on reverse if necessary and identify by block number)		
FIELD	GROUP	SUB GR.		
17	09		Radar Detection of Birds	
13	12		Bird Aircraft Strike Hazard	
19. ABSTRACT (Continue on reverse if necessary and identify by block number) Following a dangerous CSA birdstrike incident in late January 1983, CINCMAC urgently requested that HQ AFSC provide an immediate radar capability for detecting bird hazards at Dover AFB, DE. HQ AFSC, in turn, tasked RADC to provide an immediate bird hazard warning capability for the spring migration season and to recommend radar systems that could provide an adequate capability for interim and far term use. RADC (OCTS) quickly analyzed the problem and obtained an ARMY tactical GCA radar and crew to provide a bird hazard warning for the spring migration season. Subsequently, RADC conducted an extensive study on the bird strike problem which (1) developed the bird threat model, (2) identified the estimation and decision processes required in a BIRDWATCH warning system, (3) quantified the relationship between the detection coverage requirements and the time delay required to detect a bird hazard and communicate the hazard to the threatened aircraft, (4) determined the capabilities and limitations of radar systems that are in inventory and potentially available for interim use, and (5) obtained simultaneous				
20. DISTRIBUTION/AVAILABILITY OF ABSTRACT UNCLASSIFIED/UNLIMITED <input type="checkbox"/> SAME AS RPT <input checked="" type="checkbox"/> DTIC USERS <input type="checkbox"/>		21. ABSTRACT SECURITY CLASSIFICATION UNCLASSIFIED		
22a. NAME OF RESPONSIBLE INDIVIDUAL William L. Simkins		22b. TELEPHONE NUMBER (Include Area Code) (315) 330-4437	22c. OFFICE SYMBOL RADC (OCTS)	

DD FORM 1473, 83 APR

EDITION OF 1 JAN 73 IS OBSOLETE

UNCLASSIFIED
SECURITY CLASSIFICATION OF THIS PAGE

UNCLASSIFIED

SECURITY CLASSIFICATION OF THIS PAGE

detection performance on five candidate radar systems during one-on-one tests at Dover AFB.

This report contains the detailed results obtained during a ten-month intensive effort including; bird strike damage to C5A aircraft, bird hazard corridors and radar bird detection performance data during the fall migration including a single bird flock fifteen miles in extent.



Accession For	
DTIC AAA&I	<input type="checkbox"/>
DTIC TAB	<input checked="" type="checkbox"/>
Unannounced	<input type="checkbox"/>
Justification	
By	
Distribution/	
Availability Codes	
Dist	Avail and/or Special
B-3	

UNCLASSIFIED

SECURITY CLASSIFICATION OF THIS PAGE

ACKNOWLEDGEMENTS

The successful accomplishment of this mission was the result of cooperation by many individuals and organizations. First, we want to acknowledge our RADC Management for their guidance in achieving this successful mission. They are Fred Demma, Frank Rehm, and our former Commander, Brigadier General P. Bouchard. In particular we would like to thank Clarence Silfer our immediate supervisor who provided technical and administrative support throughout the duration of the program.

Other valuable contributors were the following:

* RADC photographers Sam Badolato, Leslie Ceigler, James Lyons, Larry Rocco, TSgt Sammie Williams, and Peter Zizzi (RADC/TSVF) who produced an impressive series of time-lapse photography that has had wide distribution in the Air Force.

* Technicians TSgt David Guiney (RADC/OCDS), Anthony Lattanzio and Anthony Lovaglio (RADC/OCTS) who maintained and operated the test equipment used in performing the various field tests. Of particular note is a unique modular camera control unit developed and fabricated for this effort by Mr. Lovaglio.

* Don Hershkovitz and John Antonucci (RADC/EEC) who not only provided expertise on bird migration habits but also provided a valuable interface with the FAA and AFGL, flagging information and articles that were pertinent to the bird hazard problem.

* Major James Foster and Dominick Blase (416BMW/DOTB) who provided extensive information on the availability and logistical

requirements of several candidate radar sensors.

* Secretaries Teresa Lamb, Angela Tarbania, and Carolyn Franco who patiently typed (and retyped) major sections of this report and other documents throughout this effort.

The organizations outside of RADC that contributed to this effort are too numerous to be named here, but are documented in Appendix E. However, the RADC team would like to provide a special acknowledgement to the efforts of the United States Army Communications Command, the 7th Signal Corp., and the 58th and 57th ATC Battalions who performed the immediate BIRDWATCH functions at Dover AFB in a timely, effective, and professional manner.

TABLE OF CONTENTS

	PAGE
1.0 INTRODUCTION	1
2.0 THE BIRD/AIRCRAFT STRIKE HAZARD (BASH) AT DOVER AFB, DELAWARE	7
3.0 DEFINITION OF A BIRDWATCH WARNING SYSTEM	25
3.1 Bird Threat Definition	25
3.2 Radar Cross Section (RCS) of Minimum Threat .	30
3.3 Primary and Secondary Coverage Requirements .	32
3.4 Warning System Timing	36
4.0 EVALUATION OF CANDIDATE RADAR SENSORS	43
4.1 Radar Range Equation and a Figure of Merit .	43
4.2 Comparison of Available Sensors	48
4.3 Evaluation of the AN/TPN-18A Birdwatch Performance, spring 1983	52
4.4 Analysis of Potential Interim Sensors	60
4.4.1 Free Space Detection Range Versus Requirements	64
4.4.2 Detection Limitations Due to Ground Clutter	69
4.4.3 Detection Limitations Due to Weather Clutter	77
4.4.4 Detection Limitations Due to Screening.	80
4.4.5 Detection Limitations Due to Multipath.	82

	PAGE
4.5 ONE-ON-ONE PERFORMANCE TESTS	85
5.0 THE INTERIM BIRDWATCH SYSTEM: AN OVERVIEW AND RECOMMENDATIONS	117
6.0 SUMMARY AND CONCLUSION	123
APPENDIX A CLUTTER PROFILE OF THE AN/TPN-18A RADAR . .	125
APPENDIX B CLUTTER FENCE MEASUREMENTS	135
APPENDIX C INFORMATION ON HAZARDOUS BIRD SPECIES . . .	143
APPENDIX D LOSS OF DETECTED BIRD TRAFFIC	149
APPENDIX E SUPPORTING ORGANIZATIONS	151
APPENDIX F DERIVATION OF RADAR RANGE EQUATIONS	155

LIST OF ILLUSTRATIONS

		PAGE
Figure 1.1	Photograph of the AN/MPN-14 Radar PPI Display2
Figure 1.2	Bird Strike Damage on a C5A Jet Engine Causing Engine Failure	4
Figure 2.1	Map of Dover and Nearby Towns6
Figure 2.2	Map of the City of Dover and Dover AFB	8
Figure 2.3	Bird Strike Damage - Snow Goose Passes Thru Radome and Protruded Half Way Out The Other Side10
Figure 2.4	Bird Strike Damage - Broken Fan Blade	11
Figure 2.5	Bird Strike Damage - Snow Goose Passed Thru Wing Flap11
Figure 2.6	Bird Strike Damage - Snow Goose Jammed in Wing Flap Causing Mechanical Failure	12
Figure 2.7	Bird Strike Damage Caused by Broken Blade Fragments Flying Out12
Figure 2.8	Aerial Photograph of Dover AFB15
Figure 2.9	Worst Case Example of Bird Hazard	17
Figure 2.10	Time 1659, 2nm Range Rings, 20nm Total Diameter, AN/MPN-14 Radar PPI, March 10, 198319
Figure 2.11	Time 1700, 2nm Range Rings, 20nm Total Diameter, AN/MPN-14 Radar PPI, March 10, 198320
Figure 2.12	Time 1712, 2nm Range Rings, 20nm Total Diameter, AN/MPN-14 Radar PPI, March 10, 198321

LIST OF ILLUSTRATIONS

	PAGE	
Figure 2.13	Time 1715, 2nm Range Rings, 20nm Total Diameter, AN/MPN-14 Radar PPI, March 10, 198322
Figure 2.14	Time 1720, 2nm Range Rings, 20nm Total Diameter, AN/MPN-14 Radar PPI, March 10, 198323
Figure 2.15	Photograph of the AN/MPN-14 Radar at Dover AFB	24
Figure 3.1	Bird Weight, Number Per Event and Engine Failure Distribution (DOT/FAA/CT-82/144, G FRINGS, March 1983)	28
Figure 3.2	Radar Cross Section Formulas31
Figure 3.3	Radar Cross Section of Bird Species (X-Band)32
Figure 3.4	Warning System Timing	37
Figure 3.5a	Threat Corridors for Landing Aircraft . . .	39
Figure 3.5b	Threat Corridors for Aircraft Taking Off .	.39
Figure 3.6a	Required Birdwatch Coverage For Landing Aircraft (Bird Speed = 40 Knots at Constant Altitude).	41
Figure 3.6b	Required Birdwatch Coverage for Take-off (Bird Speed = 40 Knots at Constant Altitude)	41
Figure 3.7	Required Birdwatch Coverage for Landing Aircraft (Bird Has A Vertical Velocity of 6 Knots)	42
Figure 4.1	AN/MPN-14 Radar PPI, 2nm Range Rings, 20nm Diameter, Time 1718, March 10, 1983 .	.47

LIST OF ILLUSTRATIONS

		PAGE
Figure 4.2	A Scatter Diagram Comparing Available Sensors With Requirements	49
Figure 4.3	AN/TSQ-71B System Consisting of AN/TPN 18A Radar, Operator Shelter, Diesel Generator and Repair Shelter	54
Figure 4.4	AN/TPN-18A Radar PFI, 1nm Range Rings 10nm Diameter, Time 1755, March 10, 1983	55
Figure 4.5	AN/TPN-18A Radar PPI, 1nm Range Rings, 10nm Diameter, Time 1800, March 10, 1983	56
Figure 4.6	AN/TPN-18A Radar PPI, 1nm Range Rings, 10nm Diameter, Time 1805, March 30, 1983	57
Figure 4.7	Clutter-Limited Coverage of AN/TPN-18A Radar vs. Bird Traffic Thru Air Corridor (Air Corridor From Reference [7])	59
Figure 4.8	Photograph of the AN/GPN-21 Radar's Antenna on 66 Foot Tower	61
Figure 4.9	Photograph of the Van-Mounted X-Band Marine Radar Tested at Dover AFB	65
Figure 4.10a	Detection Range of the AN/TPN-18A Versus Coverage Requirements	67
Figure 4.10b	Detection Range of the Raytheon 165018X Marine Radar Versus Coverage Requirements	67
Figure 4.11	AN/GPN-21 Radar PPI, 2nm Range Rings, 30nm Diameter, Ground Clutter	70
Figure 4.12	Theoretical Calculations of Power Returns From Ground Clutter, Aircraft, and Birds as a Function of Range	71

LIST OF ILLUSTRATIONS

	PAGE
Figure 4.13a	Attenuation of Bird Returns By MTI Filter . 72
Figure 4.13b	Attenuation of Bird Returns by a 8-pulse Discrete Fourier Transform 72
Figure 4.14	Detection Performance of AN/GPN-21 as a Function of Bird Radial Velocity and STC . 74
Figure 4.15	Raytheon 162512X Marine Radar PPI Display of Ground Clutter, 1nm Range Rings, 12nm Diameter, October 25, 1983 76
Figure 4.16	Degradation of AN/TPN-18A Detection Range Due to 0.5 Degree Screening 81
Figure 4.17	Degradation of AN/TPN-18A Detection Range Due to 1.25 Degree Screening 81
Figure 4.18	Effects of Multipath on Coverage of Raytheon 165018X Marine Radar 83
Figure 4.19	Time 1720, 2nm Range Rings, 24nm Total Diameter, AN/GPN-21 Radar, October 25, 1983 87
Figure 4.20	Time 1725, 2nm Range Rings, 24nm Total Diameter, AN/GPN-21 Radar, October 25, 1983 88
Figure 4.21	Time 1730, 2nm Range Rings, 24nm Total Diameter, AN/GPN-21 Radar, October 25, 1983 89
Figure 4.22	Time 1735, 2nm Range Rings, 24nm Total Diameter, AN/GPN-21 Radar, October 25, 1983 90
Figure 4.23	Time 1740, 2nm Range Rings, 24nm Total Diameter, AN/GPN-21 Radar, October 25, 1983 91
Figure 4.24	Time 1750, 2nm Range Rings, 24nm Total Diameter, AN/GPN-21 Radar October 25, 1983 92

LIST OF ILLUSTRATIONS

		PAGE
Figure 4.25	Time 1755, 2nm Range Rings, 24nm Total Diameter, AN/GPN-21 Radar, October 25, 1983	93
Figure 4.26	Time 1800, 2nm Range Rings, 24nm Total Diameter, AN/GPN-21 Radar, October 25, 1983	94
Figure 4.27	Time 1805, 2nm Range Rings, 24nm Total Diameter, AN/GPN-21 Radar, October 25, 1983	95
Figure 4.28	Time 1810, 2nm Range Rings, 24nm Total Diameter, AN/GPN-21 Radar, October 25, 1983	96
Figure 4.29	Time 1815, 2nm Range Rings, 24nm Total Diameter, AN/GPN-21 Radar, October 25, 1983	97
Figure 4.30a	AN/GPN-21 Radar PPI Taken At The Same Time As Figures 4.30b and 4.30c. 2nm Range Rings, 24nm Total Diameter	98
Figure 4.30b	AN/TPN-18A Radar PPI Taken At The Same Time As Figures 4.30a and 4.30c. 1nm Range Rings, 20nm Total Diameter	100
Figure 4.30c	X-Band Marine Radar PPI Taken At The Same Time As Figures 4.30a and 4.30b. 1nm Range Rings, 12nm Total Diameter	101
Figure 4.31	Time 1620 AN/GPN-21 Radar PPI, 2nm Range Rings, 24nm Total Diameter, November 3, 1983	102
Figure 4.32	Time 1625 AN/GPN-21 Radar PPI, 2nm Range Rings, 24nm Total Diameter, November 3, 1983	103

LIST OF ILLUSTRATIONS

	PAGE
Figure 4.33	Time 1630 AN/GPN-21 Radar PPI, 2nm Range Rings, 24nm Total Diameter, November 3, 1983 104
Figure 4.34	Time 1635 AN/GPN-21 Radar PPI, 2nm Range Rings, 24nm Total Diameter, November 3, 1983 105
Figure 4.35	Time 1640 AN/GPN-21 Radar PPI, 2nm Range Rings, 24nm Total Diameter, November 3, 1983 106
Figure 4.36	Time 1645 AN/GPN-21 Radar PPI, 2nm Range Rings, 24nm Total Diameter, November 3, 1983 107
Figure 4.37	Time 1650 AN/GPN-21 Radar PPI, 2nm Range Rings, 24nm Total Diameter, November 3, 1983 108
Figure 4.38	Time 1655 AN/GPN-21 Radar PPI, 2nm Range Rings, 24nm Total Diameter, November 3, 1983 109
Figure 4.39	Time 1700 AN/GPN-21 Radar PPI, 2nm Range Rings, 24nm Total Diameter, November 3, 1983 110
Figure 4.40	Time 1705 AN/GPN-21 Radar PPI, 2nm Range Rings, 24nm Total Diameter, November 3, 1983 111
Figure 4.41a	AN/GPN-21 Radar PPI Taken At The Same Time As Figures 4.41b and 4.41c. 2nm Range Rings, 20nm Total Diameter 112
Figure 4.41b	AN/TPN-18A Radar Taken At The Same Time As Figures 4.41a and 4.41c. 1nm Range Rings, 20nm Total Diameter 114

LIST OF ILLUSTRATIONS

	PAGE
Figure 4.41c	S-Band Marine Radar PPI Taken At The Same Time As Figures 4.41a and 4.41b. 2nm Range Rings, 24nm Total Diameter . . .115
Figure 4.42	Modified S-Band Marine Radar (Raytheon S-Band Electronics With MPN-13 Antenna And Van)116
Figure A.1	PPI Display, 0dB Attenuation - 10nm Total Diameter (Clutter Map)128
Figure A.2	PPI Display, 12dB Attenuation - 10nm Total Diameter (Clutter Map)129
Figure A.3	PPI Display, 24dB Attenuation - 10nm Total Diameter (Clutter Map)130
Figure A.4	PPI Display, 36dB Attenuation - 10nm Total Diameter (Clutter Map)131
Figure A.5	PPI Display, 48dB Attenuation - 10nm Total Diameter (Clutter Map)132
Figure A.6	PPI Display, 66 dB Attenuation - 10nm Total Diameter (Clutter Map)133
Figure B.1	AN/TPN-18A Radar With Clutter Fence 35 Feet Behind The Radar 138
Figure B.2	Clutter Fence Geometry139
Figure B.3	Calculated Knife - Edge Diffraction Pattern 140
Figure B.4	AN/TPN-18A Radar PPI Display of Clutter, Without Clutter Fence 141
Figure B.5	AN/TPN-18A Radar PPI Display of Clutter, With Clutter Fence 35 Feet Behind The Radar 142
Figure E.1	Roadmap of Support From Contributing Organizations 152

LIST OF TABLES

		PAGE
Table 2.1	Hazardous Bird Species At Dover AFB, DE . . .	9
Table 2.2	Estimated Canadian Goose Populations, 1978 - 1982	13
Table 2.3a	Average Snow Goose Populations, 1977 - 1982	.14
Table 2.3b	Peak Snow Goose Populations, 1977 - 1982 . .	14
Table 2.4	Typical Rate of Climb For C5A16
Table 3.1	Bird Strikes By Impact Points On Aircraft .	.27
Table 3.2	Percentage Of Strikes By Phase Of Flight . .	33
Table 3.3	Bird Ingestion Summary For Civilian Aircraft.	34
Table 3.4	Bird Strikes By Altitude, 1968 - 197134
Table 3.5	Safety Corridor Boundaries As A Function Of Time And Position Along Planes Path	38
Table 4.1	Definition Of Terms For Radar Range Equation.	44
Table 4.2	Comparison Of Potentially Available Radars.	.50-51
Table 4.3	Parameters And Detection Performance Of GPN-21, TPN-18A, And Raytheon Marine Radar .	68
Table 4.4	Weather Backscatter And Attenuation Relationships78
Table 4.5	Detection Performance Of Candidate Radars In Rain79
Table D-1	Sample Of Bird Detection Log For 15 March 1983	149
Table D-2	Summary Of Bird Detections, 15-21 March, 1983	150
Table F-1	Definition Of Terms For Radar Range Equation.	154

1.0 INTRODUCTION

The Bird/Aircraft Strike Hazard (BASH) problem has always been an issue of concern at Dover Air Force Base, Delaware, primarily due to the large number of native Canadian geese that winter in the area. However, with the recent increase in Snow geese wintering in the local wildlife areas, the Dover birdstrike problem has increased significantly over the past several years. On 23 January 1983, a fully loaded C5A Galaxy aircraft was nearly lost after colliding with a large flock of geese during takeoff. This near fatal collision again brought the hazardous bird strike condition at Dover AFB to the attention of General James Allen, Commander-in-Chief, Military Airlift Command (CINCMAC). General Allen requested that General Marsh and Air Force Systems Command (AFSC) provide an immediate capability for the detection of hazardous bird conditions at Dover AFB in all weather conditions. The authors from Rome Air Development Center initiated Project BIRDWATCH and the results are presented in this report.

We will show the results of radar detection of birds employing five different radars at Dover Air Force Base. An illustration of bird detection employing a radar is given in Figure 1.1. The AN/MPN-14 Mobile Ground Control Approach (GCA) radar's Plan Position Indicator (PPI) display has two nautical mile range rings with a total diameter of 20 nautical miles. The radar has a Moving Target Indicator (MTI)

**ILLUSTRATION OF THE DOVER AFB BIRD STRIKE HAZARD PROBLEM
ROME AIR DEVELOPMENT CENTER**

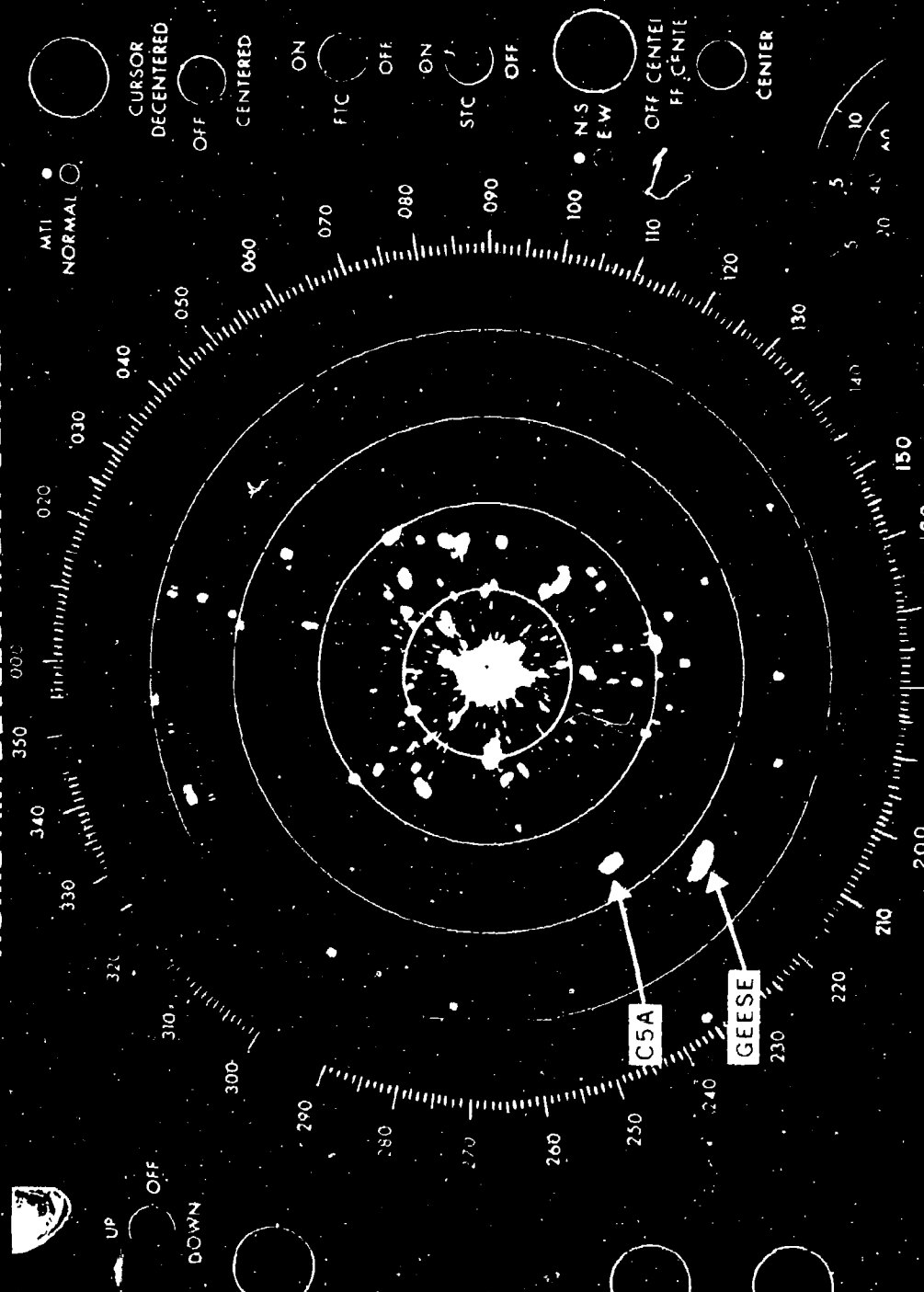


Figure 1.1 PHOTOGRAPH OF THE AN MPN 14 RADAR PPI DISPLAY

where most of the moving targets displayed are birds. As noted on the display, the radar return from a large flock of geese appears as large as the radar return from the C5A aircraft. An example of the costly and severe damage caused by a bird strike is shown in Figure 1.2. The debris from the damaged C5A engine pod was sucked into the engine, chipping the high speed rotor blades and destroying their delicate balance. Such damage can cause a vibration that can literally rip the engine apart.

This report documents the efforts performed by the RADC team to define, analyze, and provide a radar-based bird hazard warning system. The report begins by briefly describing in Section 2 the Bird/Aircraft Strike Hazard (BASH) problem at Dover AFB, Delaware. Section 3 defines the basic parameters of a bird warning system including an important analysis that determined the sizing requirements of a BIRDWATCH radar sensor and provided important guidelines for the development of an operational concept. Section 4 describes the evaluation of available sensors and analyzes the performance of several radars tested at Dover AFB. PPI photos and audio/video recordings were taken during the performance tests of the radars for future use by USAF personnel. The Dover AFB Wing Safety office has expressed an interest in using this data in their annual safety training and review programs for aircrews, ground crews and control tower and air traffic control personnel. Copies of this data have also been sent upon request to HQ MAC personnel, for use in briefing CINCMAC on the problem and in planning future BIRDWATCH surveillance efforts and procurements; to USAFALCENT personnel for use in evaluating operational procedures in hazardous



Figure 1.2 Bird Strike Damage On A C5A Jet Engine
Causing Engine Failure 23 January 1983
(Courtesy of 436 MAW, DAFB, DE)

bird environments; and to the BASH squadron at Tyndall AFB, the Air Force focal point for bird strike problems. Section 5 provides an overview of the interim BIRDWATCH system currently operating at Dover AFB, DE and offers recommendations on how the system could be improved in the future. Section 6 concludes the report with a summary of the effort's accomplishments.

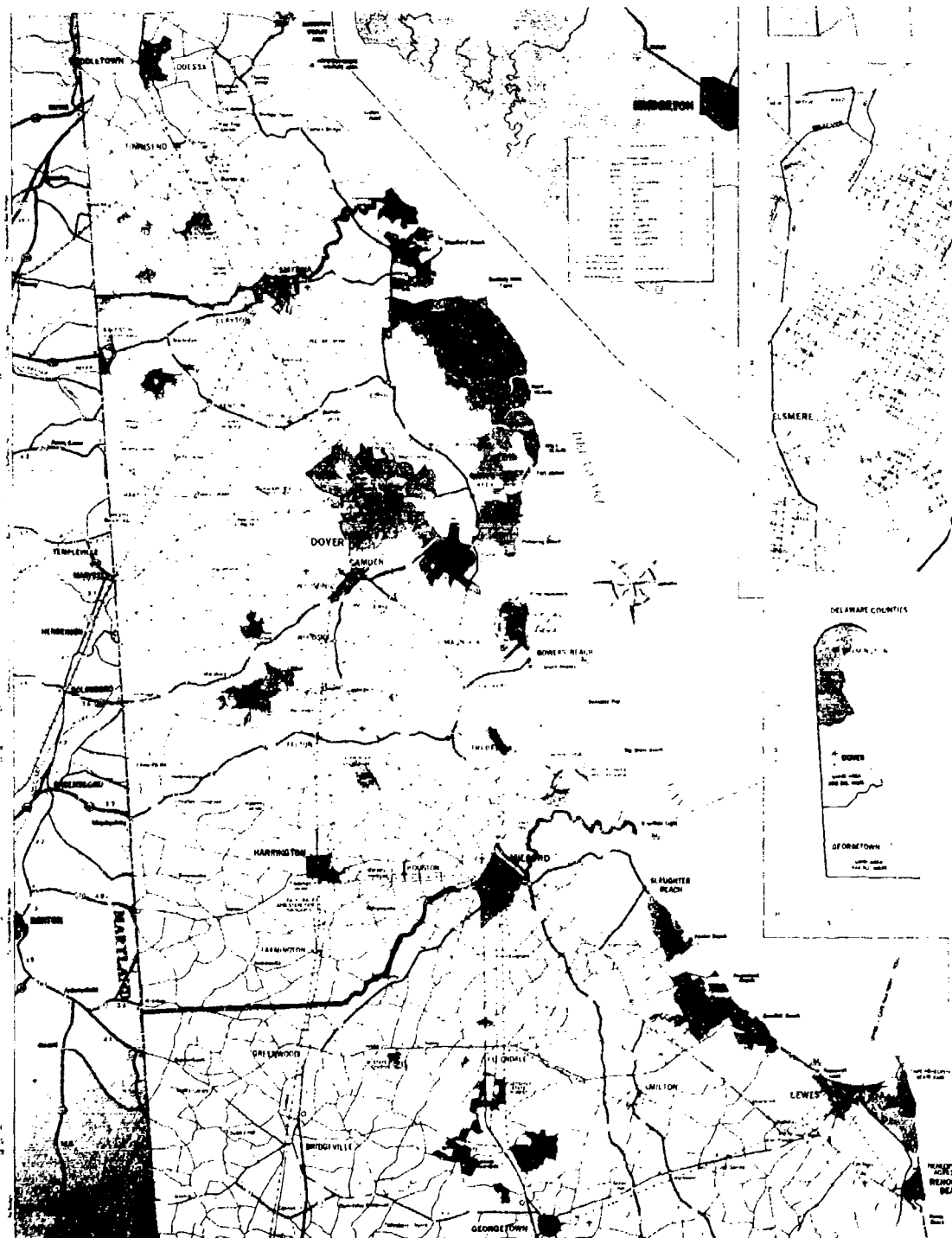


Figure 2.1 Map Of Dover And Nearby Towns

2.0 THE BIRD/AIRCRAFT STRIKE HAZARD (BASH) AT DOVER AFB, DELAWARE

Dover Air Force Base (DAFB) is a Military Airlift Command (MAC) installation occupying approximately 1477 hectares on the Piedmont Plateau in Kent County, Delaware. Figure 2.1 shows the location of the base in relation to the nearby towns, bodies of water and other physical and cultural features. Residential and small commercial districts adjoin the base to the west and northwest with the city of Dover, the capital of Delaware, centered approximately 3 nm to the north-northwest. Farmland adjoins the base on the north, east, south, and southwest sides. A civilian airport is also located at the northern boundary. Other cultural features that exist within 5 nm of DAFB include residential housing, commercial structures typically less than 5 stories high, and farms with large grain silos and barns.

Figure 2.2 shows the location of several wildlife refuges that are located near the base. The abundance of water and the location along the Atlantic Flyway make the region a prime waterfowl habitat. Most of the larger refuges (the Woodland Beach Wildlife Area, the Bombay Hook National Wildlife Refuge and the Little Creek Wildlife Area) are located in a stretch of coastal land ranging from approximately 15 nm north of the base to within a few hundred feet to the east-northeast. To the southeast lies Logan Lane Wildlife Refuge, a recent annex to the Little Creek Wildlife Refuge. South of Dover Air Force Base are other noteworthy migratory areas including the Milford Neck Wildlife Area and an area near Frederica. The bird strike hazard at Dover AFB is, to a large degree, caused by the proximity of these refuges.

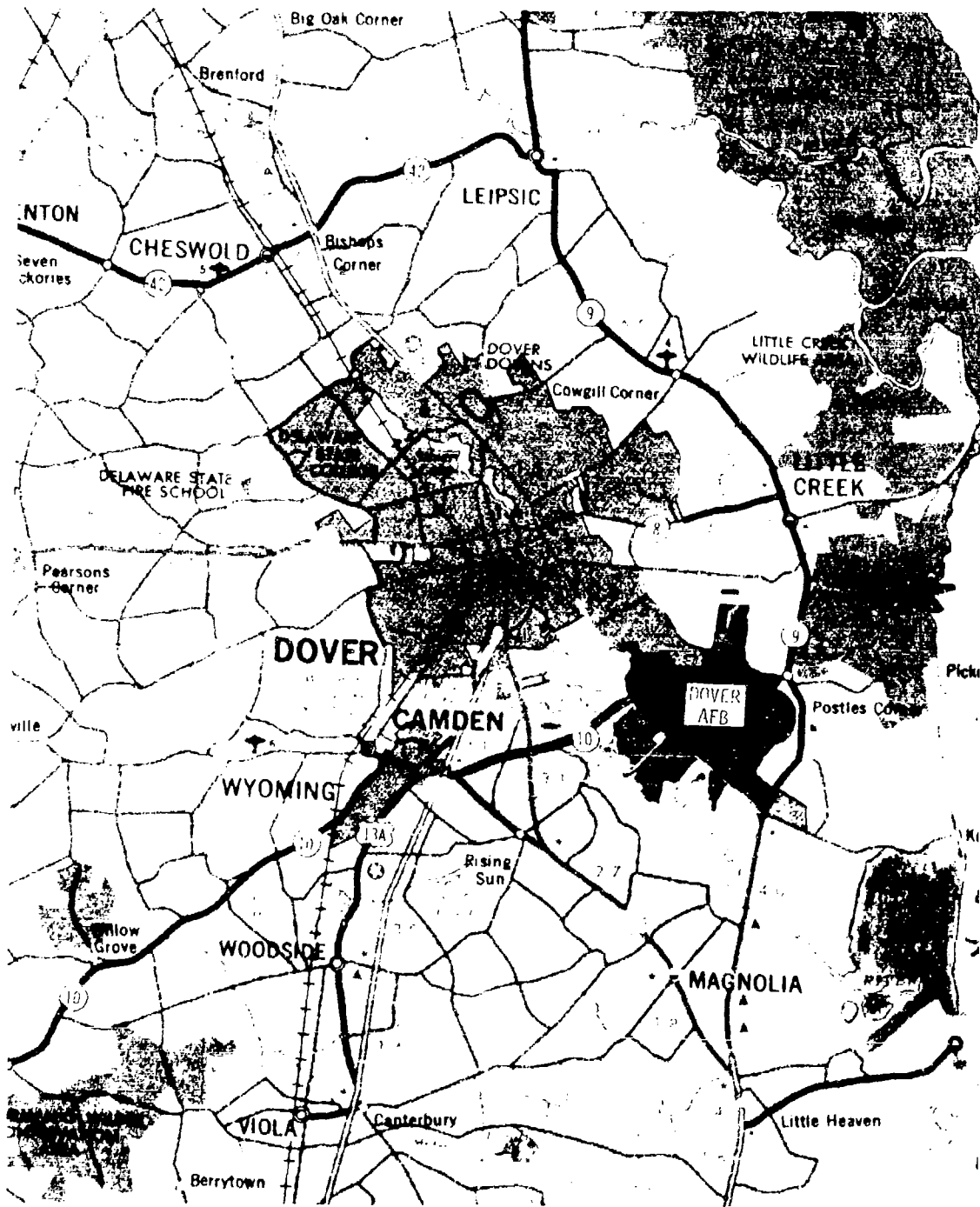


Figure 2.2 Map Of The City Of Dover And Dover AFB

Bird Species	Size (in)	Weight (avg)	Wintering Population	General Comments
Common Canada Goose	32-40	8lb,7oz (M) 7lb,5oz (F)	>70,000 pk 30,000 avg	*1 Oct-15 Apr threat *Threat altitude: migrating:< 5000 ft. wintering:< 1500 ft. *Typical flock sizes: 5-15 birds
Greater Snow Goose	23-38	7lb,4oz (M) 6lb,2oz (F)	50,000 pk 20,000 avg	*1 Oct-15 Apr threat *Threat altitude: migrating:< 5000 ft. wintering:< 1000 ft. *Typical flock sizes: 10-30 birds
American Brant	24	3lb,5oz (M) 2lb,12oz (F)	>1,000	*Not an important threat due to small population in Dover area
Whistling Swans	48	16lb (M) 14lb (F)	2,000 pk 700 avg	*Not an important threat due to small population in Dover area
Black Duck Mallards	21-25	2lb,11oz (M) 2lb,6oz (F)	50,000 pk 30,000 avg	*1 Oct-15 Apr threat *Threat altitude: migrating:< 4000 ft. wintering:< 500 feet *Typical flock sizes: 5-10 birds
Marsh Hawks Ospreys	20-26	2lb	Not Available	*Threat period: all year *Threat altitude: typ. above 1000 ft. *Usually flies alone or in pairs
Gulls Blackbirds Starlings	18-28 15 15	1-4lb 1lb 1lb	Not Available	*Threat period: all year *Threat altitude: typ. below 500 feet *Typical flock sizes: > 100 in fall/spring

TABLE 2.1 - HAZARDOUS BIRD SPECIES AT DOVER AFB, DE [1],[2],[3]

Among the major species of waterfowl that winter in the area are the Canada Goose, Greater Snow Goose, Whistling Swans, and several species of duck. Table 2.1 lists the size, weights, and other general information on the waterfowl in the Dover area. The Canadian and snow geese present an especially dangerous hazard below 1500 feet due to their large size and the large numbers that winter in or migrate thru the area. Figures 2.3 thru 2.7 depict the damage incurred by a C5A when it struck a flock of snow geese while taking off. Not only can radomes and windshields be shattered but ingestion of a single snow goose can chip an engine blade, causing an imbalance. If the engine is not immediately shut off, it can virtually self-destruct sending



Figure 2.3 Bird Strike Damage - Snow Goose Passed Thru Radome And Protruded Halfway Out The Other Side
(Courtesy of 436 MAW, DAFB, DE)

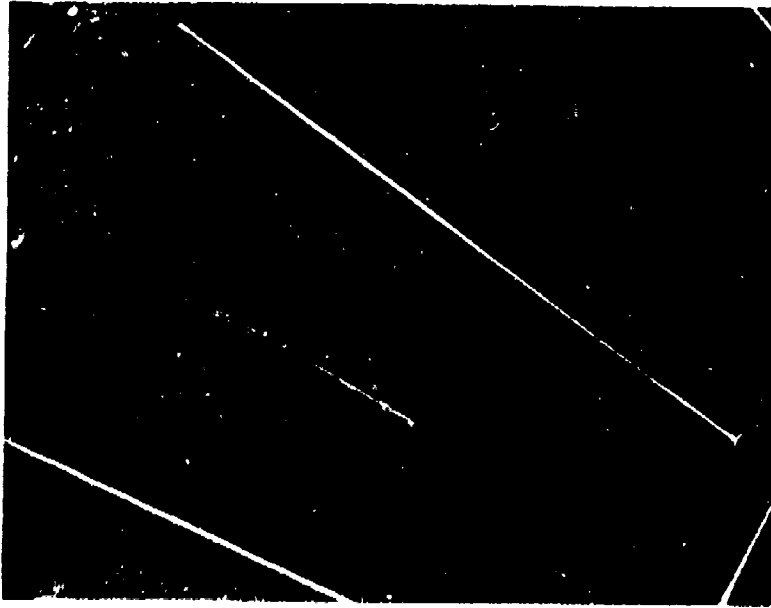


Figure 2.4 Bird Strike Damage - Broken Fan Blade



Figure 2.5 Bird Strike Damage - Snow Goose Passed Thru Wind Flap
(Courtesy of Dale MAW, DAPIS, DII)

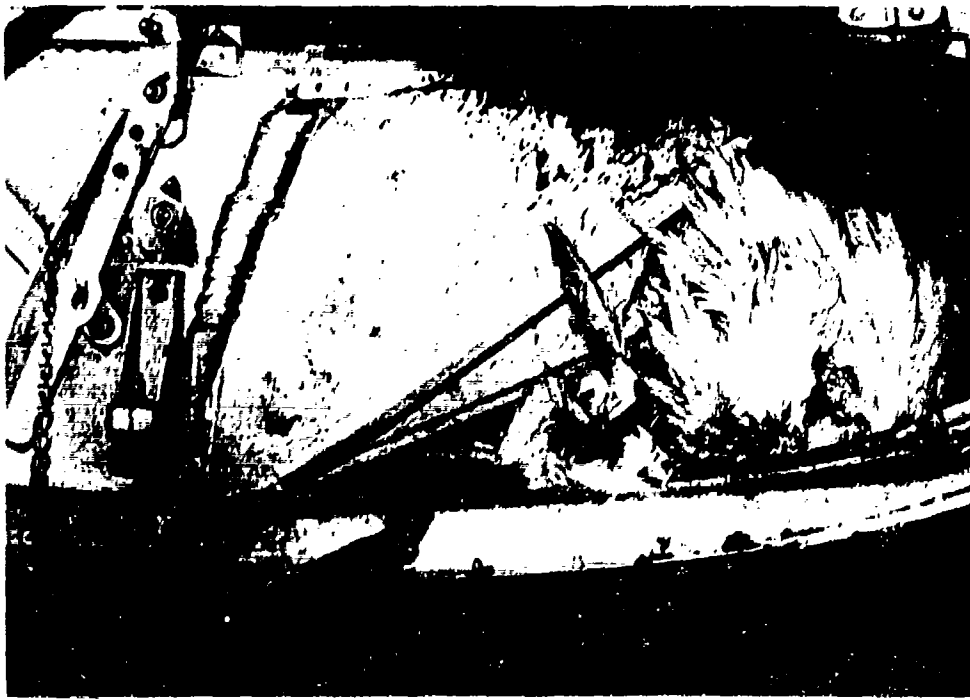


Figure 2.6 Bird Strike Damage - Snow Goose Jammed In Wing Flap Causing Mechanical Failure

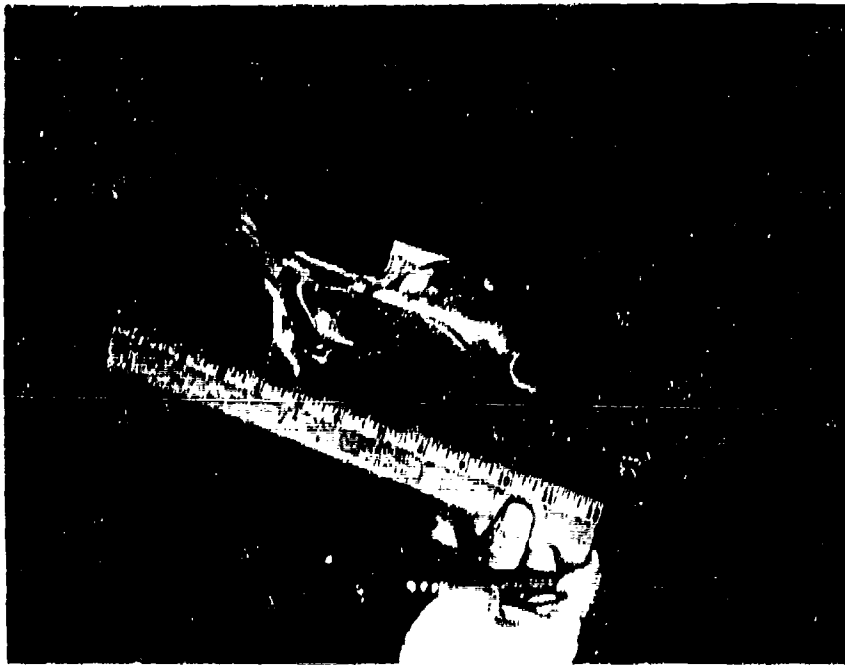


Figure 2.7 Bird Strike Damage Caused by Broken Blade Fragment Protruding Out
(All Corridor Obtained From Ref [7])
(Courtesy of A30 MW, BAPB, DR)

fragments thru the engine housing and wings and into the fuselage of the plane.

Waterfowl census estimates of the last few years [4] are given in Tables 2.2 and 2.3. Note the large increase in snow goose population during the last 6 years from a peak of 4200 in 1977 to 35,000 in 1982! An aerial survey taken during 22-23 November, 1983, counted over 94,000 waterfowl in the Dover area including 45,383 ducks, 32,726 Canada geese, 15,765 Snow geese, 257 Whistling swans, and 250 Brant.[5] One practice that has contributed to this increase is the renting of refuge land to local farmers. As part of the rental agreement, the farmers will raise certain grain crops, leaving approximately 10 % of the grain in the fields as feed for the migrating waterfowl. Since the geese tend to migrate only as far south as necessary to find food, the availability of grain in fields relatively safe from hunters and predators encourages the migrating geese to stay.

<u>Month</u>	<u>1978</u>	<u>1979</u>	<u>1980</u>	<u>1981</u>	<u>1982</u>
October	73,108	74,106	82,011	51,530	65,386
November	24,408	17,483	34,850	22,659	24,171
December	35,711	18,485	27,563	35,289	37,939
January	31,802	20,206	27,633	15,806*	27,347
February	n/a	n/a	n/a	54,812	n/a

* Due to severe cold, many snows and Canadas went south and returned after the survey; n/a - not available

TABLE 2.2 ESTIMATED CANADIAN GOOSE POPULATIONS 1978-1982 [4]

<u>MONTH</u>	<u>1977</u>	<u>1978</u>	<u>1979</u>	<u>1980</u>	<u>1981</u>	<u>1982</u>
JAN	800	425	6200	10000	17000	8000
FEB	1445	375	3400	12000	23000	35000
MAR	----	125	2675	17000	2250	23000
APR	150	225	150	900	900	1200
SEP	30	250	25	75	200	250
OCT	275	2938	1950	5400	6800	15000
NOV	4200	4150	5250	16500	7500	10000
DEC	1300	4825	7200	16500	7500	15000

TABLE 2.3a AVERAGE SNOW GOOSE POPULATIONS
(BOMBAY HOOK NATIONAL WILDLIFE REFUGE) [4]

<u>MONTH</u>	<u>1977</u>	<u>1978</u>	<u>1979</u>	<u>1980</u>	<u>1981</u>	<u>1982</u>
JAN	1600	850	10000	16000	22000	9500
FEB	1445	700	6500	16500	17000	42000
MAR	0	300	2800	20500	2500	50500
APR	250	550	300	1500	1500	2000
SEP	30	500	25	75	200	250
OCT	650	3750	3440	6900	8100	22050
NOV	5500	5575	7450	20000	12500	22000
DEC	1800	6200	8500	20000	8835	27500

TABLE 2.3b PEAK SNOW GOOSE POPULATIONS
(BOMBAY HOOK NATIONAL WILDLIFE REFUGE) [4]

Figure 2.8 is an aerial photo of Dover AFB and introduces the two categories of bird hazards. The first category of bird hazard includes the gulls, starlings and other pest birds that loaf and feed on or near the runway and fly up in front of approaching aircraft. While a specialized pulse doppler radar may be capable of detecting the presence of movement on the base or in the adjacent fields [6], a sophisticated processing capability would be required to reliably identify the detected movement as dangerous bird activity. Furthermore, even if a radar system could reliably detect gulls on the runway or starlings in an adjacent field, a ground crew would still be required to disperse the birds from the intended path of arriving or

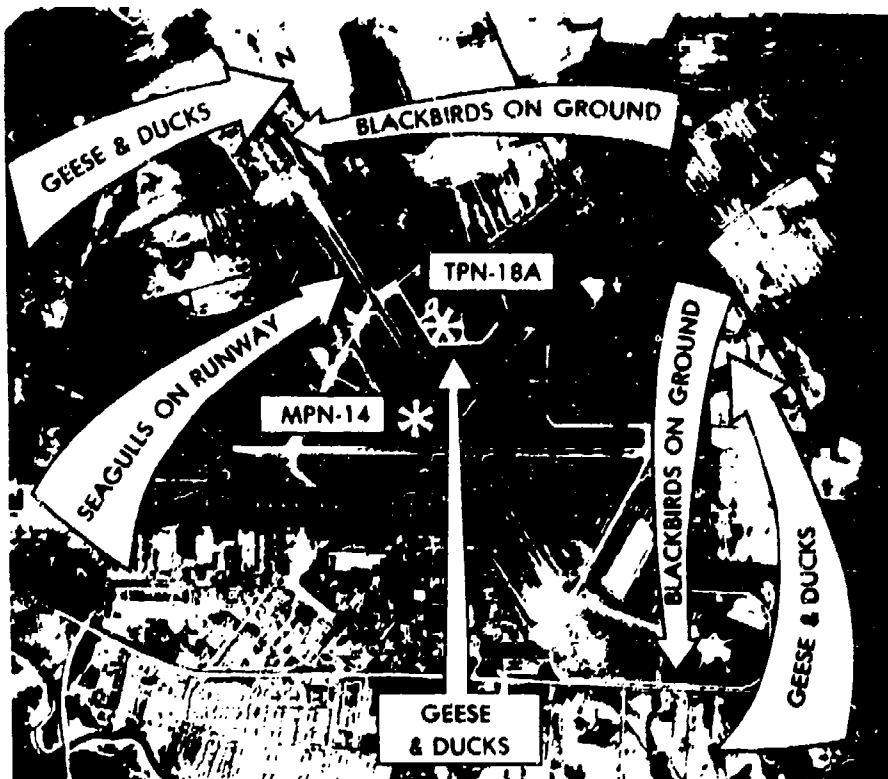


Figure 2.8 Aerial Photograph of Dover AFB

departing aircraft. The best defense against this hazard is to turn the base grounds, runway areas, and the land off the end of the runways into undesirable feeding or resting grounds. An assessment of this BASH problem at Dover AFB and suggestions for reducing the hazard are contained in an April 1978 report [1] published by AFCEC/DEVN, Tyndall AFB, FL.

The second category includes the waterfowl and raptors which threaten the Dover aircraft by flying over the base or thru the approach and takeoff corridors. Figure 2.9 gives an example of typical bird traffic thru the takeoff corridors during the late afternoon and early evening. During the morning, the bird traffic is along the same paths but in the opposite direction. The "air corridor" areas are centered around the typical takeoff paths. If birds are within this corridor when a fully-loaded C5A begins to roll down the runway, the birds may represent a hazard to the departing aircraft. The altitude of the aircraft as a function of time and distance is given in Table 2.4. Note that the aircraft is in the hazardous region below 1500 feet for as long as 60 seconds after beginning takeoff!

TIME (SEC)	ALTITUDE (FT)	GROUND DISTANCE (FT)
0 (begin roll)	0	0
32	0 (lift off)	6500
40	100	9500
49	500	16500
60	3000*	25000

*For ambient temperatures < 40 degrees F, gross weights < 650,000.
1500 ft for temperatures > 50 degrees F, gross weights 760,000 lbs. [8]

TABLE 2.4 TYPICAL RATE OF CLIMB FOR C5A [7], [8]

LEGEND: AIR CORRIDOR 

BIRD FLIGHT PATHS 

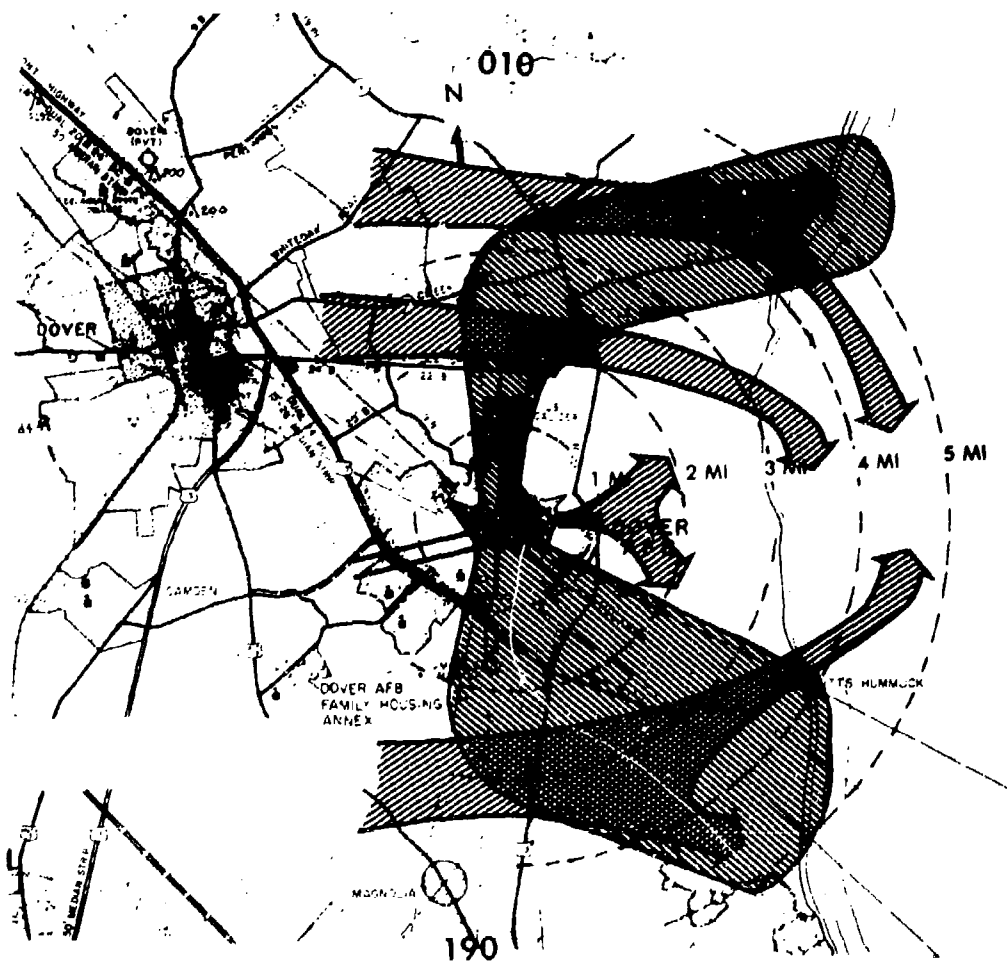


Figure 2.9 Worst Case Example of Bird Hazard
(Air Corridor Obtained From Ref [7])

Figures 2.10 thru 2.14 give an indication of the intense bird activity that can be detected by a surveillance radar sensor. The figures show a Plan Position Indicator (PPI) output of the AN/MPN-14 GCA radar (Figure 2.15) after processing by a Moving Target Indicator (MTI) filter. The radius of the display represents 10 nm with range rings that are spaced 2 nm apart. Excluding the clutter residue ring within 1 nm of the radar, most of the detections represent flocks of low-flying birds. In Figure 2.10, notice the large flock at a range of 9 nm and an azimuth of 230 degrees. The successive figures show this flock flying directly over the base and landing in the Little Creek Wildlife Refuge northeast of the base. Other large flocks from the northwest can also be noted traveling toward the base. Most of the detections within 4 nm also represent flocks of birds which can easily be distinguished from ground clutter residue and vehicles by scan-by-scan tracking.

Therefore, a surveillance radar can provide some capability for detecting the large numbers of birds flying in the vicinity of the base. On clear days, visual sightings by the control tower personnel and pilots will remain the best technique for avoiding birdstrikes on or near the airfield. However, during rainy or foggy weather when visibility is impaired, a radar sensor may provide the only means of detecting a hazard. By combining the two techniques in a warning system, an all-weather capability for reducing the probability of a catastrophic bird strike can be obtained.

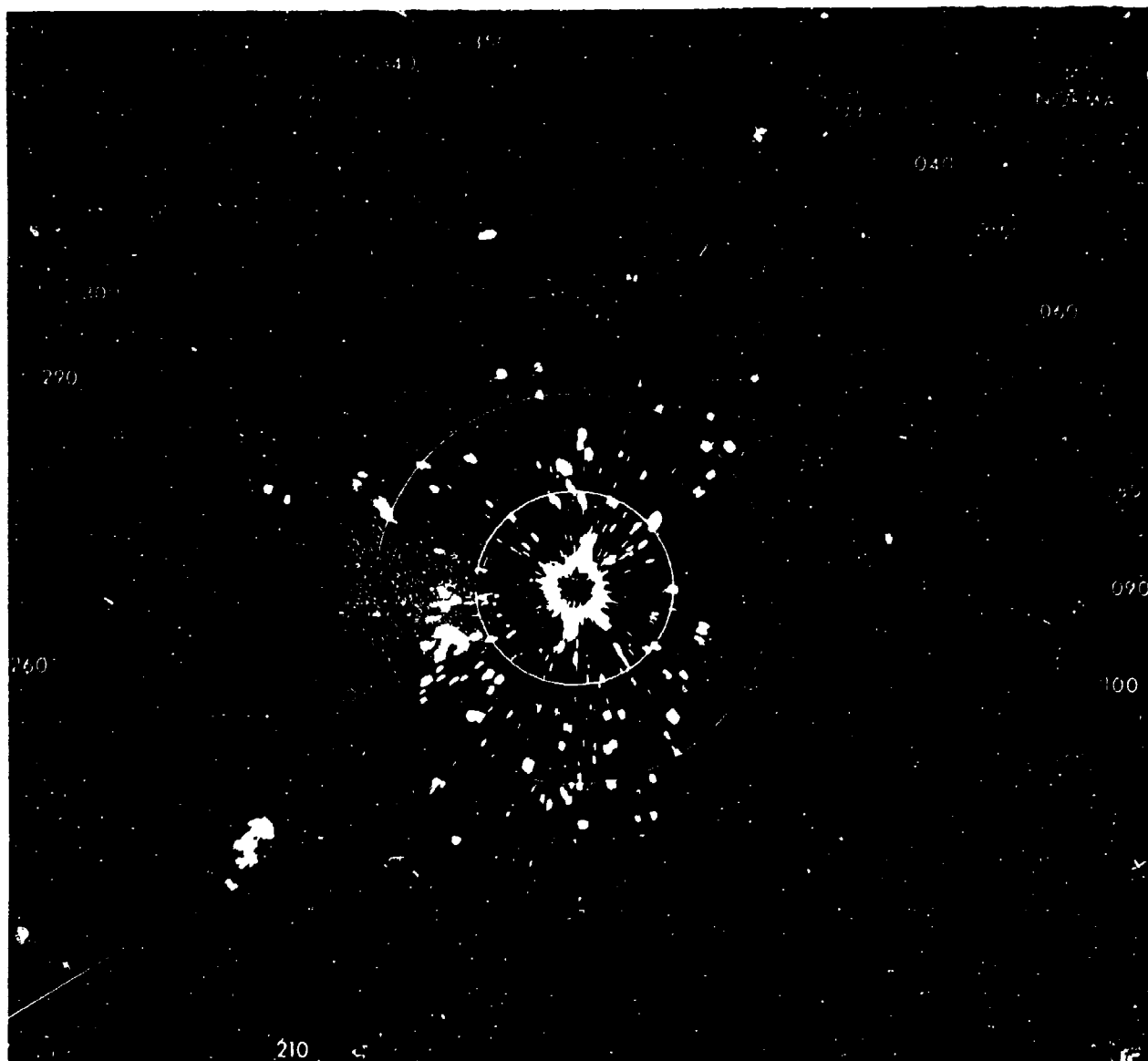


Figure 2.10 Time 1659, 2nm, Range Rings 20nm, Total
Diameter AN/MPN-14 Radar PPI, March 10, 1983

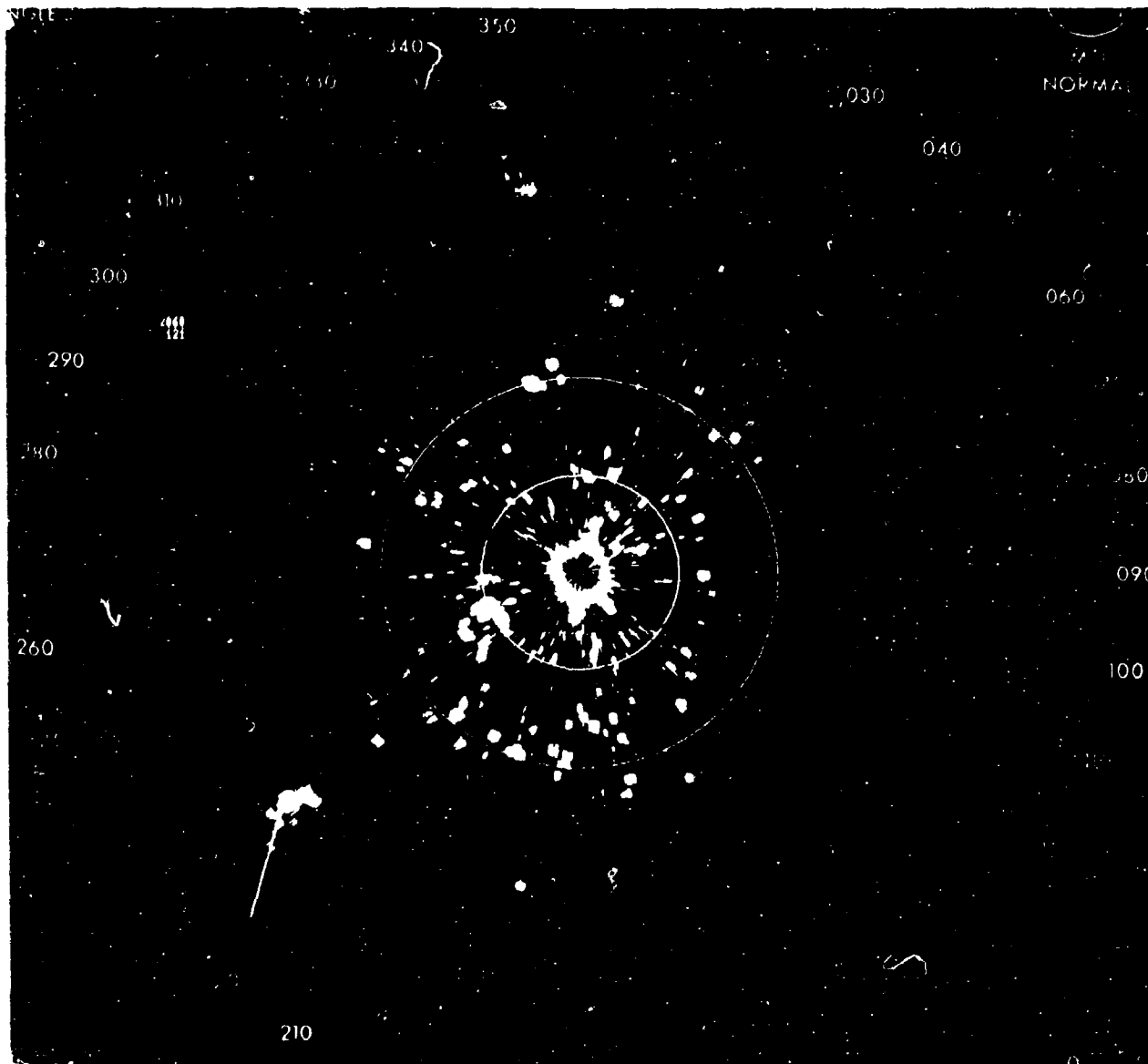


Figure 2.11 Time 1700, 2nm, Range Rings 20nm, Total
Diameter AN/MPN-14 Radar PPI, March 10, 1983

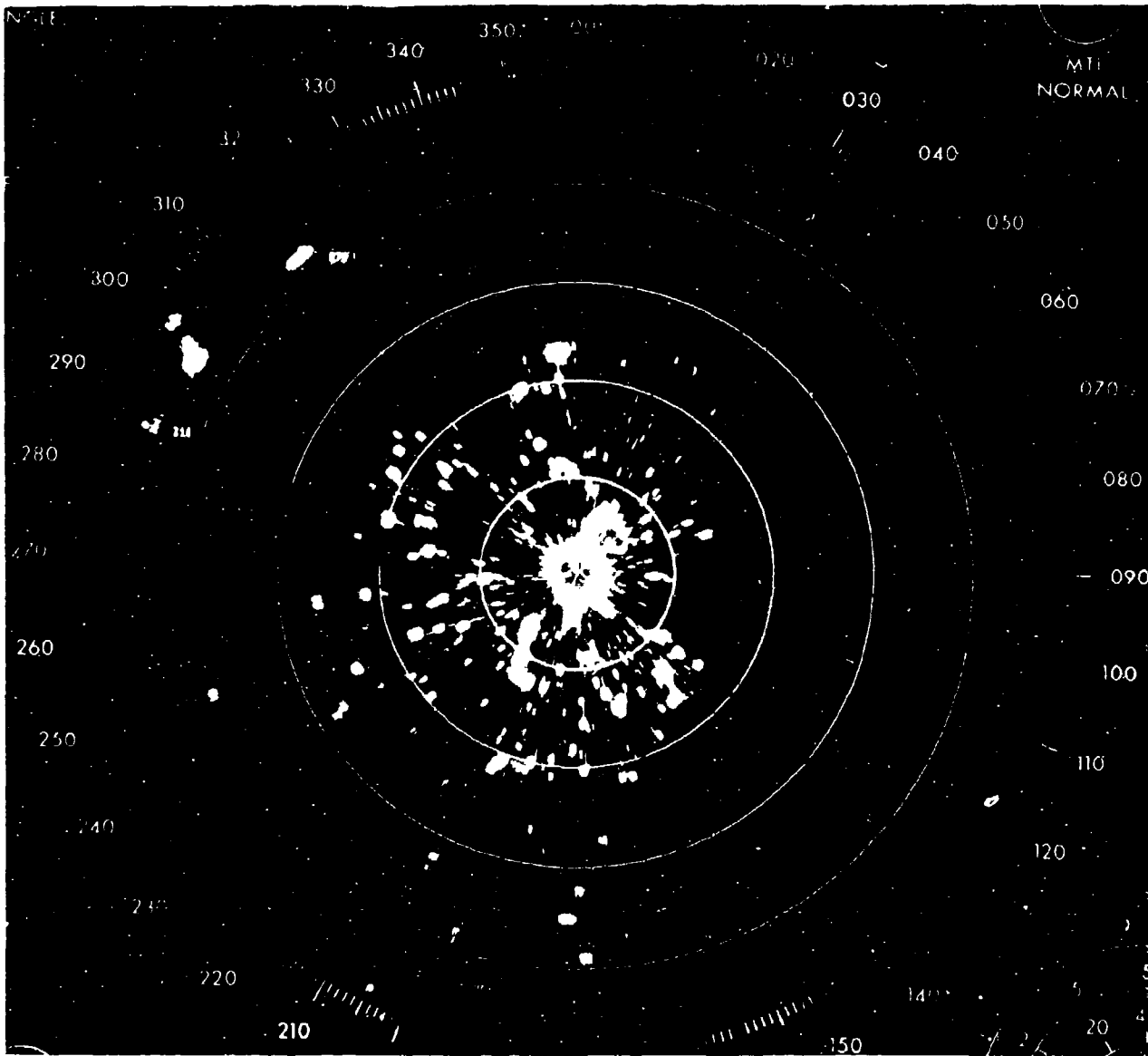


Figure 2.12 Time 1712, 2nm, Range Rings 20nm, Total Diameter AN/MPN-14 Radar PPI, March 10, 1983

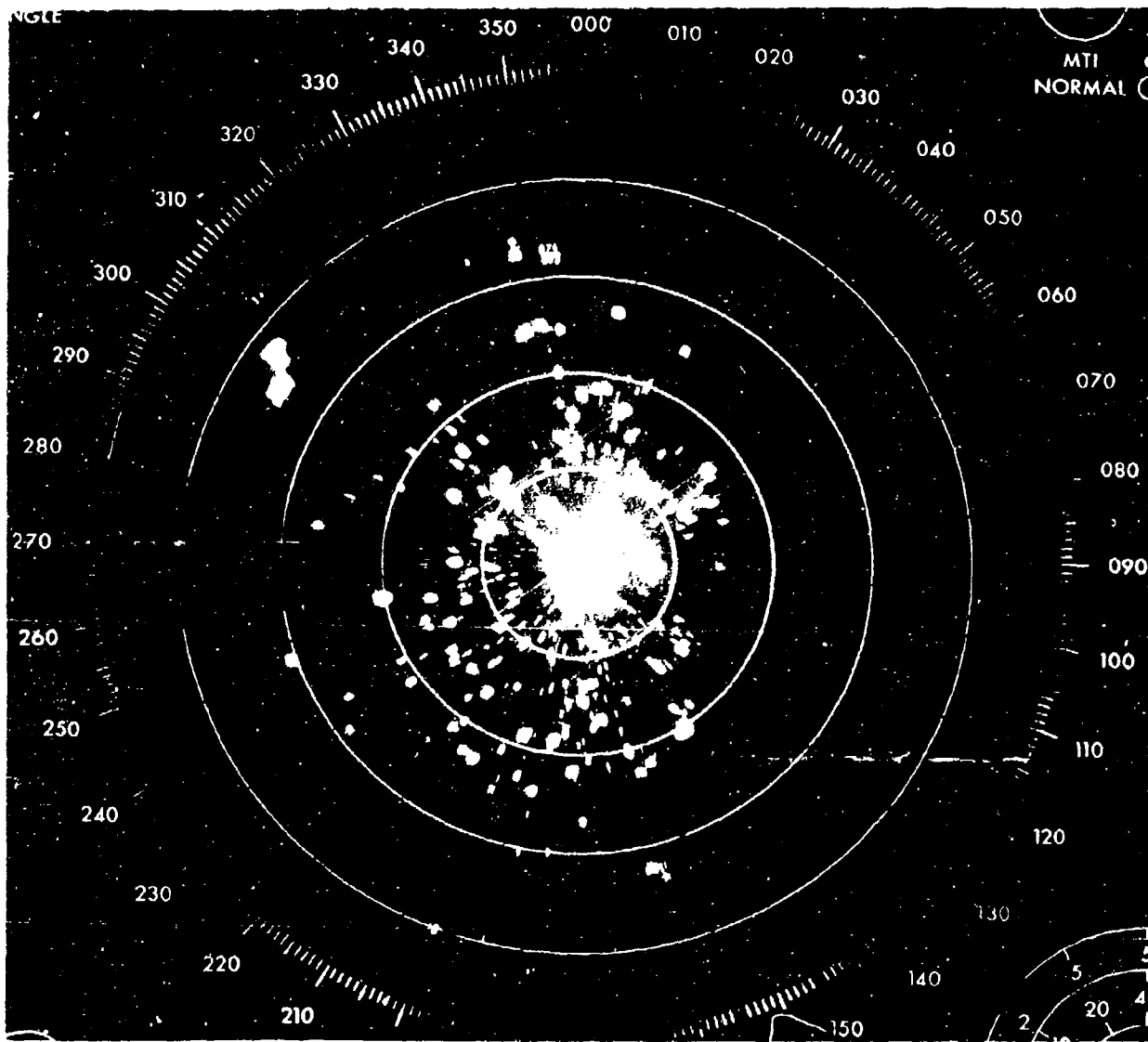


Figure 2.13 Time 1715, 2nm, Range Rings 20nm, Total Diameter AN/SPN-14 Radar PPI, March 10, 1983

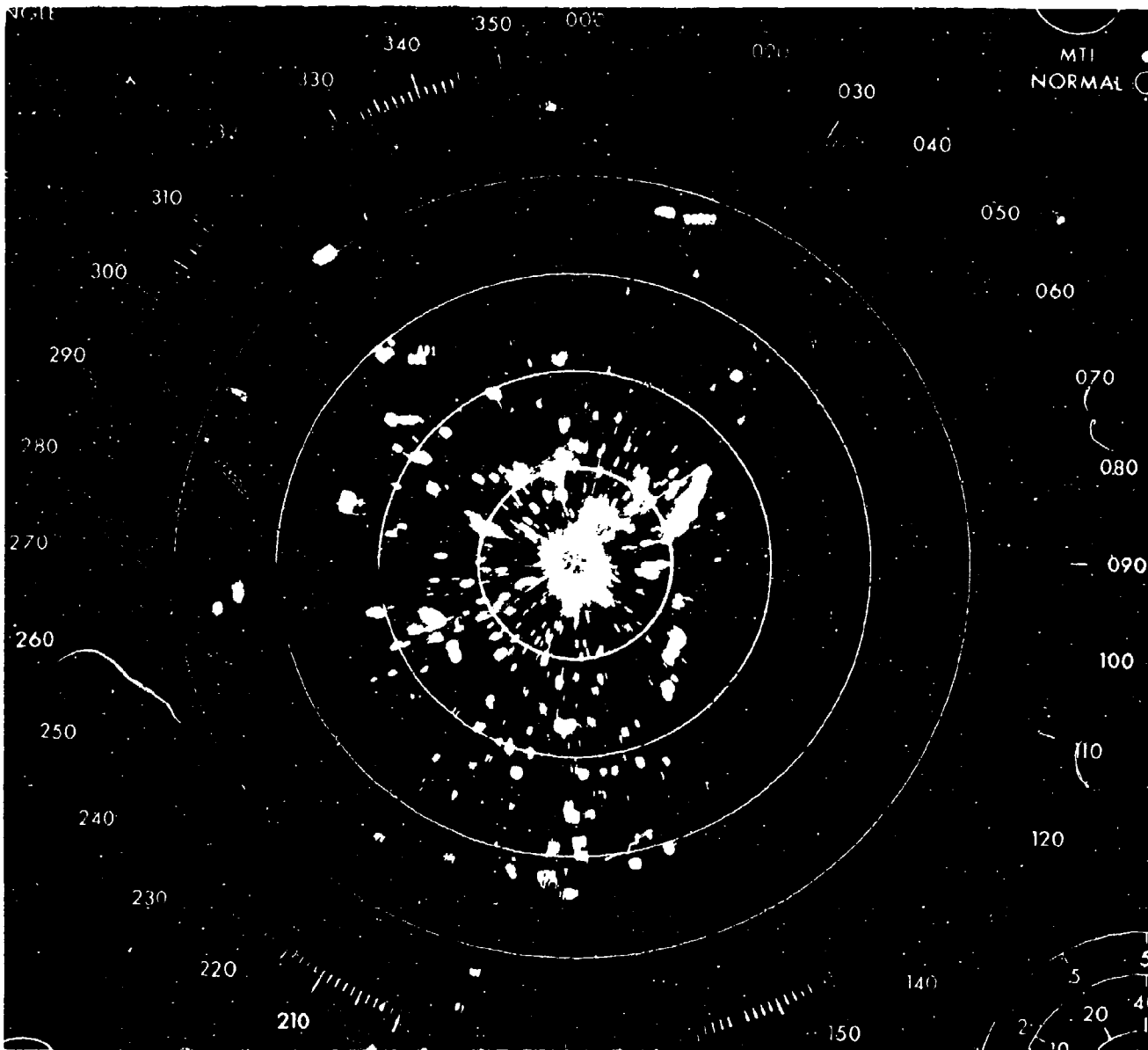


Figure 2.14 Time 1720, 2nm, Range Rings 20nm, Total
Diameter AN/MPN-14 Radar PPI, March 10, 1983

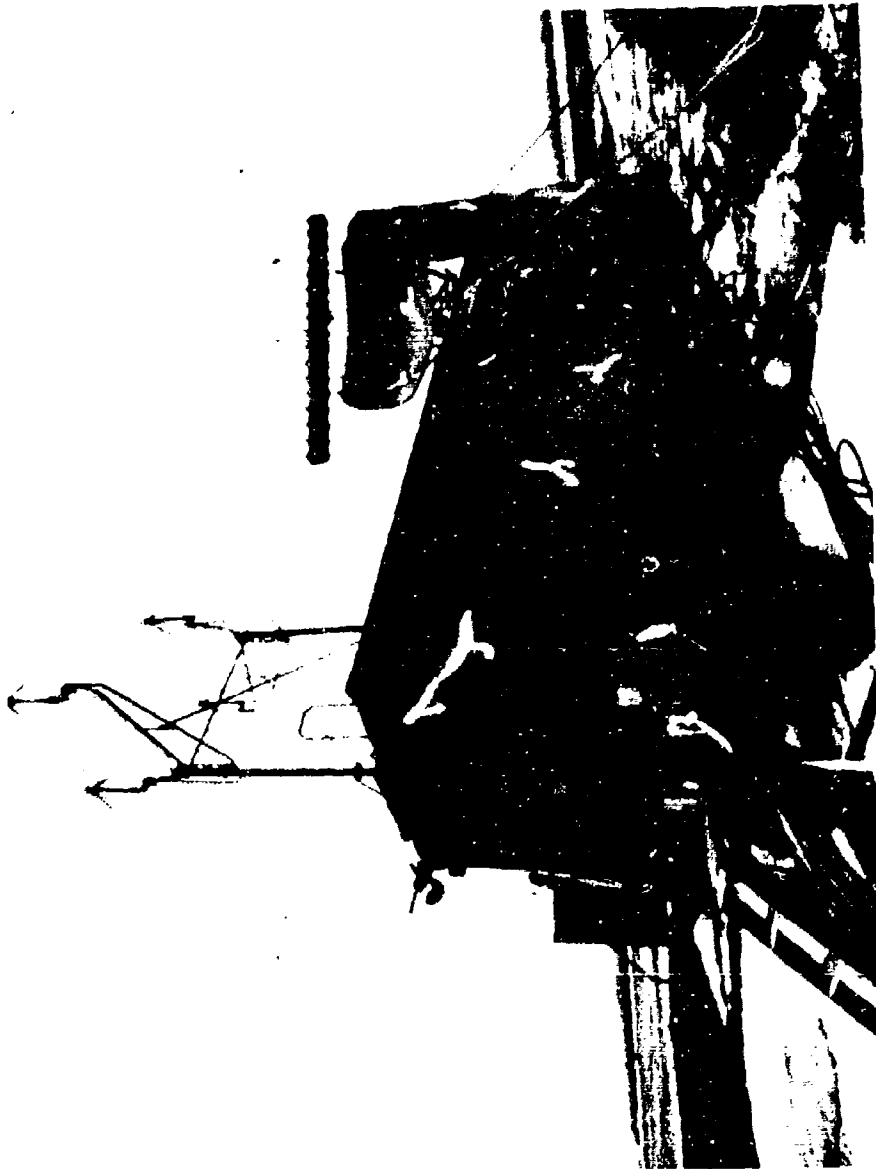


Figure 2.15 Photograph Of The AN/MPN-14 Radar At
Dover AFB

3.0 DEFINITION OF A BIRDWATCH WARNING SYSTEM

In order to design a warning system that will indicate the presence of a bird threat to aircraft pilots in sufficient time to prevent an incident, four basic parameters of the problem must be defined. First, the minimum threat must be defined quantitatively in terms that can be related to the safety of the aircraft and crew, i.e., that number or size of a bird threat which may smash a windshield or cause engine failure if ingested. Secondly, the dangerous air spaces around the base, i.e. those regions most occupied by birds, must be identified. Since local aircraft fly at specific various altitudes and ranges around the base when performing various phases of flight, the degree of danger can be related directly to those phases of flight. Thus, the required altitudes and ranges to be covered by the warning system can be defined in terms of a primary coverage area for the more dangerous volumes and a secondary coverage area for local volumes presenting a lesser though not insignificant hazard. Third, a warning system must work within the framework of an operational concept that allows sufficient time for the detection and communication processes. With the target size, the coverage area and the timing defined, the final warning system parameter, the size and characteristics of the warning radar sensor can then be determined.

3.1 Bird Threat Definition

When a threat had to be established during February 1983, the preliminary threat definition ranged from an initial conjecture of 5-10 geese [9] (40-80 lbs of bird mass) to 5-10 ducks [10] (15 lbs. of bird

mass). However, a study on the Dover AFB birdstrike problem performed by the BASH squadron in 1978 [1] noted that 4 out of the 8 strikes in which the bird species could be identified were raptors which hunt singly or in pairs. Due to the immediacy of the requirement and the potential cost in lives and material at stake, the initial threat was conservatively defined as a single goose. This led to the decision to obtain an AN/TPN-18A radar and crew to meet the spring requirement.

However, these estimates were made without having a documented relationship between bird mass and plane safety. A study published by Houle (1977) [11] revealed that, in the early 1970's, the structural components that have led in strike frequency were engines, wings, nose and radome areas, and windshields/ canopies in that order. Furthermore, the study [11],[12] revealed that strikes involving "... engine and windscreen components account for approximately 43% of all reported USAF bird strikes and for 77% of all the accidents that result in the loss of aircraft and/or crew." Table 3.1 presents the results of a more recent study by Kull (1983) [13] which shows that a similar pattern still existed in bird strikes reported during the 1980-1983 period. While the extensive work being performed on impact resistant windshields [14] may reduce or eliminate the danger of strikes to this component, little improvement is expected in the susceptibility of engines to damage from bird ingestions. Therefore, to establish the bird threat, the RADC effort focused on the threat to the engines.

The FAA is currently conducting a study on bird ingestions by high bypass ratio turbine jet engines such as exists on Boeing 747, DC 9,

IMPACT POINT	PERCENT
Engine/Engine Cowling	22.5
Wing	18.0
Windshield/Canopy	15.5
Radome/Nose	13.2
Fuselage	7.8
External Tanks/Pods/Gears	6.2
Multiple	8.0
Other	8.5

TABLE 3.1 - BIRD STRIKES BY IMPACT POINTS [13]

and other aircraft including the C5A. In a recent interim report by Frings [15], the FAA revealed the analysis of reported bird strikes which occurred between May 81 to April 82. Out of the 289 strikes reported, 188 or 65% incurred engine damage. The number and weight of the ingested birds could be estimated in 145 of the damaging strikes. Figure 3.1 presents the bird strike data in terms of bird weight versus number of birds ingested. Note that 120 of these 131 strikes (91.6%) involved the ingestion of only one bird per engine. Furthermore, of the 17 strikes resulting in engine failure, 9 (53%) were the result of ingesting one bird; 5 (29%) were the result of ingesting one bird < 1.5 lbs, and 11 (65%) were the result of ingesting a bird mass < 4 lbs. The average weight of an ingested bird was 37 oz with the most likely weight being 40 oz or 2.5 lbs. The preliminary conclusion of the

2 1/2 lbs for ducks, gulls and hawks. Consequently, a more appropriate threat is a 4 lb bird (a small goose or a large duck), which has a high probability of causing damage if ingested.

The next question is whether it is reasonable to use a single bird as the threat rather than a flock. Clearly, in a region with over 100,000 waterfowl and millions of smaller birds, the chances of a takeoff corridor being completely devoid of birds is almost nil. However, the primary purpose of the single bird threat is to provide a model which allows comparison between radars, not to provide a criterion for an operational warning system. The ability of a radar to detect the presence of bird activity depends on the number of birds it attempts to detect at a given instant, i.e. the number of birds within a resolution cell. The size of the resolution cell is proportional to the antenna elevation and azimuthal beamwidths and pulse width of the radar and the range from the radar.

$$RC = R^2 * \theta * \phi * (ct/2)$$

where

RC = resolution cell in cubic meters

R = range in meters

θ = two-way elevation beamwidth of the antenna in radians

ϕ = two-way azimuthal beamwidth of the antenna in radians

c = speed of light = 300,000,000 meters/second

t = pulse width in seconds

Since the resolution cells of typical search radars vary from less than 10,000 cubic meters to over 10,000,000 cubic meters, the density of the flock in terms of the number of birds per cubic meter would have to be known to allow comparison. Since flock density is not known, a chosen approach was to compare performance for a single bird and extrapolate performance for the case when a larger number of birds exists within a resolution cell.

3.2 Radar Cross Section (RCS) of Minimum Threat

Several models have been suggested for describing the radar backscatter from birds[16],[17],[18]. The most meaningful models are those that give a good approximation of the mean radar cross section (RCS) at microwave frequencies: the water sphere, the prolate spheroid of water, and the cylinder model. Figure 3.2 presents the RCS formulas and a sample calculation of the RCS for a 4 lb. bird using each model. The models describe the optical RCS and do not predict the fluctuations that would be expected as a function of incident wavelength, bird movement, or aspect angle.

RCS predictions at X-Band (wavelength = 3.2 cm) using the water sphere and cylinder models are plotted in Figure 3.3 for the hazardous bird species in the Dover area. Note that the predicted RCS values are a strong function of the model chosen, i.e., the cylinder model is 8 dB below that predicted by the water sphere. However, since all models relate RCS to the 2/3 power of weight, the differences in RCS between species is less than 4 dB. Also note that the RCS of a large goose is far below the 100+ square meters of the C5A and other large aircraft that frequent Dover AFB. This large difference in RCS can present

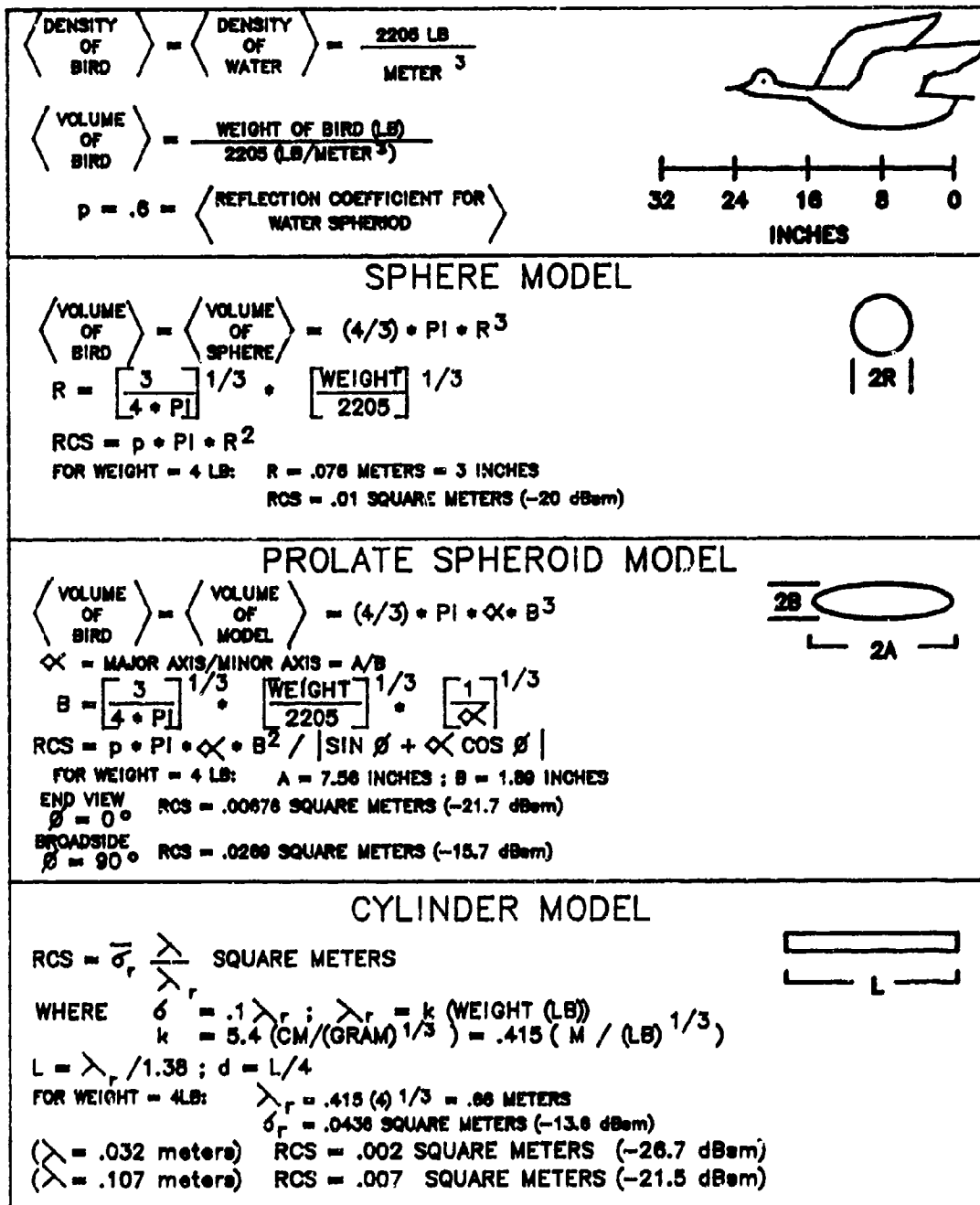


Figure 3.2 Radar Cross-Section Formulas

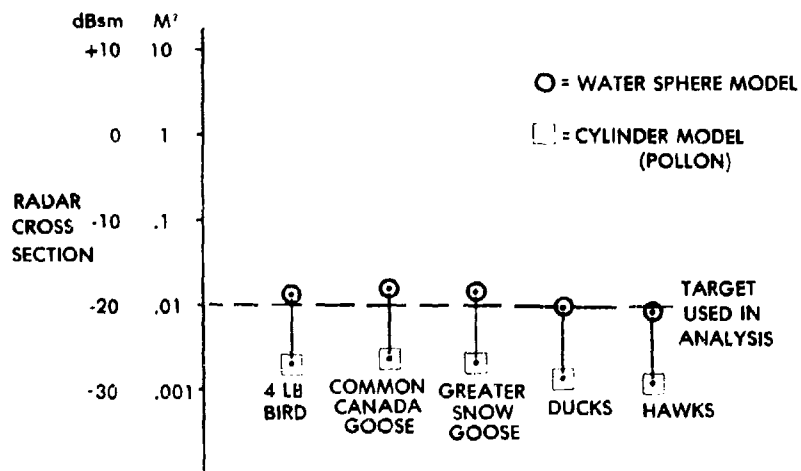


Figure 3.3 Radar Cross-Section of Bird Species (X-Band)

significant problems and limitations if a sensor is used to perform both the Air Traffic Control function on the large aircraft and the BIRDWATCH function on a small number of geese.

3.3 Primary and Secondary Coverage Requirements

When RADC was first introduced to the problem at DAFB, opinions were sought from the BASH squadron at Tyndall AFB [9] on the coverage that should be provided around the base. The recommendations given were that primary coverage should be provided down the corridors used for takeoff and landing out to about 6 nm with secondary 360 degree coverage of the traffic pattern out to 10 nm. The height coverages recommended were from treetop level to 1700 ft within 6 nm and from 5000 ft down to 300 ft or lower, if possible, out to 10 nm.

PHASE OF FLIGHT	MILITARY (1967-1972) 2173 DAMAGING STRIKES	CIVILIAN (MAY 81-APR 82) 188 DAMAGING STRIKES
TAKEOFF/ CLIMB	26%	56%
APPROACH/ LANDING	30%	21%
LOW LEVEL OPERATIONS	27%	N/A
OTHER	17%	23%

TABLE 3.2 - PERCENTAGE OF STRIKES BY PHASE OF FLIGHT [11,15]

Subsequent investigations supported these original recommendations. Table 3.2 gives the percentages of damaging strikes by phase of flight for military and commercial aircraft. The military statistics were documented by a report by Houle (1977) [11] and represent bird strike data taken over a 6 year period in which 65 million dollars worth of damage was incurred. Recent conversations [19] with the BASH squadron revealed that the percentages in each category have held constant over the recent years as well. The civilian percentages were obtained from the FAA interim report by Frings [15]. In each case, approximately 80% of the strikes occurred during low-level operation. While the primary

PHASE OF FLIGHT	TOTAL INGESTIONS (289 EVENTS)	DAMAGING INGESTIONS (188 EVENTS)	ENGINE FAILURE INGESTIONS (17 EVENTS)
TAKEOFF/ CLIMB	43%	56%	75%
APPROACH/ LANDING	28%	21%	25%
OTHER	29%	23%	0%

MULTIPLE BIRD INGESTIONS PER ENGINE	13 (5%)	11 (6%)	8 (47%)
MULTIPLE ENGINE INGESTIONS	11 (4%)	5 (3%)	1 (6%)

TABLE 3.3 - BIRD INGESTION SUMMARY FOR CIVILIAN AIRCRAFT [15]

<u>ALTITUDE</u>	<u>FREQUENCY</u>
< 100 FT	21.3%
100 FT - 500 FT	19.5%
500 FT - 1000 FT	21.2%
1000 FT - 2000 FT	22.8%
2000 FT - 3000 FT	7.7%
> 3000 FT	7.5%

TABLE 3.4 - BIRD STRIKES BY ALTITUDE (1968 - 1971) [20]

aircraft at Dover AFB, the C5A, may perform low level operations during local training missions, its operational missions have more in common with the large passenger jets than fighters and bombers. Thus the civilian data, which is expanded in Table 3.3, provides statistics more appropriate to C5A operational missions. Note that over half of the damaging strikes and three-quarters of the strikes resulting in engine failure occur during takeoff when engine thrust is most important and the plane is most vulnerable!

Another statistic supporting the original recommendations is the distribution of bird strikes by altitude presented in Table 3.4. This information, derived from a study by Southern (1978) [20], emphasizes that 85% of the damaging strikes reported between 1968 thru 1971 occurred below 2000 ft. Of the strikes that occurred below 100 ft, 75% occurred while the plane was on the ground. Discussions with BASH personnel indicated that current bird strike data follow a similar distribution [19]. Since a radar warning system will not be effective for bird activity on or very near the ground or runway, the major impact of the system will be to provide coverage between 100 ft and 2000 ft where approximately two-thirds of the strikes occur.

Thus, the primary coverage should be the takeoff and landing corridors originally recommended by the BASH squadron with secondary coverage in the traffic corridors within 10 nm of the base highly desirable. In order to define the boundaries of the primary coverage volume, the timing and processes of a warning system will now be addressed.

3.4 Warning System Timing

The development of a warning system must include the timing required for the following processes to occur:

1. initiation of warning system (request for advisory)
2. detection and assessment of potential threats
3. perform binary decision on threat existence
4. report advisory to aircraft
5. aircraft takes appropriate action

The time required to perform the above processes and the speeds of both the aircraft and threatening bird flock determine the range requirements of the radar sensor.

Figure 3.4 presents an example of warning system timing similar to that used in the adhoc BIRDWATCH system at Dover AFB between March 7 and April 15, 1983. During this time, the BIRDWATCH system incorporated an AN/TPN-18A GCA radar and crew. Assume that time 0 is chosen to represent the time at which a plane begins to roll for a take-off or begins down the glide slope for landing. Two minutes before time 0, the BIRDWATCH monitor is notified and begins to monitor the Plan Position Indicator (PPI) scope for bird activity around the intended path of the plane. Within 60 seconds (approximately 16 scans for the AN/TPN-18A radar), a trained operator can estimate the size, speed, and heading of potentially hazardous bird activity. (Highly trained operators of the AN/TPN-18A also demonstrated an ability to obtain crude but useful height estimates to assist in judging the threat potential of detected bird flocks.) At time -50 seconds, the

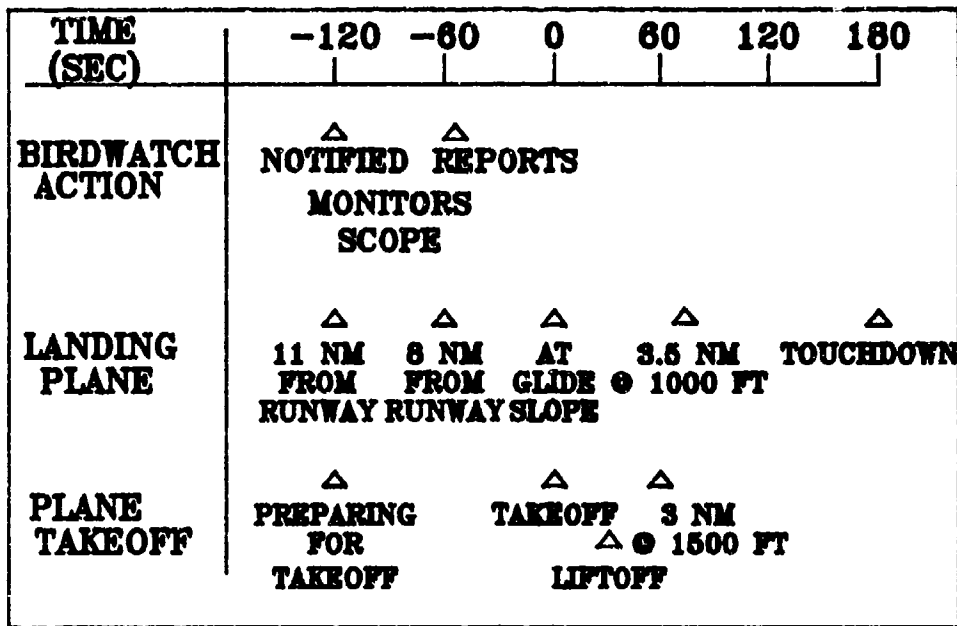


Figure 3.4 Warning System Timing

operator makes a binary decision as to whether the threat exists or not and relays this decision to the requestor. Since the adhoc system used the Dover AFB Command Post as a middleman between the BIRDWATCH monitor and the pilots, approximately 50 seconds are allotted for communication of the advisory to the pilot and for the pilot to take action. Note that after -50 seconds, no further BIRDWATCH action is assumed to take place. Therefore, the BIRDWATCH monitor must be able to detect potential threats within a volume around the intended path of the

<u>Down Range (nm)</u>	<u>Ground Speed* (knots)</u>	<u>Time (seconds)</u>	<u>Cross Range (nm)</u>
0.0	0	0 (begin roll)	---
1.0	233	31	1.44
1.5	286	38	1.52
2.0	330	44	1.58
2.5	369	49	1.64
3.0	404	53	1.69
3.5	436	58	1.74
4.0	467	62	1.78
4.5	495	65	1.82

*Assumes a constant horizontal acceleration of 12.86 feet/(second squared) or .0021 nautical miles/(second squared). Derived from data in Table 2.4 for future C5 capabilities with a gross weight of 760,000 lbs and ambient temperatures > 50 degrees F.

Note: Cross Range is the distance between the plane's path and the position of an intercepting bird at $t = -100$ seconds. Velocity of the bird is 40 knots or .011 nm/sec.

TABLE 3.5 SAFETY CORRIDOR BOUNDARIES AS A FUNCTION OF TIME AND POSITION ALONG PLANE'S PATH

plane, i.e. a safety corridor, to get the plane safely airborne or landed.

Figure 3.5 presents the shapes and dimensions of the safety corridors for the takeoff and landing cases as would be viewed on a PPI indicator. When a plane is taking off, the advisory must be adequate for approximately 60 seconds after the plane begins rolling down the runway or 180 seconds after the initial request. Table 3.5 provides approximate values for the range and velocity of a fully-loaded C5 at various times after the plane begins to roll down the runway. The cross range distance between the plane's path and the boundaries of the safety corridor are also given as a function of time and are plotted in

Figure 3.5a. Since a plane taking off is accelerating, the corridor has curvilinear sides. A trapezoidal approximation (dashed line) could be more easily calculated for a worst case example and used in operational environments.

For the landing case given in Figure 3.5b, the advisory must be valid for a full 180 seconds after time 0 or 5 minutes after the original request. The 6 nm corridor is assumed to begin at the top of the glide slope (time 0) and terminate at the end of the runway. When approaching the landing corridor, a C5A typically travels at

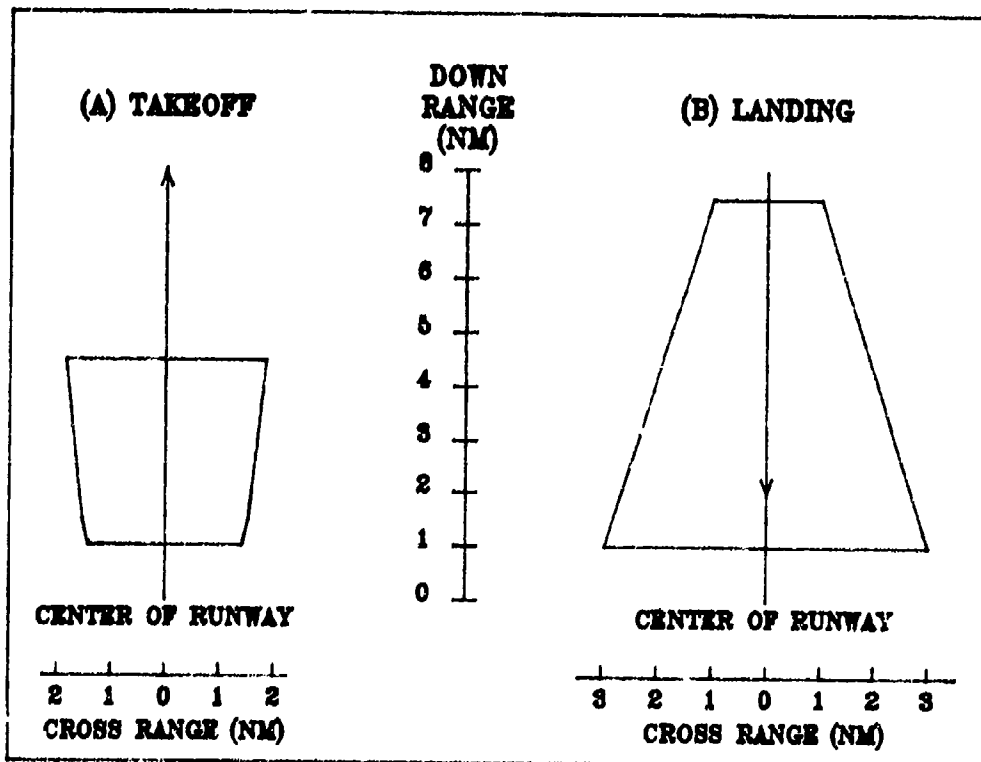


Figure 3.5a Threat Corridors for Landing Aircraft

Figure 3.5b Threat Corridors for Aircraft Taking Off

approximately 140 knots slowing down to about 120 knots down the glide path.[8] If an intercepting bird has a velocity of 40 knots, then the distance that the bird can travel between time of the BIRDWATCH monitor period ($t = -100$ seconds) and intercept time determines the boundary of the safety corridor. Since the speeds of the bird and aircraft are assumed to be constant, this corridor has the shape of a trapezoid.

Figure 3.6 presents the contours of the "safety corridors" as a function of altitude and range. For the landing case (Figure 3.6a), coverage is required to approximately 7.5 nm at 1500 feet dropping to 4 nm for birds flying at treetop levels. The more hazardous takeoff case (Figure 3.6b) requires less range (5.5 nm at 1500 feet and 2.25 nm at treetop levels).

These contours assume that the birds fly at a constant altitude. If the birds were assumed to gain altitude, then birds flying under the glide path can be further out and still intercept the plane at a higher altitude. This has the effect of requiring more range coverage at the lower altitudes. Figure 3.7 presents an example of this effect assuming a vertical velocity of 6 knots. This figure also emphasizes the seriousness of the "pop-up" problem, i.e. the birds that feed at the end of the runway and fly up in front of an approaching plane. As stated in section II, the warning system described in this section has no capability in providing a reliable warning for the "pop-up" hazard.

In summary, to provide a safety corridor for both landing and takeoff, a BIRDWATCH radar sensor must be capable of detecting a -20 dbsm bird at a range of at least 7.5 nm at 1500 ft altitude and 4 nm range for birds flying at treetop heights. The next section will

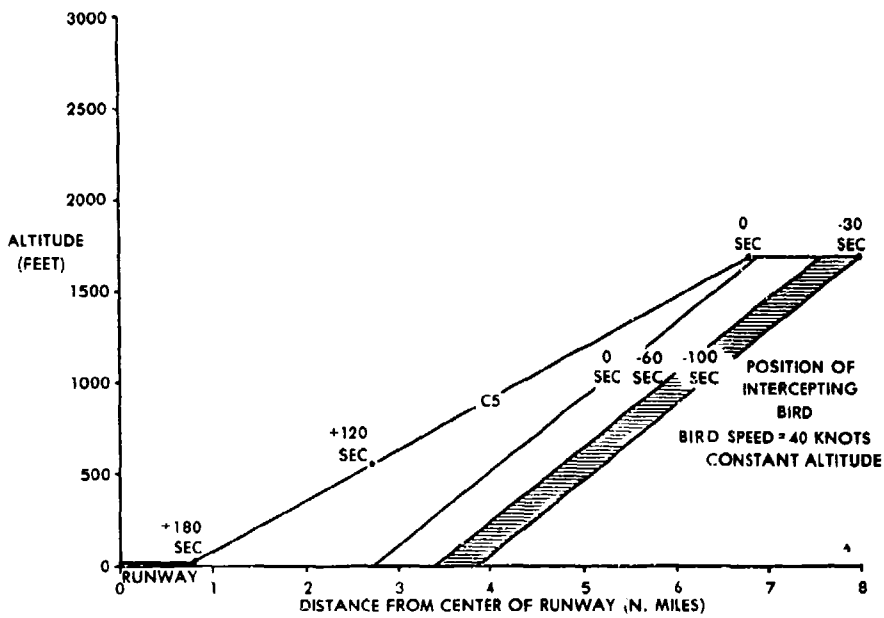


Figure 3.6a Required Birdwatch Coverage For Landing Aircraft (Bird Speed = 40 Knots At Constant Altitude)

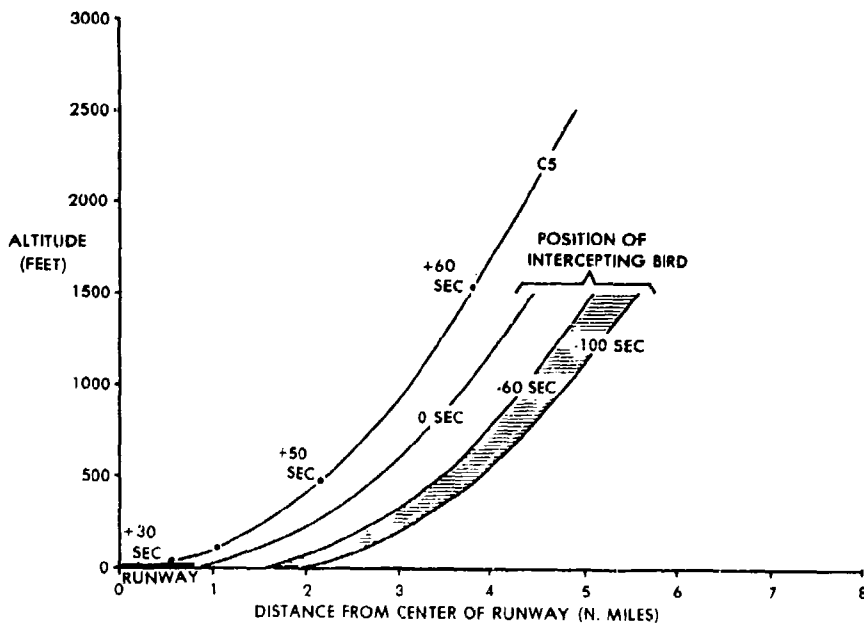


Figure 3.6b Required Birdwatch Coverage For Take-Off (Bird Speed = 40 Knots At Constant Altitude)

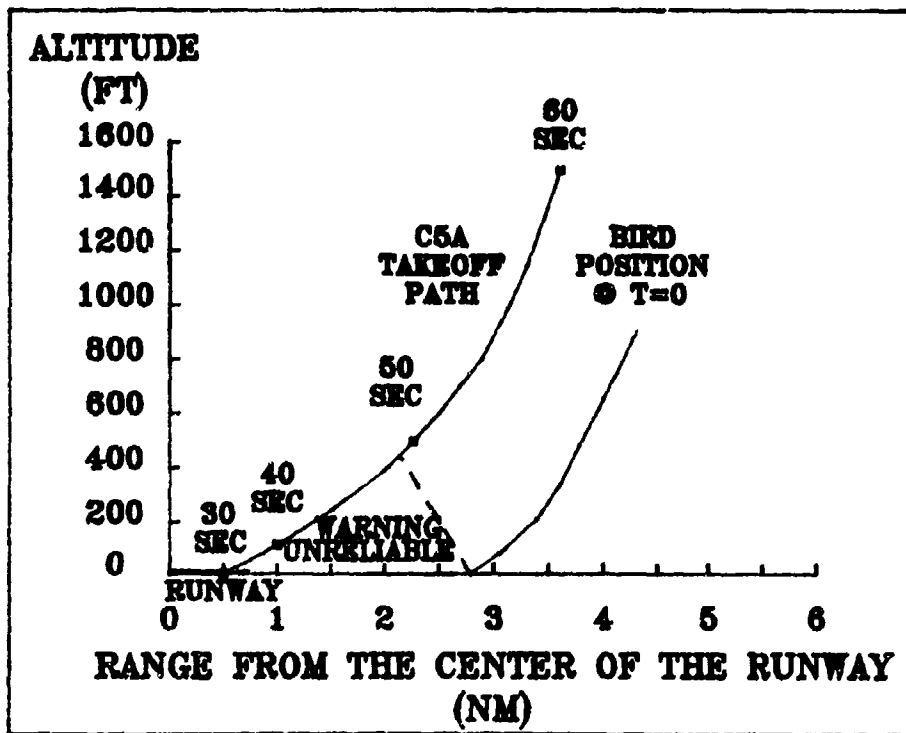


Figure 3.7 Required Birdwatch Coverage For Landing Aircraft
(Bird Has A Vertical Velocity of 6 Knots)

determine the size and parameters of the radar sensor necessary to achieve this performance.

4.0 EVALUATION OF CANDIDATE RADAR SENSORS

This section will describe the approach and efforts expended in selecting a BIRDWATCH sensor. First, the range equation for search radar will be introduced as a figure-of-merit (FOM) for evaluating sensors. The primary and secondary coverage requirements and the bird threat developed in the last section will be used to establish a minimum FOM for the birdwatch sensor. Since the immediate requirement demanded the use of an existing system, several radars listed in The Handbook of U.S. Radar Equipment, MIL-HDBK-162B, and a recent survey of U.S. Navy radars were screened for potential use. An evaluation of the radar chosen to satisfy the immediate requirement in March 1983 is provided and the experience is used to help analyze three candidate systems for the interim requirement. The section ends with an analysis of the one-on-one tests performed during the fall of 1983.

4.1 Radar Range Equation and a Figure of Merit

The range equation for a search radar provides a first-order figure of merit (FOM) for comparing the detection performance of various radar sensors. A useful form of the range equation, derived in Appendix F, is given in equation (4.1) which relates the requirements of the system to radar parameters commonly listed in specification summaries.

$$(4.1) \quad \text{FOM} = \frac{P_t A_e t_s}{K T_s} = \frac{(4\pi) \psi R^4 (S/N)}{\sigma (\Sigma \text{ losses})}$$

Table 4.1 lists the definitions of the important parameters. This FOM compares the effective radiated energy of the sensor to the noise energy competing with the return. To allow candidate radars to be

P_t	= average transmitter power (watts)
t_s	= time taken to perform one volume scan (seconds)
RPM	= revolutions per minute
A_e	= effective aperture (square meters) = $\frac{G_r \lambda^2}{4\pi}$
G_r	= power gain of the receiving antenna
λ	= wavelength (meters)
σ	= radar cross section of target (square meters)
ψ	= angular volume searched (steradians) $\approx 2\pi\theta_e$
θ_e	= one-way 3 dB elevation beamwidth (radians) $\approx \frac{\lambda}{L_e h}$
h	= height of antenna aperture (meters)
L_e	= inefficiency of antenna due to weighting
(S/N)	= minimum integrated signal-to-noise ratio at threshold detector $\Delta 17.7$ dB (sw I, $P_d = .8$, $P_{fa} = 10^{-6}$)
K	= Boltmann's constant = 1.37×10^{-23} w-s/ K = -228.6 dBw-s/ K
T_s	= system noise temperature (degrees Kelvin) $\Delta T_a + T_{tr} + L_{tr} T_o$ (NF-1)
NF	= noise figure of the receiver
T_a	= antenna noise temperature (degrees Kelvin) $\Delta 100$ K
T_r	= noise temperature of transmission line and passive components connecting the antenna and the receiver (degrees Kelvin) = $T_o(L_{tr}-1)$
L_a	= transmitter power loss due to azimuth weighting
$F^4(\theta, \phi, R)$	= propagation factors = 1 for free space
L_b	= mismatch loss of receiver bandpass filter $\approx B_n T$
B_n	= noise bandwidth of the receiver (Hz) ≈ 3 dB bandwidth
τ	= pulse width (seconds)
L_i	= non-coherent integration inefficiency of equal amplitude pulses ($2.4 \log N_p$ ($5 < N_p < 30$); $3 \log N$ ($30 < N_p < 100$))
N_p	= number of pulses per one-way antenna beamwidth = $\frac{T_a \phi_a \text{ PRF}}{360}$
ϕ_a	= one-way azimuthal beamwidth (degrees)
PRF	= pulse repetition rate (pulses per second)
L_p	= pattern loss ≈ 1.6 dB
L_t	= plumbing loss in transmitter
L_r	= non-ohmic loss and ohmic loss not included in noise temperature or receiving antenna gain
L_{atm}	= loss in atmosphere (2 way)
L_{rain}	= loss in absorption by rain = $.0011 (3.2/f)^{-2} \cdot R_r$ (dB/Km)
f_r	= radar operating frequency (GHz)
r	= rain rate (mm/hr)
L_{log}	= additional loss in non-coherent integration when a logarithmic detector is used $\sim .5 \log N_p$
L_{ftc}	= loss in S/N by FTC ~ 3 dB
R	= range (meters)

TABLE 4.1 DEFINITION OF TERMS FOR RADAR RANGE EQUATION

screened quickly, the FOM uses only four parameters commonly given in specifications: the average transmitter power (P_t); the effective aperture of the receiving antenna, (A_e); the time required to scan the volume, (t_s), and the system noise temperature, (T_s).

To establish the minimally acceptable FOM, the four system parameters listed on the left of the equal sign in equation (4.1) must be defined by the sensor requirements established in the previous section. These parameters are the detection range; the angular volume to be searched; the cross section of the bird threat to be detected and the signal-to-noise ratio required to provide a minimum probability of detection (P_d) at an acceptable probability of false alarm (P_{fa}).

The detection range is the maximum detection range requirement in the BIRDWATCH system for a 4 lb bird, i.e. the landing coverage requirement of 7.5 nm at an altitude of 1500 feet. The angular volume searched is defined by the elevation and azimuthal angles required to be searched in the system. The requirements for coverage down the 2.7 degree glide slopes and for 300 to 5000 feet altitude coverage at 10 nm leads to a minimum elevation coverage from the horizon up to about 4.5 degrees. For the landing/takeoff corridors, only four 20 degree azimuth sectors are necessary. However, to provide the secondary coverage, a 360 degree capability is required. Since many of the systems considered are 360 degree scanning systems, a 360 degree (azimuth) by 4.5 degree (elevation) volume is assumed in the calculations. Therefore, the required angular search volume is approximately 0.5 steradians.

The average radar cross section (RCS) of a 4 lb bird threat was

shown in the last section to be - 20 dBsm. However, this value is averaged over all aspects of the bird. The instantaneous RCS of a bird or a flock of birds fluctuates over a periods exceeding two seconds. Therefore, for radars that have scan periods exceeding 2 seconds, the RCS of a bird flock fluctuates about the mean value of -20 dBsm from scan-to-scan and, for single frequency channel systems, the fluctuations are assumed to follow Swerling 1 statistics.

The last parameter, the signal-to-noise ratio, was not explicitly defined in the last section but is related to the assumptions on what is required for a human operator to reliably detect, acquire, track and assess the size of a bird hazard within a given time limit. In the warning system timing example described in Section 3, the BIRDWATCH monitor was allocated 60 seconds to detect birds in the vicinity of the aircraft's path and identify potentially hazardous traffic. The detection of a bird flock requires at least two hits on the PPI display within 2 to 4 scans (blip scan ratio = 2/2 to 2/4). Crude estimates of speed, heading, and relative size requires one or two more detections within the next two or three scans. Thus for one flock at least three or four detections in a minimum of three to seven scans (blip scan ratios = 3/3 to 3/7) are necessary to allow the operator to make a reasonable estimate of a single isolated threat. Unfortunately, as shown in Figure 4.1, the operator is often forced to make estimates on several targets simultaneously within a small period of time. In such cases, the quality of the estimates will increase significantly with an increase in the blip scan ratio or probability of detection (P_d). For the purposes of this analysis, a (P_d) of .8 (blip scan of 4/5)

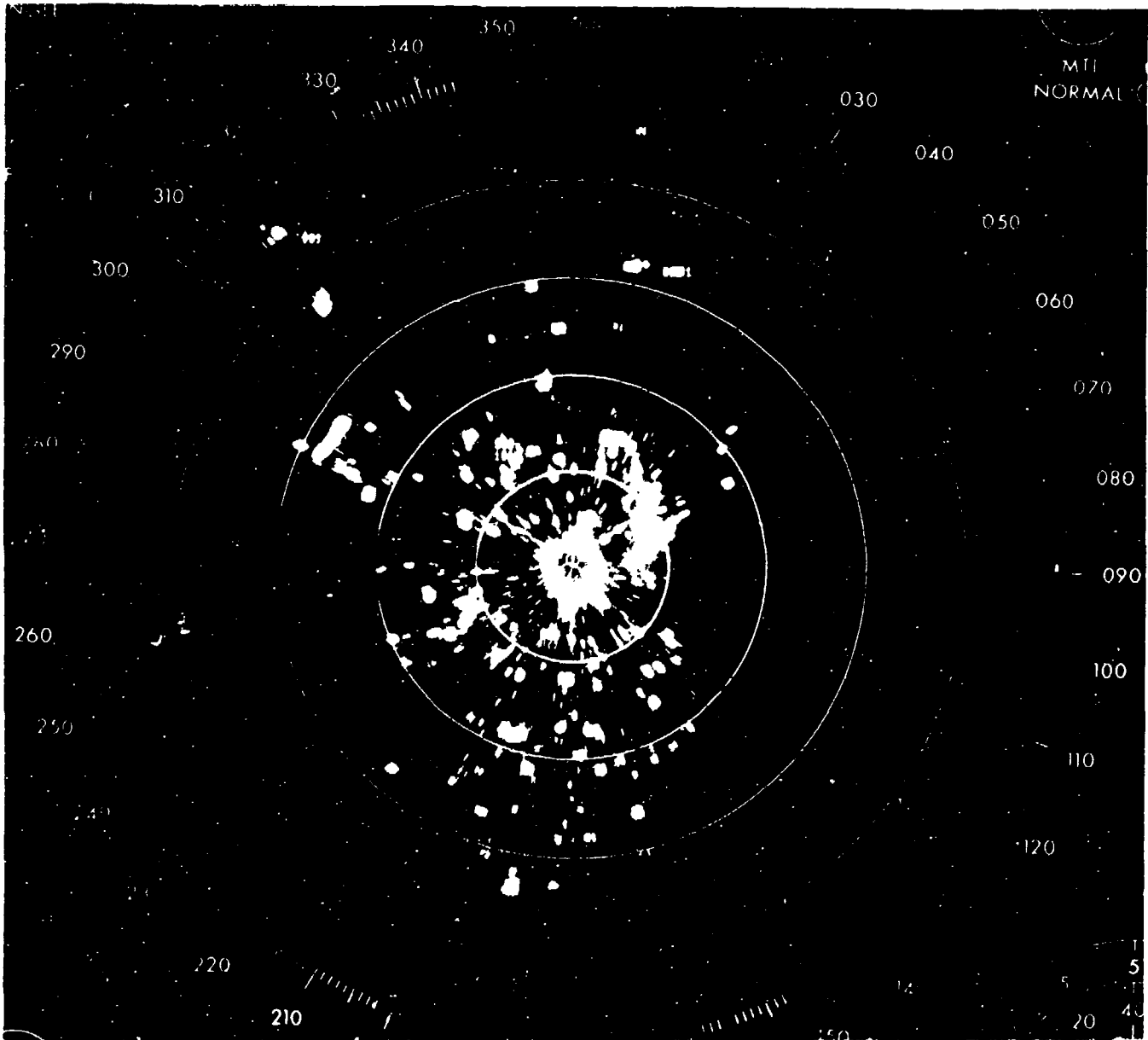


Figure 4.1 AN/MPN-14 Radar PPI, 2 nm Range Rings, 20nm Diameter, Time 1718, March 10, 1983

has been chosen as a reasonable compromise, requiring approximately 4 to 5 scans to perform the required estimates. Since Swerling 1 fluctuation statistics are assumed to describe the RCS of the bird, this (P_d) corresponds to a S/N = 17.7 dB ($P_{fa} = 10^{-6}$).

Inserting these values into equation (4.1), the figure of merit required for the candidate sensors is -221.5 dB watt-seconds/degree Kelvin (w-s/K) or 7.08×10^{-23} w-s/K. Finally, note that with 5 or more scans required to perform the required estimates on multiple detections within the allocated 60 seconds, the maximum allowable scan period of a potential BIRDWATCH sensor is 12 seconds.

4.2 Comparison of Available Sensors

Figure 4.2 presents a scatter plot of a few of the sensors initially considered for meeting the immediate BIRDWATCH requirement during February 1983. The ordinate is the FOM and the abscissa is scan time (t_s). Potential candidate sensors were those that met or exceeded both requirements. Since the FOM is only a first-order screening tool, those sensors near the boundary such as the larger marine radars were also considered as potential candidates.

Table 4.2 provides the various merits and demerits of several candidate systems. One surprise to the investigators was that few radar sensors listed in the DOD inventory offered a three dimensional (3-D) surveillance capability, i.e. range, azimuth, and altitude information on target detections, or modern doppler processing. Altitude estimates on the detected bird traffic would allow better discrimination between true hazards and bird traffic that is safely below or above the intended path of the aircraft. Doppler processing, such as MTI, allows the detection of targets moving to or from the

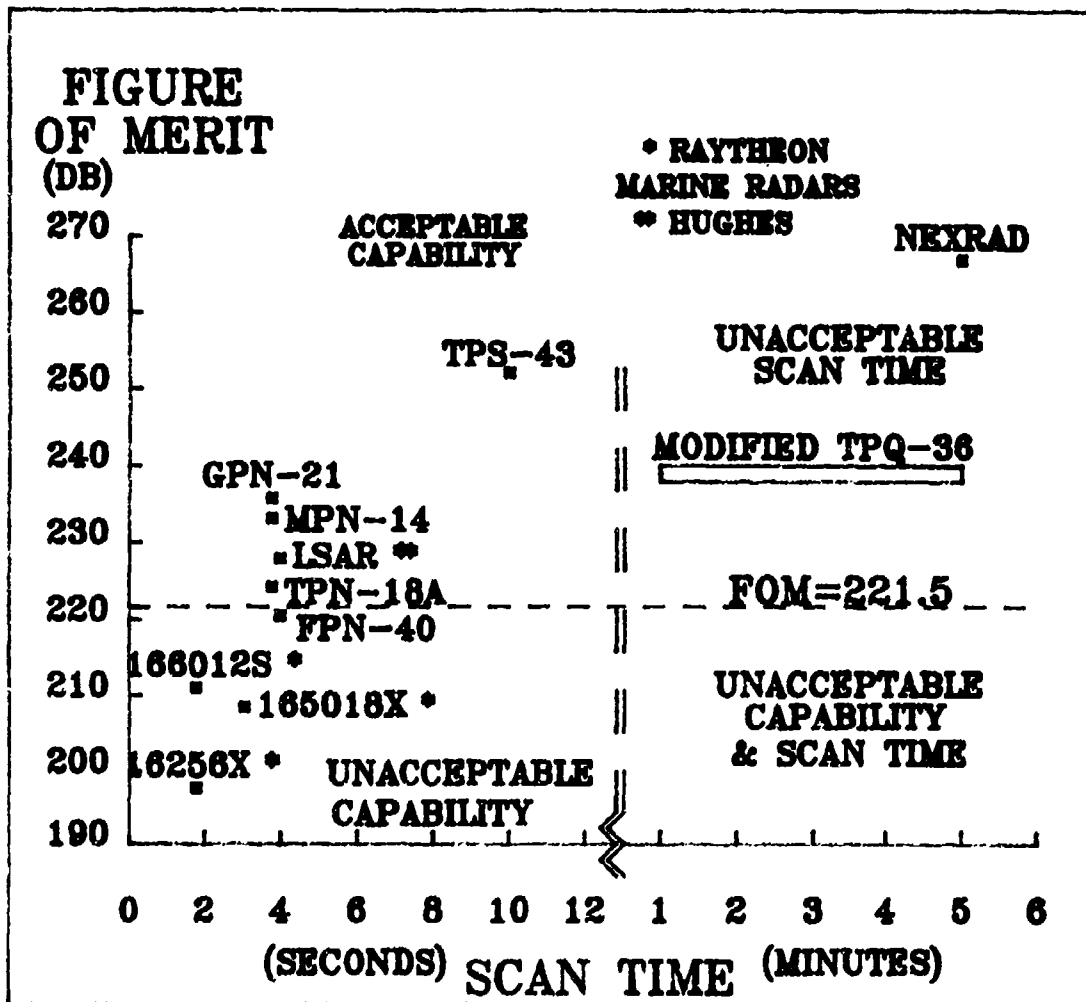


FIGURE 4.2 A Scatter Diagram Comparing Available Sensors With Requirements

radar sensor in the presence of stronger radar reflections from trees, buildings, and other stationary scatterers on the earth's surface.

While many radar systems were considered and several systems met or exceeded the FOM requirement, most were unacceptable for one reason or another. Some of the sensors were eliminated as viable alternatives because although, they were in the DOD inventory, they could not be obtained for the BIRDWATCH effort, or could not be

PARAMETER	GPN-21	TPN-18A	FPN-40	MPN-14	TPS-43	TPQ-36
Average Power (Watts)	400 (X2)	168	200	600	4700	250
Effective Aperture (Square Meters)	1.8	.5	.5	1.26	4	1.3
Scan Time (Seconds)	3.75	3.75	4.0	3.75	10	>60
System Noise Temperature (Degree K)	965	965	2700	1000	870	1550
Figure of Merit	235.6	223.8	220.3	233	252	239
(Estimated Free Space Detection Range) X100% Requirement	225%	115%	93%	194%	579%	274%
MTI	yes	no	no	yes	yes	yes
Circular Polarization	yes	yes	yes	yes	no	no
All Weather Capability	yes	no	no	yes	yes	Limited
Screening Limitations	no	yes	yes	yes	yes	yes
Contractor Maintenance	no	no	Negotiable	no	no	Negotiable
3-D Capability	no	Limited (PAR)	Limited (PAR)	Limited (PAR)	yes	yes
Off-The-Shelf Procurable	N/A	yes	yes	no	yes	yes
Doppler Processing	no	no	no	no	no	yes
Conflict W/ATC Functions	Possible	no	no	yes	Possible	no
Availability	April 1983	7 March for 60 days	Fall 1983	none	-	none
Manpower	USAF Operators & Maintenance	Army Personnel	USAF Operators & Maintenance	N/A	USAF Operators & Maintenance	USAF Operators & Maintenance
Cost	<10K	15K for 60 days Good	Negotiable	N/A	-	1.5M
Overall spring '83 Assessment	Good	Possible	Possible	N/A	N/A	N/A
Future				N/A	Possible	N/A

TABLE 4.2 COMPARISON OF POTENTIALLY AVAILABLE RADARS

	Raytheon 166012S	Raytheon 165018X	Raytheon 16256X	NEXRAD	LSAR (Hughes Prototype)
Average Power (Watts)	54	40	22.5	600	250
Effective Aperture (Square Meters)	.5	.2	.058	29	1.3
Scan Time (Seconds)	1.82	3	1.82	300	4 (assumed)
Receiver Noise Temperature (Degrees F)	2700	2700	2700	870	1500 (assumed)
Figure of Merit	211	208.4	197.9	266.6	227.7
(Estimated Free Space Detection Range) X100% Requirements	54%	49%	26%	1340%	143%
MTI	no	no	no	yes	yes
Circular Polarization	no	no	no	no	no
All Weather Capability	Limited	no	no	yes	Limited
Screening Limitations	yes	yes	yes	Site Dependent	Site Dependent
Contractor Maintenance	yes	yes	yes	Negotiable	Negotiable
3-D Capability	no	no	no	yes	yes
Off-The-Shelf Procurable	yes	yes	yes	no	no
Doppler Processing	no	no	no	yes	yes
Conflict w/ATC Function	no	no	no	no	no
Availability	7 Mar 83	7 Mar 83	7 Mar 83	none	none
Manpower	USAF Operator team	USAF Operator team	USAF Operator team	N/A	USAF Operator team
Cost	~40K per channel	~40K per channel	~20K per channel	N/A	N/A
Overall	Unacceptable	Unacceptable	Unacceptable	N/A	N/A
Assessment Future	Unacceptable	Unacceptable	Unacceptable	Unacceptable	Possible

TABLE 4.2 COMPARISON OF POTENTIALLY AVAILABLE RADARS (Cont'd)

installed within a week's time. Others were rejected because they were no longer in DOD inventory or available from a contractor. Some, like the AN/TPS-43 radar, far exceeded the FOM requirements and offered 3-D and signal processing advantages. However, the recovery time of the TR components limited the short range capability to approximately 3 to 5 nm, making it useless for a BIRDWATCH function. Furthermore, if installed at Dover AFB, this long-range S-Band system, which transmits a multimegawatt phase-coded pulse, could interfere with the AN/MPN-14 or AN/GPN-20 GCA systems located within a few thousand feet and operating at a slightly lower frequency.

The surveillance radar of the AN/MPN-14 performing the GCA function during February and March 1983 offered Moving Target Indicator (MTI) processing and was potentially able to provide a useful all weather two dimensional BIRDWATCH capability. In addition, the Precision Approach Radar (PAR) associated with the AN/MPN-14 system offered 3-D information on one landing corridor. However, the AN/MPN-14 shelter contained no extra scopes or space for a BIRDWATCH operator. Furthermore, uncertainty of the system's ability to simultaneously perform its primary Air Traffic Control function and BIRDWATCH function excluded the use of the AN/MPN-14 for the spring of 1983.

The AN/GPN-21 surveillance radar, which with the AN/GPN-22 PAR and various communications and supporting equipment form the AN/GPN-20 GCA system, offered capabilities similar to the AN/MPN-14. Unfortunately, it was being installed during that winter and would not be available until April 1983.

Even modification of modern short range systems like the AN/TPQ-36 and prototype systems like the Hughes LSAR were investigated in an attempt to provide modern 3-D and Doppler processing capabilities. However, by the end of February, it was concluded that the best radar available to meet the immediate BIRDWATCH sensor and manning requirements by early March was the ARMY AN/TPN-18A, which was available with well-trained ARMY operators and maintenance personnel. The AN/GPN-21 was tagged as a promising interim sensor for use beginning in the fall of 1984 and until a far term solution is procured. In the event that the AN/GPN-21 may not be able to simultaneously perform the ATC and BIRDWATCH functions or was found to be unsuitable for other reasons, the AN/TPN-18A and the older AN/FPN-40, as well as their modern commercial counterparts, the Mark V and the Mark VI, were identified as backup sensors.

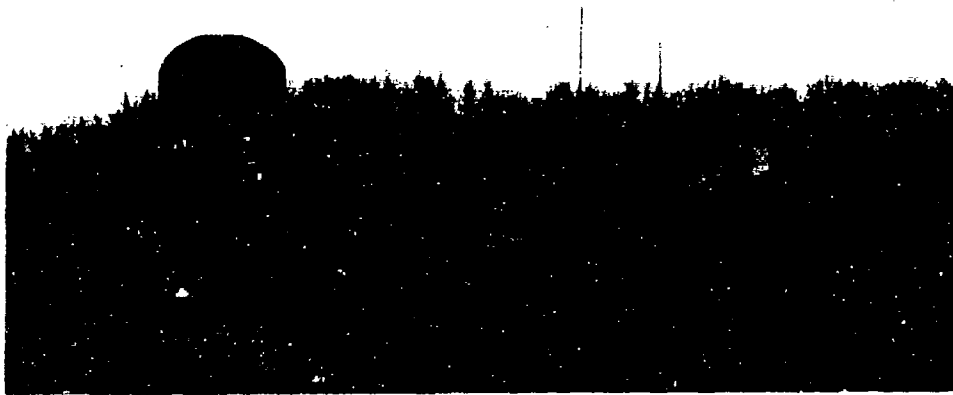


Figure 4.3 AN/TSQ-71B System Consisting Of AN/TPN-18A Radar, Operator Shelter, Diesel Generator And Repair Shelter.

4.3 Evaluation of the AN/TPN-18A BIRDWATCH Performance, Spring 1983

Figure 4.3 is a picture of the AN/TSQ-71B tactical GCA radar system. In the foreground is the AN/TPN-18A radar which consists of both a search and precision approach antennas. In the background are the diesel power generators, the operators shelter, and, barely visible, the maintenance shelter.

Figures 4.4 through 4.6 present the PPI display viewed by the AN/TPN-18A BIRDWATCH operators. The range rings are spaced 1 nm apart giving a maximum display radius of 5 nm. The photographs were taken approximately 4 minutes apart. Most of the detections on these photos represent backscatter from buildings, trees, and other objects on the ground. These returns are distinguished from moving targets in that

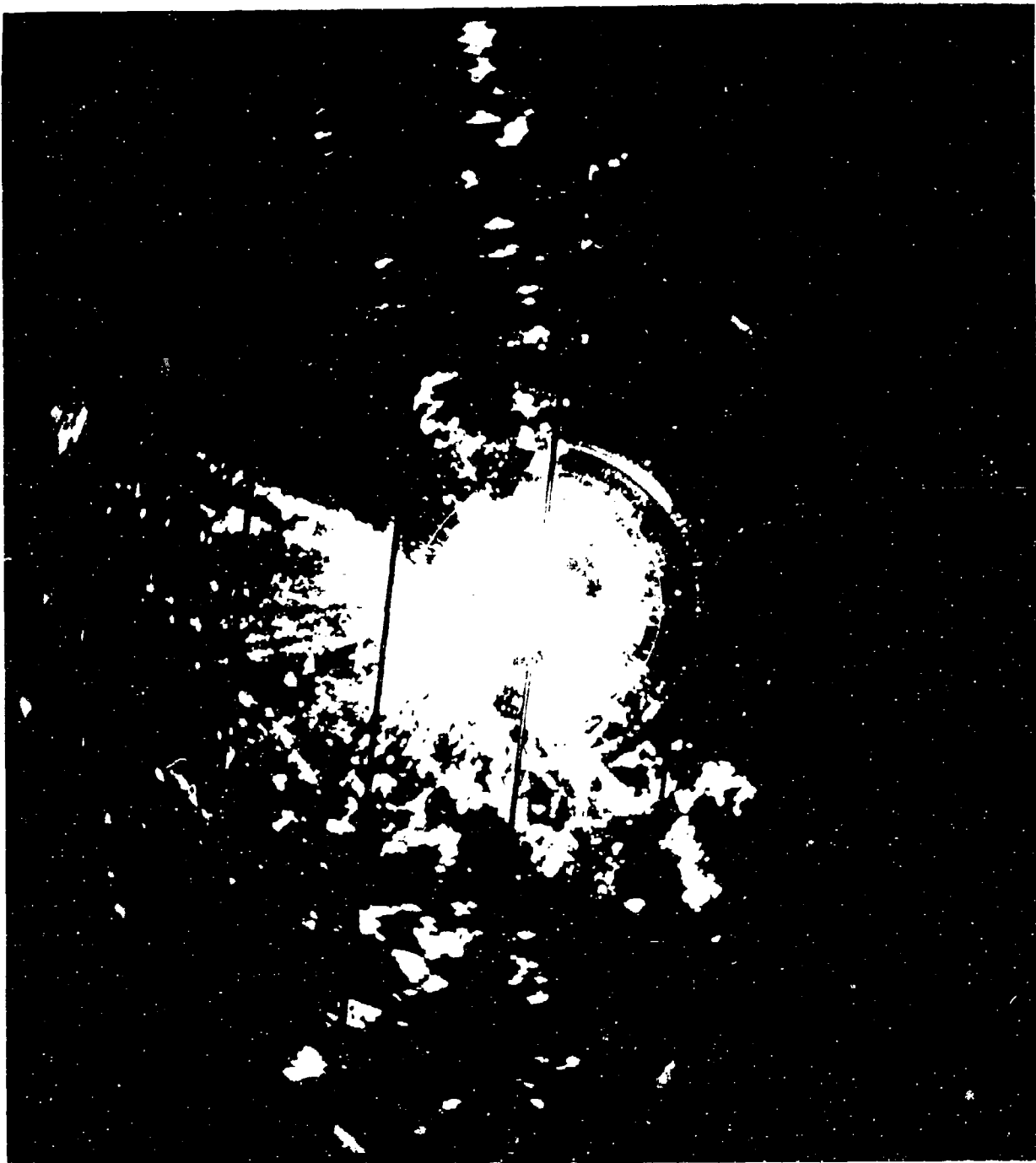


Figure 4.4 AN/TPN-18A Radar PPI, 10nm Range Rings, 10nm Diameter, Time 1755, March 30, 1983



Figure 4.5 AN/TPN-18A Radar PPI, 1nm Range Rings, 10nm Diameter, Time 1800, March 30, 1983

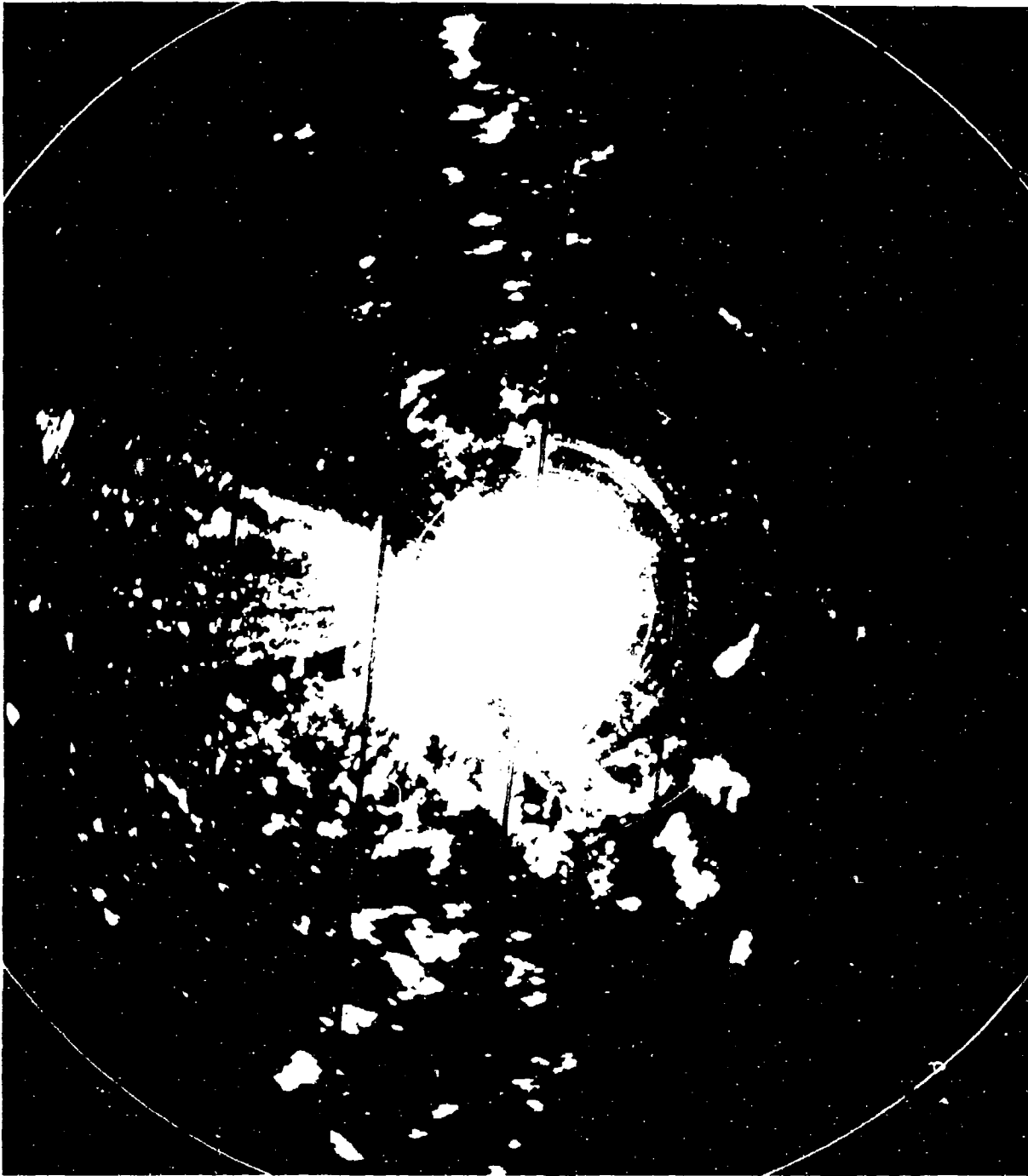


Figure 4.6 AN/TPN-18A Radar PPI, 1nm Range Rings, 10nm Diameter, Time 1805, March 30, 1983

they do not move as a function of time. Birds, as well as planes, cars, etc. can be identified on the photos by their movement. For example, the Figures 4.4 through 4.6 show bird activity approximately 1.5 nm east of the radar. The photos also show how much the return from the birds can fluctuate, complicating the detection and tracking problem for the operator.

The AN/TPN-18A was operational on 7 March 1983 and a BIRDWATCH warning system similar to that described in Section 3 was operational on 8 March 1983. By 11 March 1983, a preliminary assessment of the advisory's capabilities and limitations was completed and briefed to the 436 MAW Vice Wing Commander and the 436 MAW Chief of Safety. Figure 4.7 shows how the coverage of the AN/TPN-18A corresponds to the air corridors and typical bird traffic. Important points brought out in the assessment were the following:

- * Within 1 nm: The ability of the system to monitor birds is limited by the ground clutter returns from the grassy surface, trees, buildings and stationary aircraft. The system provides no warning capability for avoiding birds that fly up from the ground in front of approaching aircraft. While experiments showed that raising the antenna elevation angle will reduce the clutter from the runway to the point that sea gulls flying 20-50 feet above the runway can be seen on the PPI display, this antenna position does not allow good observation of the geese approaching the takeoff and landing corridors. An antenna tilt of 2-3 degrees was chosen as a compromise to provide good detection of the geese flying off the end of runway 010/190. This angle also reduced the backscatter from the runway to the point that

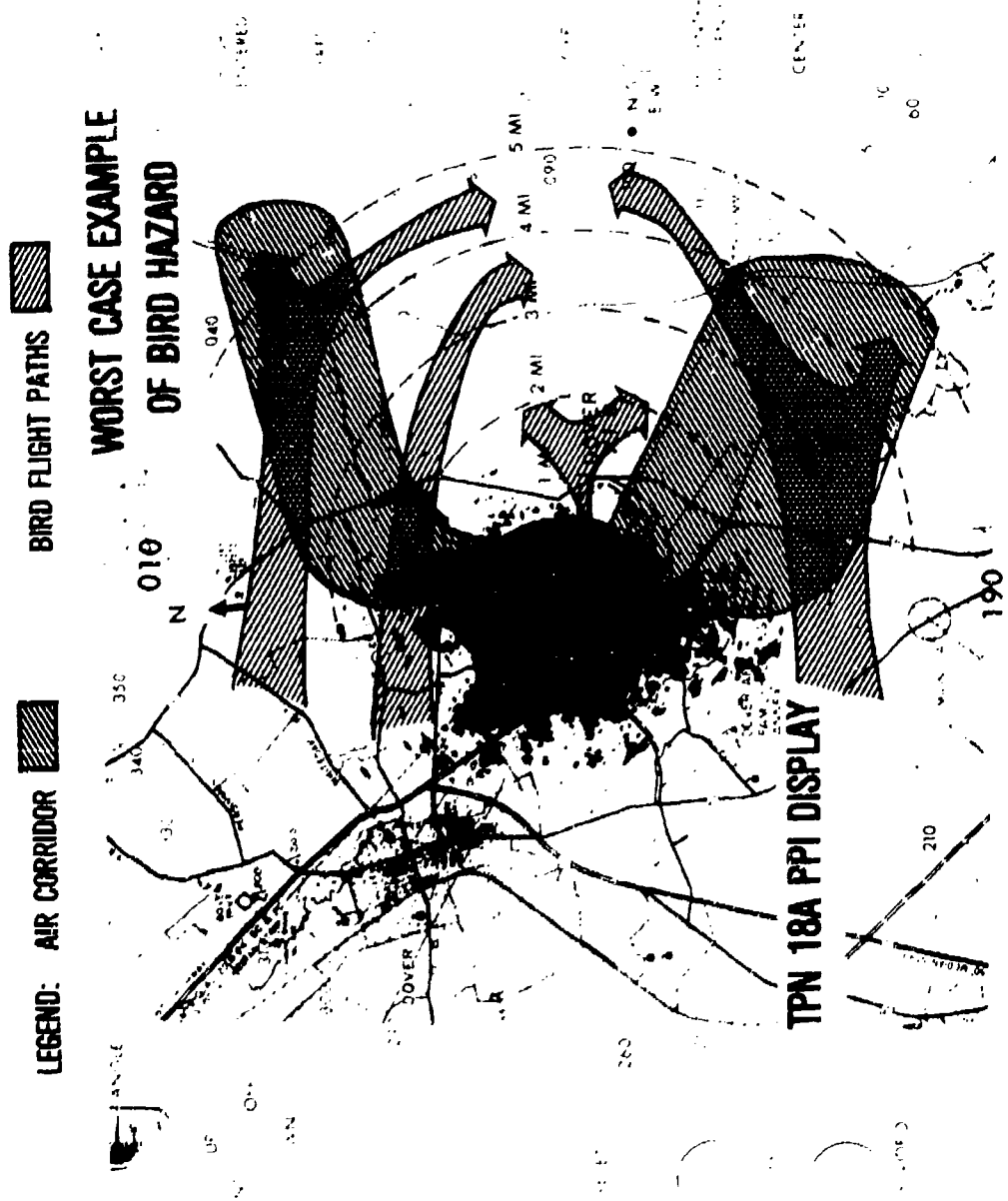


Figure 4.7 Clutter-Limited Coverage of AN/TPN-18A Radar vs. Bird Traffic Thru Air Corridor (Air Corridor From Reference [7])

the operator could clearly define the takeoff and landing corridors and track a large plane rolling down the runway.

* 1 to 2 nm: Due to screening, clutter returns were from structures above the surface i.e., tree lines, buildings, telephone and power line poles, etc. From the northwest thru the north, and east to the southeast, clutter returns were sparsely distributed allowing a trained operator to reliably monitor bird activity. From the northwest thru west to the southeast, clutter returns from the buildings and other structures prevented any reliable coverage. The antenna elevation angles between 2 and 3 degrees represented a compromise between ground clutter-limited close-in coverage (within 1.5 nm) and good detection of low-flying birds beyond 2 nm. For the main runway 010/190, the AN/TPN-18A provided fair-to-good coverage of the landing corridor to the north. The major blind spot is for low-flying birds coming from the west or southwest and flying directly over the runway.

* Beyond 2 nm: Close-in buildings and tree lines screened the surface of the ground and most of the structures beyond 2 nm. This provided large areas with no interfering clutter and allowed good to excellent coverage for birds flying above 300 feet from the northwest thru the north to the southwest and poor to excellent coverage over the remaining azimuths. Again, due to the height of some of the hangars, the radar was essentially blind at certain western azimuths for low-flying bird hazards. Other details are given in Appendix D.

4.4 Analysis of Potential Interim Sensors

During July 1983, tests were performed on the AN/GPN-21 (Figure 4.8) to determine its capabilities and limitations for performing the

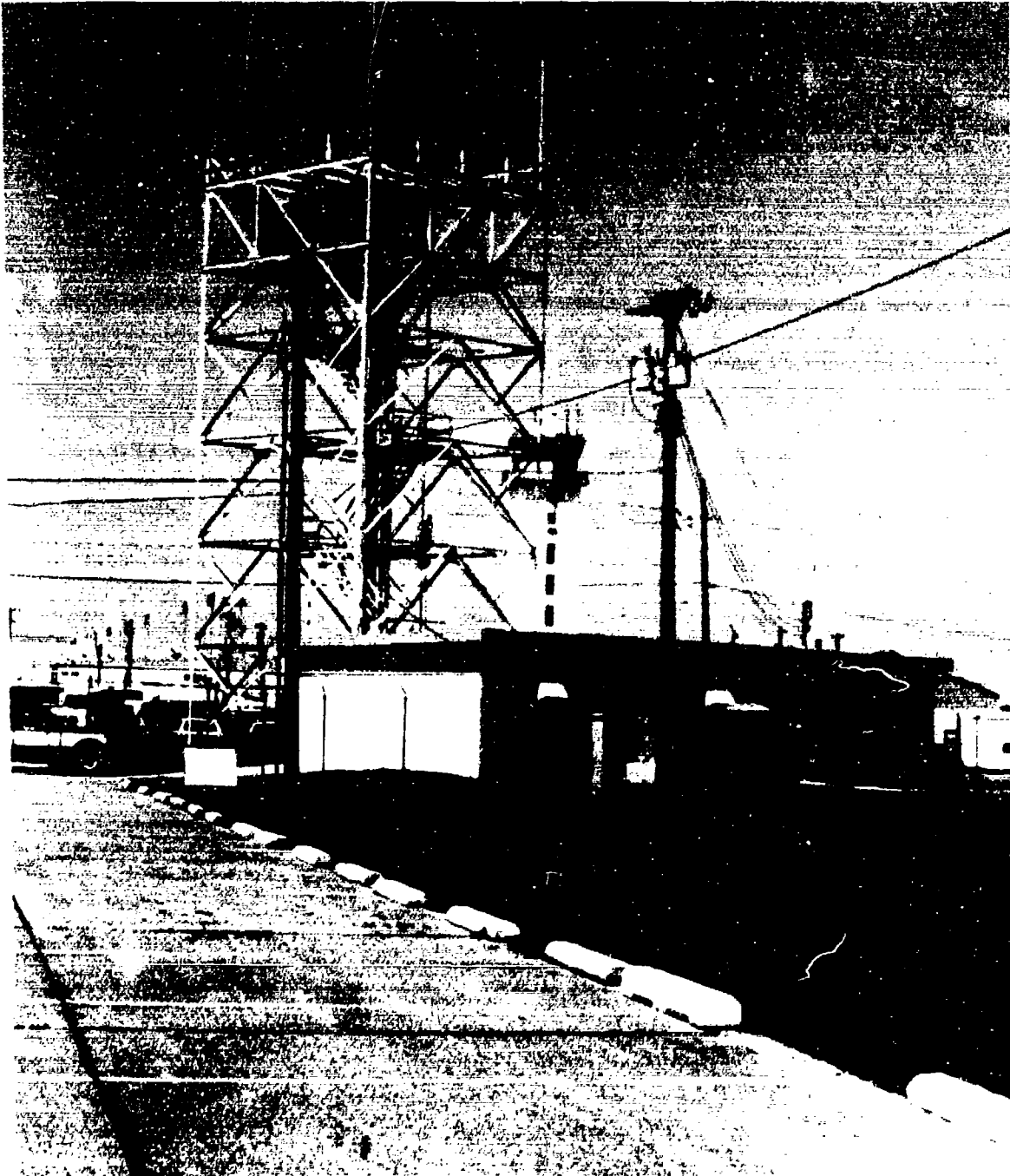


Figure 4.8 Photograph Of The AN/GPN-21 Radar's Antenna
On 66 Foot Tower

BIRDWATCH function. Parameters measured or documented included the subclutter visibility (SCV), the sensitivity time control (STC) waveforms, the use of the passive antenna beam, the electrical tilt of the main antenna beam and the use of range-azimuth gating (RAG) of additional attenuation to inhibit clutter breakthru. One of the problems encountered, however, was the lack of bird-like test targets to test the capability of the MTI and demonstrate the effects of screening and multipath in the local environment.

Using theoretical estimates for clutter amplitudes typical of the Dover environment, it was estimated that the radar had to have a subclutter visibility (SCV) factor, as defined by the measurement instructions given in the Technical Order 31P5-2GPN21-2, of at least 30 dB to adequately detect a -20 dBsm bird flying off the end of runway 01. Unfortunately, the measured SCV of the GPN-21 system after calibration was only 22 dB, or 8 db short.

An attempt to detect a radio controlled model airplane at the end of the runway verified this shortcoming. Except for the electronics, control cables and the engine, the plane was fabricated of low backscattering balsa wood. The radar cross section of the small airplane was assumed to be dominated by the engine which was estimated to have an RCS of approximately -21 dBsm, roughly the RCS of a 4 lb bird. The aircraft was operated at the end of runway 010 approximately 1 nm from the AN/GPN-21. Since the radio controlled aircraft had to stay within visual range of the operator, the plane flew in a race track pattern of less than 1/4 mile. Unfortunately, the target could not be detected among the clutter residue and false alarms due to

noise. Since adequate detection performance of birds could not be adequately demonstrated at this time and the potential conflict with the AN/GPN-21's ATC function could not be satisfactorily resolved, alternative sensors were pursued to provide a BIRDWATCH operation in October 1983 and to allow one-on-one tests with the AN/GPN-21 later in the fall.

The backup candidates identified in Section 4.2 were the AN/TPN-18A, the AN/FPN-40, and their commercial variants. The AN/TPN-18A is a solid-state ARMY system that is currently replacing the older tube version AN/FPN-40 systems operating overseas. Furthermore, the available AN/TPN-18A systems are scheduled to be upgraded by providing an MTI capability. Since these systems were in demand, they were not available for a long term loan to the Air Force. The commercial variants would cost up to 2 million dollars per copy and could be obtained with some MTI capability. However, the systems would have no more capability in rain than the TPN-18A. Since the RADC team believed that the AN/GPN-21 would ultimately prove to be a far better system in a one-on-one test, these systems were not proposed.

However, the AN/FPN-40 systems being replaced by the AN/TPN-18A would be available from the ARMY for the cost of transporting the hardware to Dover AFB and could be logistically supported through a nearby ARMY depot for this fall and winter. With the addition of an inexpensive low-noise amplifier, the performance of the AN/FPN-40 would be identical to the AN/TPN-18A. Due to the low initial costs and availability of logistic support from the ARMY, installation of the AN/FPN-40 was initially proposed to HQ/MAC personnel in August 1983 to

provide a BIRDWATCH capability until one-on-one tests with the AN/GPN-21 could be performed. However, due to concern expressed by HQ/MAC and AFCC personnel on the reliability and maintainability of this older tube-type system, other alternatives were investigated.

Since the initial attempt to provide a bird hazard capability involved the use of a marine radar loaned by NRL, there remained significant interest in the possibility of using one or more marine radars for the interim sensor. The main advantages of these systems, shown in Figure 4.9 were their low acquisition costs and reputation for reliability. The main disadvantage was that their figure of merit given in Figure 4.2 and Table 4.2 predicted detection performances ranging from 10 to more than 23 dB below the required capability. However, for completeness, they were included as a alternative sensor with and without modifications that would improve their performance.

4.4.1 Free space detection range versus requirements

The free space detection range of a radar sensor can be calculated using another form of the range equation given in equation (4.2).

$$(4.2) \quad (S/N) = \frac{P_t \sigma A_e L_e L_a L_b L_i L_o L_t L_r L_{atm} L_{rain} F^4 (\theta, \phi, R)}{(4\pi)^4 R^4 K T_s \psi}$$

The term "free-space" means that propagation, multipath and clutter effects are not included in the calculation. In order to obtain a better estimate of performance than given by the FOM, assumptions have to be given for the losses that exist in each system. Table 4.1 gives the definitions of these losses and of the other parameters. Table 4.3 lists the calculated or assumed values for each parameter and presents

the calculation of the detection ranges at the center of the antenna beam for the AN/GPN-21, the AN/TPN-18A, two off-the-shelf marine radars, and a modified S-Band system using marine radar electronics.

The detection range for the AN/GPN-21 was close to the range estimated in Table 4.2 because the losses and antenna pattern were close to the values assumed in the FOM calculation. The range for the AN/TPN-18A was more than predicted in Table 4.2 because the loss values



Figure 4.9 Photograph of the Van-Mounted X-Band Marine Radar Tested at Dover AFB

were about 2 dB less and the 3.2 degree (-3 dB) elevation beamwidth of the antenna is smaller than the 4.5 degrees used in the FOM calculation. The lower energy short pulse mode would have a detection range of approximately 7 nm. Similarly, differences in the calculated detection ranges for the two off-the-shelf marine radars using the two equations are due primarily to the differences between the elevation beamwidth used in the FOM calculation and the marine radar's 20 to 22 degree elevation beamwidth.

Figure 4.10 compares the free-space coverage of the AN/TPN-18A and the Raytheon 125018X marine radar. Note that the free-space detection envelope of the AN/TPN-18A presented in Figure 4.10a provides a good match to the required elevation and range requirements using the lower energy short pulse (0.2 microsecond) mode, while the marine radar's free-space detection envelope in Figure 4.10b not only falls short in range but is poorly matched to the required elevation coverage.

The modifications to the S-Band marine radar improve the match to the elevation coverage requirements and double the detection range thru the use of a larger antenna aperture and the addition of a low noise amplifier. These modifications were chosen because the antenna is available from DOD warehouses and the modifications could be implemented relatively easily. Note that all calculations are "optimistic" by a couple of decibels due to uncertainties in the plumbing loss in each radar.

REQUIRED BIRDWATCH COVERAGE FOR LANDING

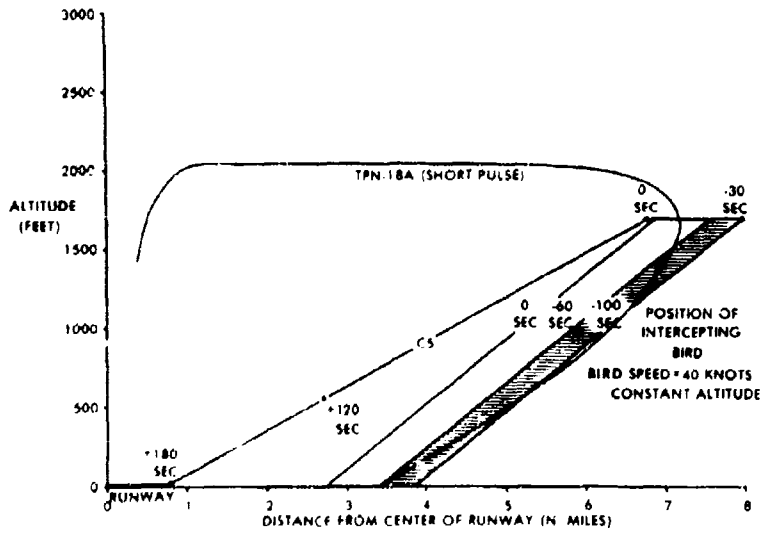


Figure 4.10a Detection Range Of The AN/TPN-18A Versus Coverage Requirements

REQUIRED BIRDWATCH COVERAGE FOR LANDING

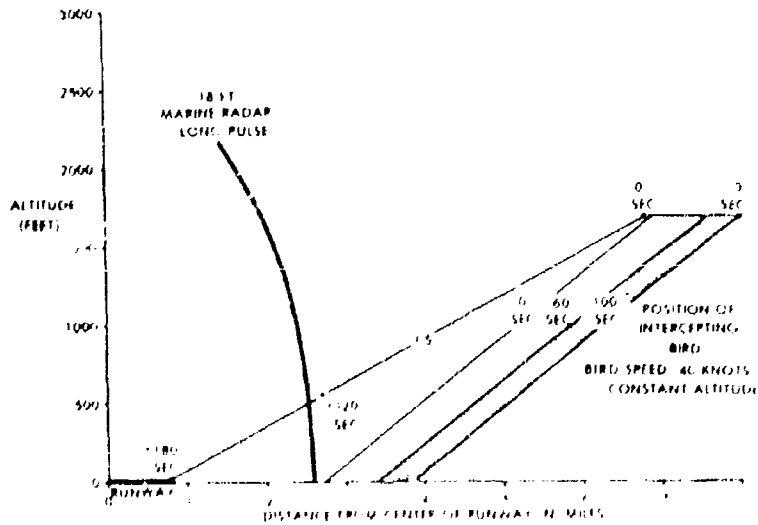


Figure 4.10b Detection Range Of The Raytheon 165018X Marine Radar Versus Coverage Requirements

PARAMETER (See table 4.1)	GPN-21 Single Channel		TPN-18A		Raytheon 125018X [21]		Raytheon 126012S [21]		Modified S-Band Marine Radar	
	value	dB	value	dB	value	dB	value	dB	value	dB
P ₀	400W	+26.0	168W	+22.2	40.5	+16.1	54	17.3	54	17.3
t ₀	3.75 sec	+5.7	3.75 sec	+5.7	3 sec	+4.8	1.82 sec	2.6	4 sec	6.0
D _A	--	-4.0	--	-1.6	--	-2.6	--	-2.0	--	-2.4
A ₀	1.8m ²	+2.5	.5m ²	-3.0	.2m ²	-7.0	.5m ²	-3.0	lm ²	0.0
A ₁	.01m ²	-20.0	.01m ²	-20.0	.01m ²	-20.0	.01m ²	-20.0	.01m ²	-20.0
L ₀	--	-0.6	--	-2.0	--	-3.0	--	-3.0	--	-3.0
L ₁	--	-2.8	--	-3.0	--	-2.0	--	-3.0	--	-5.0
L ₂	--	-1.6	--	-1.6	--	-1.6	--	-1.6	--	-1.6
L ₃	--	0*	--	0*	--	0*	--	0*	--	0*
L ₄	--	0*	--	0*	--	0*	--	0*	--	0*
L ₅	.89	-5	.91	-4	.98	-1	.98	-1	.96	-2
L ₆	N/A	N/A	N/A	N/A	--	-0.5	--	-0.6	--	-0.8
L ₇	.53	2.76	.39	4.1	2.2	-3.4	2.42	-3.8	1	0.0
	steradians		steradians		steradians		steradians		steradians	
K	12.56	-11.0	12.56	-11.0	12.56	-11.0	12.56	-11.0	12.56	-11.0
S/N	--	-17.7	59	-17.7	59	-17.7	59	-17.7	59	-17.7
K ₁	--	+228.6	--	+228.6	--	+228.6	--	+228.6	--	+228.6
K ₂	965 K	-29.	965 K	-29.8	2700	-34.3	2700	-34.3	965 K	-29.8
F ₀ (diam)	--	+177.6	--	+170.5	--	+146.3	--	+148.4	--	+160.4
Sample (Hz)	--	27.5	--	18.3	--	4.5	--	5.1	--	10.2
Range (nm)	--	14.9	--	9.9	--	2.5	--	2.8	--	5.5

* It was assumed from the literature whether the transmitter powers, antenna gains, and receiver noise temperatures included plumbing losses. Therefore, an "optimistic" value of 0 dB was assumed.

$$R^4 = \frac{P_t t_s A_e c t L_a L_b L_j L_c L_d L_e L_{ant} L_{log}}{4\pi (S/N) K T_s}$$

TABLE 4.3 PARAMETERS AND DETECTION PERFORMANCE OF GPN-21, TPN-18A, AND RAYTHEON MARINE RADAR

4.4.2 Detection limitations due to ground clutter

Figure 4.11 presents the ground clutter map of the AN/GPN-21. Except for the coast line to the east, the ground clutter extends for approximately 5 nm, requiring the use of a Doppler processing technique to obtain detection of birds and small aircraft. The AN/GPN-21 uses a Moving Target Indicator (MTI) system which allows the selection of various 2-pulse or 3-pulse canceller configurations to attenuate the stationary ground clutter. The capability of an MTI radar to reduce the large clutter background and still provide a sufficient signal-to-(clutter-plus-noise) ratio to detect a small moving target is sometimes called the "subclutter visibility" (SCV) of the radar. In the measurements defined in the AN/GPN-21 manuals, the SCV is equal to the improvement in noise-to-clutter ratio obtained by the MTI filter in decibels minus the single pulse signal-to-(clutter-plus-noise) ratio in decibels required to achieve a 50% probability of detection of the signal on an A-scope. For an MTI filter, the average power gain of the processor is equal to the power gain of a target signal averaged over all velocity. Therefore, the noise-to-clutter improvement for an MTI is equal to the "improvement factor", a standard term for the improvement in signal-to-clutter ratio. The measured SCV of the AN/GPN-21 in the 3-pulse MTI canceller configuration was approximately 22 dB, inferring an improvement factor of approximately 35 dB. The primary limitations on the AN/GPN-21's improvement factor is the frequency instability of the motion transmitter and scanning modulation.

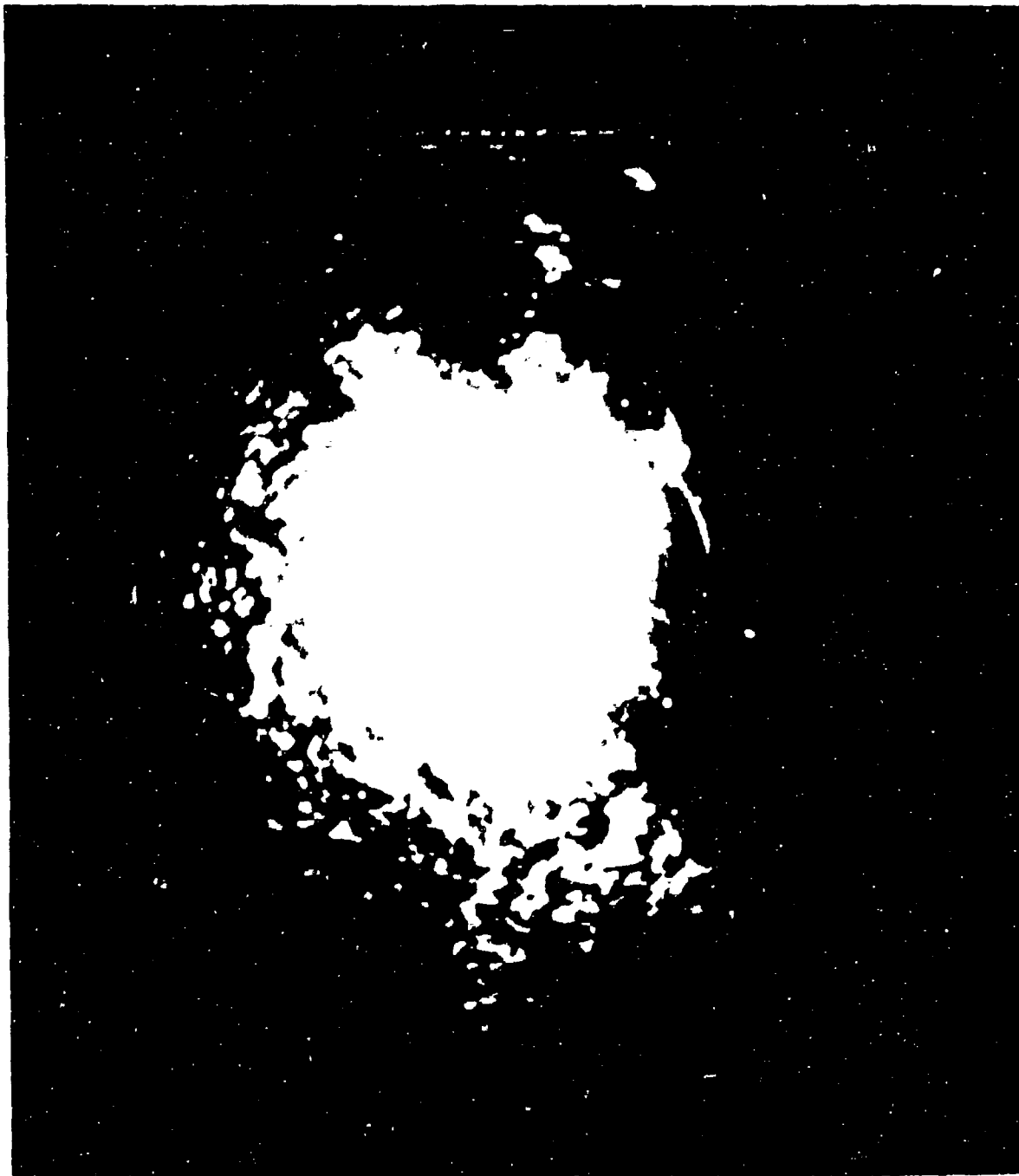


Figure 4.11 AN/GPH-21 Radar PPI, 2nm Range Rings, 30nm Diameter, Ground Clutter

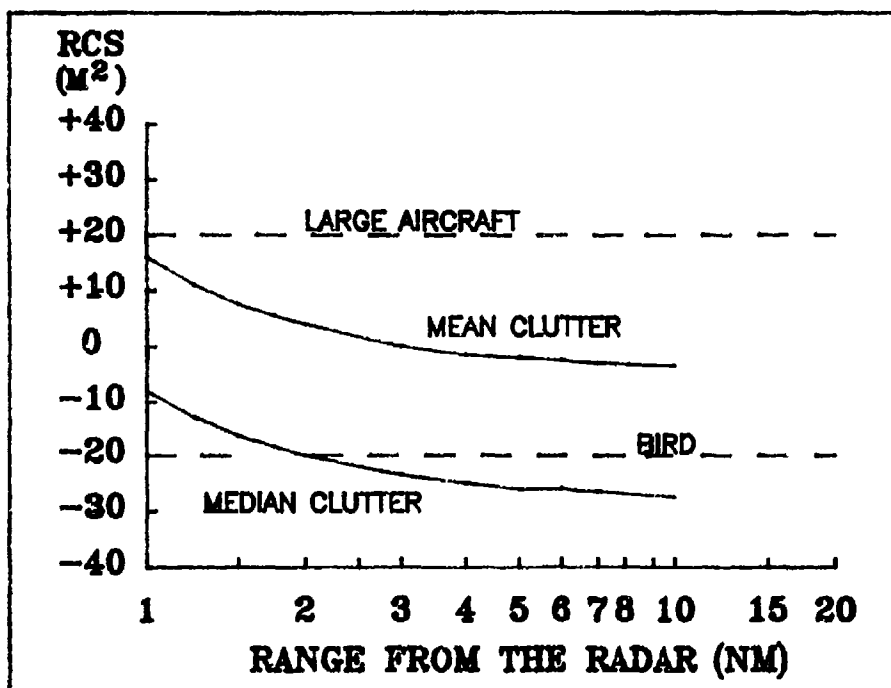


Figure 4.12 Theoretical Calculations of Power Returns From Ground Clutter, Aircraft, and Birds as a Function of Range

Figures 4.12 thru 4.14 illustrate the limitations of the AN/GPN-21 MTI capability. Figure 4.12 plots a theoretical mean (10 percentile) and median (50 percentile) clutter levels typical of the Dover environment versus the backscatter of a bird and a large aircraft. If a signal/(clutter+noise) ($S/(C+N)$) ratio equal to 17.7 dB is needed to provide adequate performance, little attenuation of the clutter is

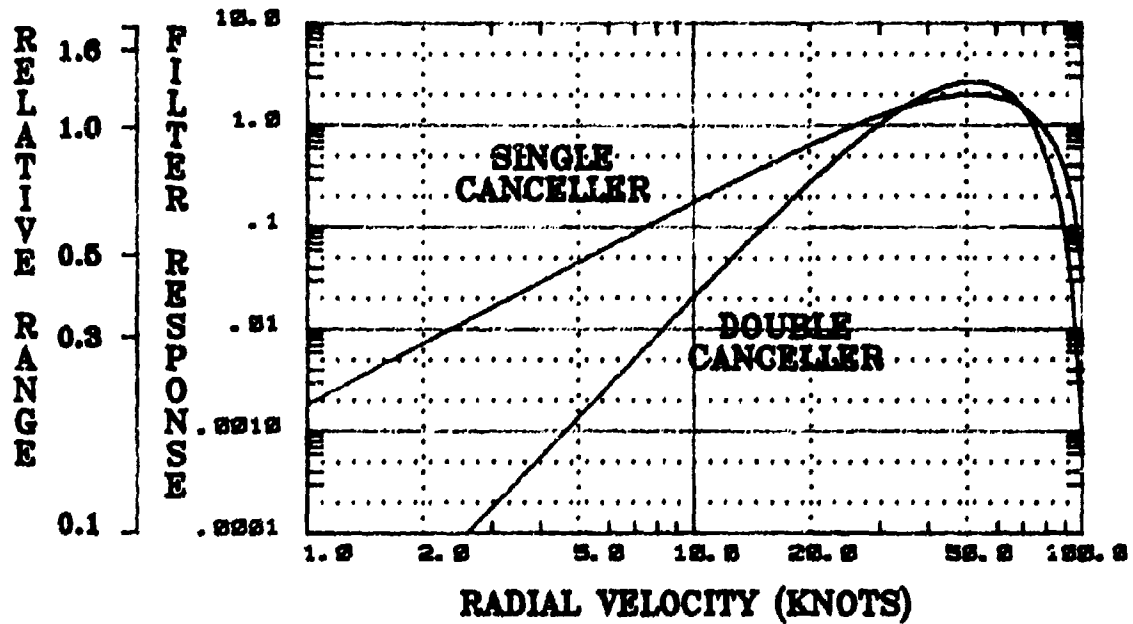


Figure 4.13a Attenuation of Bird Returns By MTI Filter

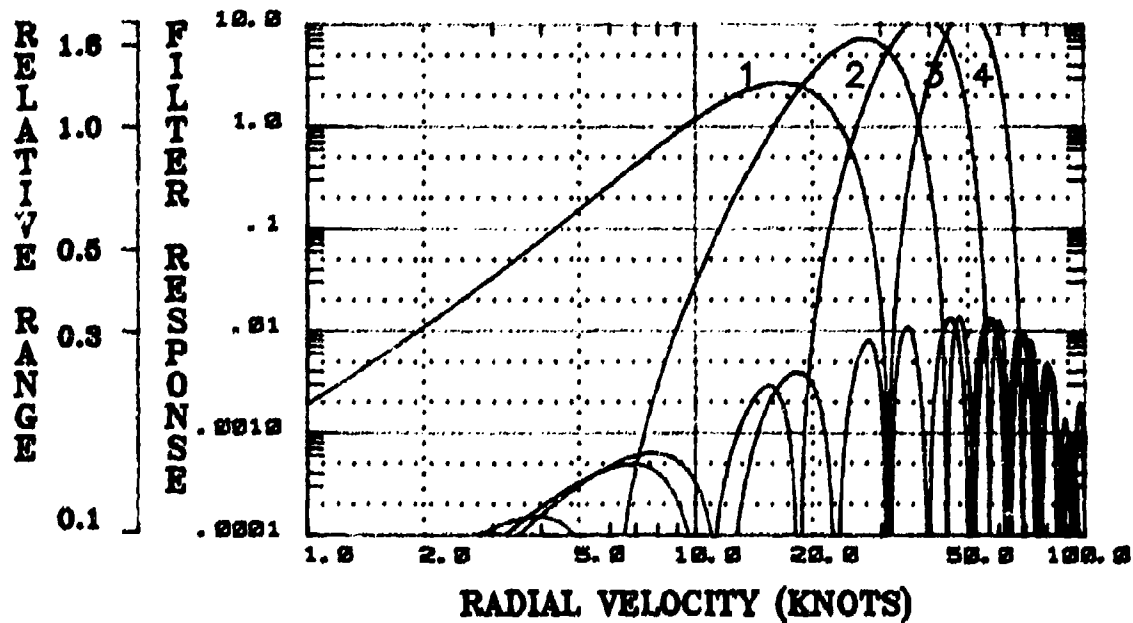


Figure 4.13b Attenuation of Bird Returns by a 8-pulse Discrete Fourier Transform

required to detect the aircraft at 1 nm. However, at the same range, the improvement factors required to provide adequate detection performance are 30 dB in the median clutter and over 50 dB in the mean clutter. At 3 nm, the required improvement factor drops to about 15 dB and 35 dB, respectively, which is within the range of the AN/GPN-21 capabilities.

However, the improvement factor describes a capability in clutter that is averaged over all possible velocities. Since the MTI is a filter, the AN/GPN-21's capability to detect a given target at a given instant depends on the radial velocity of the target, i.e. the velocity component toward or away from the radar. Figure 4.13a presents the filter responses of the two and three pulse cancellers implemented in the AN/GPN-21. The responses are normalized to the canceller gain averaged over all velocities (also known as the noise gain of the filter). Therefore, the 0 dB point on the ordinate corresponds to the improvement factor previously given and also to the detection range given in Table 4.3. Targets with radial velocities that provide integration gain can be detected at a longer distance; targets with radial velocities that provide a loss with respect to noise must be closer to be detected with a P_d of 0.8. For example, the AN/GPN-21 at Dover AFB uses a double (3-pulse) canceller. For a bird travelling toward or away from the radar at 30 knots, the filter response is approximately 1 and the estimated detection range is the 15 nm given in Table 4.3. However, for a bird travelling at 10 knots toward or away from the radar, the filter response is (.02). This corresponds to a relative detection range of (.376) and a estimated detection range of

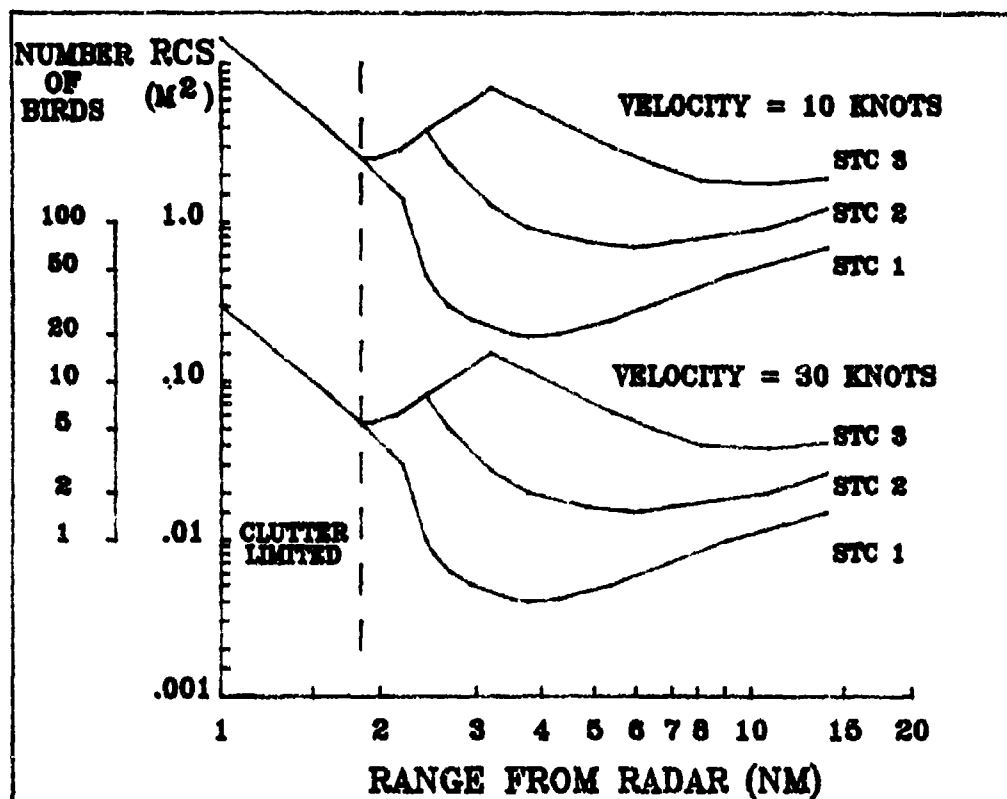


Figure 4.14 Detection Performance of AN/GPN-21 as a Function of Bird Radial Velocity and STC

(.376) x 15 nm = 5.6 nm. Finally, birds that have little or no radial velocity component will have such a low filter response that they will not be detectable at any range containing clutter.

Figure 4.13b shows a similar plot for a pulse Doppler filter as used in the AN/GPN-25. With this system, an excellent improvement

factor is combined with the integration gain of the filters to provide excellent detection of the bird activity at radial velocities as low as 4 knots.

Another parameter of the AN/GPN-21 that can severely impact detection of birds is the sensitivity time control (STC) attenuation. The STC changes the receiver gain as a function of range to prevent large returns from clutter or large aircraft from overloading the receiver. Figure 4.14 illustrates the combined effects of STC and the MTI processing on the detection performance of the AN/GPN-21 (single channel) as a function of range. Assumptions include an MTI improvement factor of 35 dB, the use of the main beam rather than the passive beam, linear polarization, and the mean clutter values given in Figure 4.12. The curves are plotted for a probability of detection of 0.8 and include the three STC waveforms implemented at Dover AFB during July 1983. No digital video integration or enhancement mode is assumed.

Within 2 nm of the radar, the poor SCV performance of the radar allows adequate detection of flocks consisting of 10 or more birds and then only if they have a radial velocity equal or exceeding 30 knots. Beyond 2 nm, the sensitivity of the radar at each radial velocity is determined by the choice of STC waveform used. Since the STC waveform is chosen primarily to satisfy the requirements of the ATC function under existing weather conditions, a simultaneous BIRDWATCH capability using the AN/GPN-21 can be severely compromised.

The limitations of the AN/TPN-18A system due to ground clutter were described in section 4.3. Since the system lacks an MTI or any

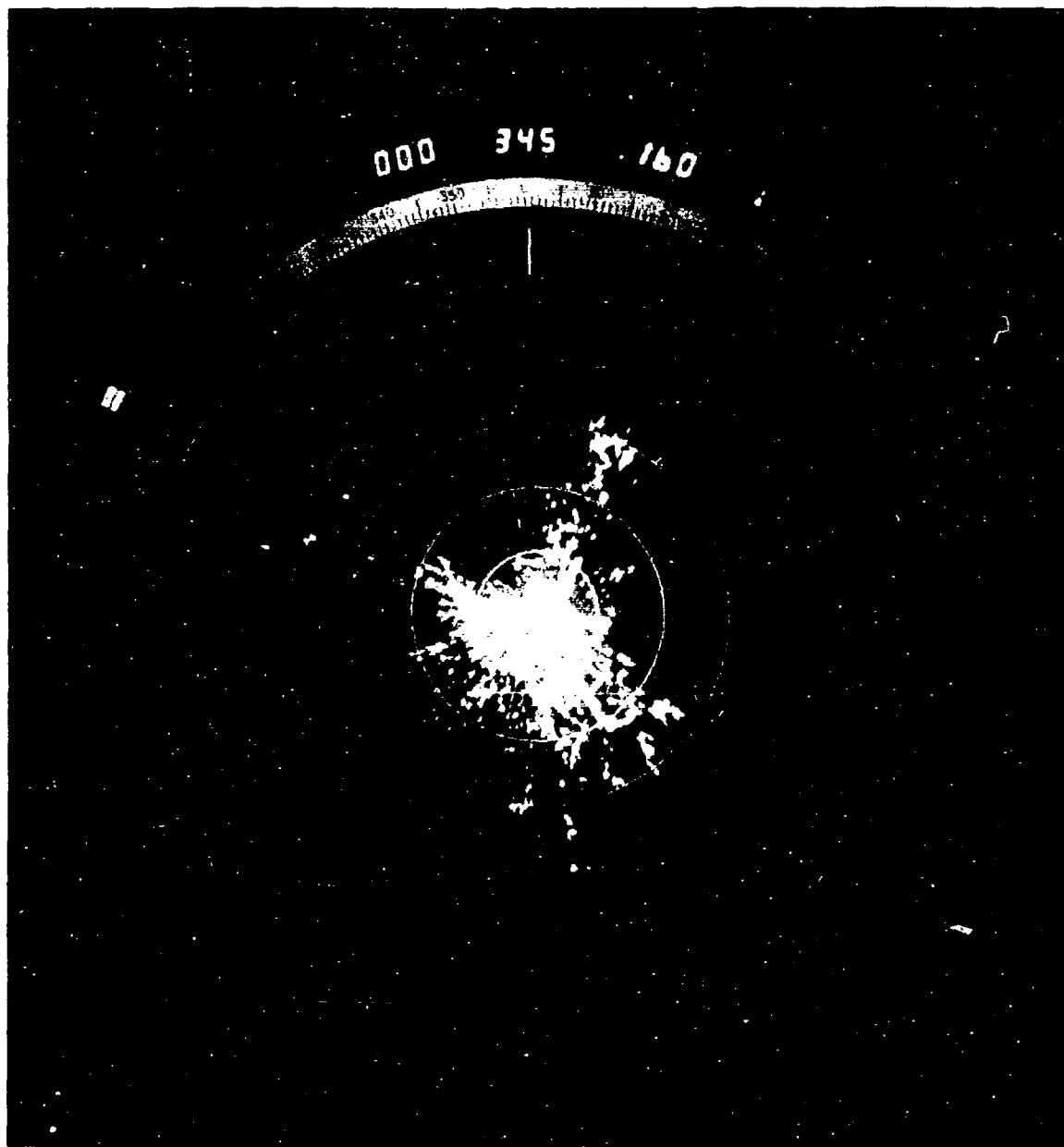


Figure 4.15 Raytheon 162512X Marine Radar PPI Display
Of Ground Clutter, 1nm Range Rings, 12nm
Diameter, Time 1138, October 25, 1983

other capability for detecting weak moving targets over stronger stationary scatterers, it derives its ability to provide some degree of performance thru the use of screening (see Section 4.4.4) and a small resolution cell.

Figure 4.15 presents the ground clutter displayed on the PPI of a 162512X X-Band marine radar while it was at Dover AFB during the last week of October 1983. Like the AN/TPN-18A, this system lacks an MTI and cannot detect small targets in stronger clutter. However, due to the higher resolution of the system, the clutter from the runways, fields and the earth's surface is reduced, allowing better detection of the planes on the base.

4.4.3 Detection limitations due to weather clutter

Weather clutter can inhibit the detection of a target in two ways. First, as the radar energy passes through a rain storm, the raindrops attenuate the energy passing on to the target thru scattering and absorption, reducing the power received from the target. Second, a portion of the scattered energy is received by the radar receiver, masking the reflected energy of the target. The equations used to estimate the attenuation and reflectivity of a volume of rain are given in Table 4.4. For short ranges within 10 nm, the attenuation of rain is negligible. Therefore, the signal-to-(clutter + noise) ratio in rain can be given by equation (4.3) where σ_c is the radar cross section of the rain clutter and Z is a function of the radar parameters given in Table 4.3. (See Appendix F)

$$(4.3) \quad S/(C+N) = (S/N) \cdot (N/(C+N)) = \frac{S \sigma L_0}{S \sigma_c + R^4}$$

Rainfall Rate -
Volume Reflectivity
Relationship (m^2/m^3)

$$N_V = 6.12 \times 10^{-14} r^{1.6}/\lambda^4$$

Attenuation Factor
(dB/m, one way)

$$k = .00013 (f)^{2.36} r$$

where

r = rainfall rate, millimeters/hour
 λ = wavelength, meters
 f = frequency, gigahertz

TABLE 4.4 WEATHER BACKSCATTER AND ATTENUATION RELATIONSHIPS

As the rain fall rates increase, the weather clutter becomes stronger and the range at which the required $S/(C+N)$ is obtained or exceeded decreases. Circular polarization reduces the backscatter from weather by up to 20 dB but also reduces the backscatter from birds as well. Table 4.5 shows how the detection range is degraded for four candidate radars. For the X-Band systems, any rain of a drizzle or more presents a severe degradation of the system performance even with the use of circular polarization, making the system useless for detecting birds in the midst of the rain. The S-Band systems, on the other hand, maintain useful detection ranges through light-to-moderate rainfall rates. Since waterfowl do not fly in rainrates above 4 mm/hr very often or for any significant distance, the S-Band systems provide essentially an all-weather bird hazard detection capability within the limits of their detection range.

4.4.4 Detection limitations due to screening

The coverages given in Section 4.4.1 assume a free space environment, i.e. no blockage of the radar beam by trees, buildings, or other structures and no nulls or extended ranges due to multipath. In the Dover AFB environment, the measured coverage of each radar will differ from the predicted free space coverages previously given due in part to diffraction, refraction, multipath, and screening. These functions are often lumped into a propagation pattern term $F(R, \theta, \phi)$ which is a complex time-varying function of range, azimuth, and elevation. At short ranges, $F(R, \theta, \phi)$ is dominated by multipath and screening effects of the local environment. While the measurement of multipath and attenuation factors at all angles, elevations and ranges were beyond the scope of this effort, their qualitative effects can be described through the following examples.

Figure 4.16 shows the effects of 0.5 degree screening on the coverage of the AN/TPN-18A system. The dashed line shows the free space coverage given earlier in Figure 4.10a; the solid curves shows the detection range assuming a knife-edge diffraction over 50 foot trees located 1 nm from the radar. While coverage of the glide slope and altitudes above 1,000 feet are not severely effected, the system can not meet the required detection coverage for a single 4 lb bird at the lower altitudes using the lower energy short pulse mode. Use of the higher energy mode allows the system to extend its coverage down to altitudes of 400-500 feet.

In Section 4.3, it was noted that the AN/TPN-18A system was blind to low flying birds approaching from the west. Figure 4.17

REQUIRED BIRDWATCH COVERAGE FOR LANDING

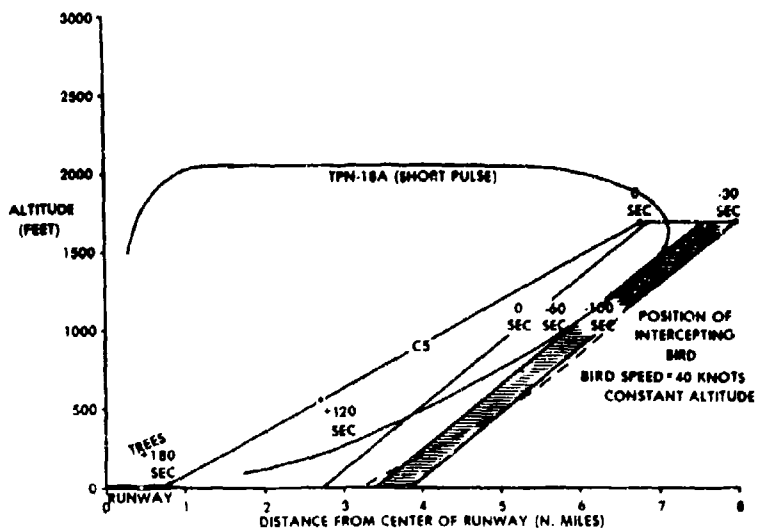


Figure 4.16 Degradation Of AN/TPN-18A Detection Range Due To 0.5 Degree Screening

REQUIRED BIRDWATCH COVERAGE FOR LANDING

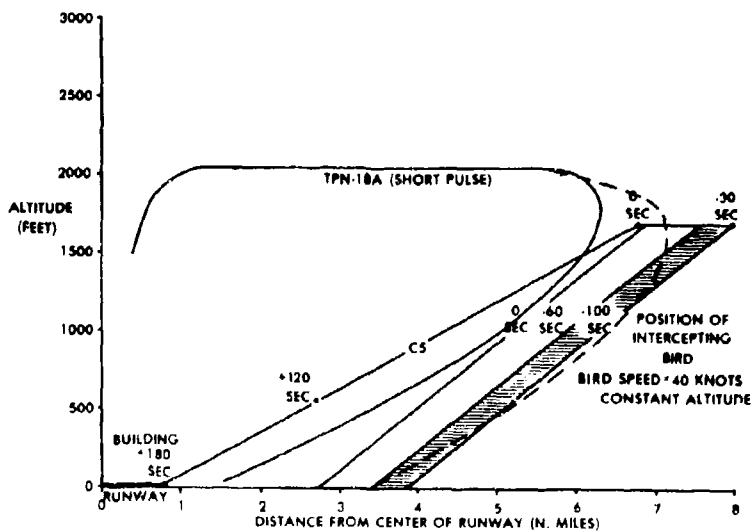


Figure 4.17 Degradation Of AN/TPN-18A Detection Range Due To 1.25 Degree Screening

demonstrates how the coverage of the system was degraded from screening by the tall hangars approximately one mile away. At 500 feet, the 4 lb bird threat could be reliably detected at ranges less than 3.5 nm, 1.5 nm short of the 5 nm requirement. It should be noted that the use of knife-edge diffraction to estimate the range reduction by screening is optimistic; actual performance could be as much as 30 dB worst.

While screening does degrade some aspects of a radar's performance, it also provides some advantages. For instance, for radars without MTI or other doppler processing capabilities, screening reduces the clutter from behind the screening structures, providing a cleaner display to the operator and better detection of the higher-flying birds. Also, since much of the low-flying bird traffic outside of the landing and takeoff corridors is not a hazard to any aircraft, the screening of such traffic reduces the load on the operator and reduces the number of false hazards that may otherwise be reported to circling planes. Since the AN/GPN-21 is mounted on a 66-foot tower and incurs little blockage by the local buildings and structures, its performance is not effected by screening. Appendix B discusses the advantages and disadvantages of screening as well as the results of some experiments performed by RADC using a manmade "clutter fence" during March-April 1983.

4.4.5 Detection limitations due to multipath

When a transmitted ray is reflected from the surface of the ground and is superimposed linearly on the ray propagating toward the target, the two rays may add to provide more energy in the direction of the

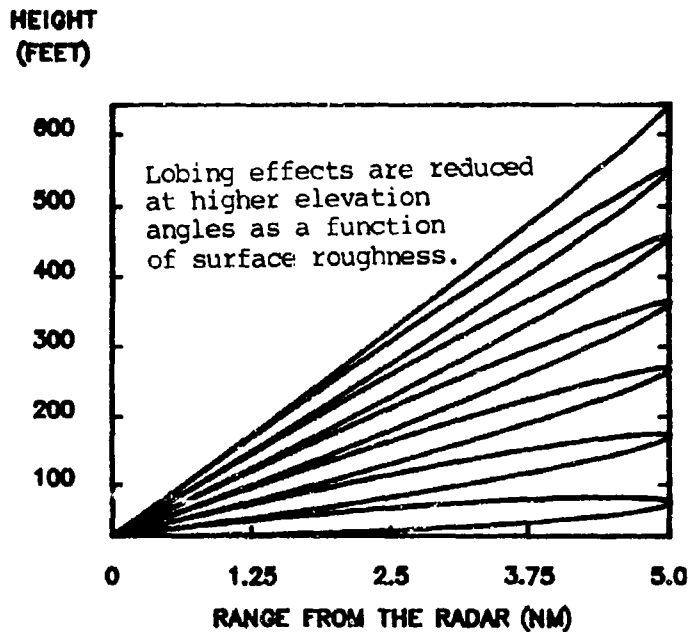


Figure 4.18 Effects of Multipath on Coverage of Raytheon 165018X Marine Radar

target (lobes) or subtract to provide less energy (nulls). Figure 4.18 demonstrates how this phenomenon effects the estimated coverage of the marine radar. At angles where the rays add, the detection range of the system can double; where the rays subtract, the detection range can be reduced to essentially zero. The figure shows how this effect could prevent the operator from obtaining a good track on an in-bound bird. At the long range, the operator may detect the bird for a few scans but will lose it as the bird approaches. During the next few scans, the operator will not know whether the bird has landed, changed direction or speed, and consequently, could give no warning of the hazard.

The AN/TPN-18A and the AN/GPN-21 are also similarly effected by multipath but to different degrees. The coverage of the AN/GPN-21 is effected less than the others due primarily to its height. First, the antenna is many wavelengths above the ground making the spacing between the multipath lobes smaller in angle. Since the nulls are narrower, the chance that a flock of birds will remain in those nulls for a significant length of time is smaller. The second advantage of height is also important. For an AN/TPN-18A or a marine radar, each with an antenna approximately 13 feet high, the reflecting multipath surface will be within a few hundred feet of the radar. Since the radar is in the middle of a relatively smooth airfield, the multipath ray will be very strong creating a lobing pattern with deep nulls. Lobing can be reduced by growing tall (12 inch) grass as proposed by Clark, et al, [1] to deter the gulls and blackbirds from feeding or resting in the fields surrounding the runway. However, the flat runways and taxiways would still cause significant lobing. Lobing can also be reduced by a low "clutter fence" around the radar to attenuate the energy incident on the ground, but only at the expense of reduced detection capability for low flying birds. (See Appendix B)

For the higher AN/GPN-21 antenna, the reflecting multipath surface for angles near the horizon is several thousand feet away and often in or near an area with trees, buildings, and other complex structures which do not reflect the strong specular ray necessary to create strong lobing patterns.

4.5 One-on-One Performance Tests

In the briefings to AFSC and HQ MAC personnel [20,21], it was recommended that one-on-one performance tests be performed between the AN/GPN-21, AN/TPN-18A, and a marine radar, if one is made available, to identify the best sensor for use in the interim BIRDWATCH system. The ARMY TPN-18A and crew were obtained to provide the BIRDWATCH function from 1 October, 1983 to mid-November when the tests were to be completed. Two tests were performed by an RADC/MAC team between 25 October 1983 and 4 November 1983. The first test compared the AN/GPN-21 and the AN/TPN-18A with the Raytheon 162512X marine radar and took place on 25 and 26 October 1983. For the second test, HQ MAC interfaced an AN/MPN-13 antenna with the transmit/receiver electronics from a 60kw S-Band marine radar in order to demonstrate the capabilities of a modified marine radar. This system was tested versus the AN/GPN-21 and the AN/TPN-18A on 2 and 3 November 1983. In order to document their relative capabilities simultaneous time-lapse photography of the best PPI presentation of each system was taken.

Figures 4.19-4.29 document the bird activity as displayed on the PPI (MTI channel) of the AN/GPN-21 on 25 October 1983. The range rings are spaced 2 nm apart with every other range ring enhanced. The maximum displayed range from the radar is 12 nm. The photos were taken in 5 minute intervals between 1720 and 1815 (except for a missing one at 1745). Most of the detections to the north, west and south is bird activity. Three notable activities are the lines of birds that form to the west and south during this sequence. The first line visible in Figure 4.19 is located almost due west between 7 and 8 nm from the

radar. Figure 4.20 clearly shows the second line at azimuth 190 extending from approximately 2.5 nm to 6 nm. By Figure 4.21, this second ring is landing at a location approximately 6.5 nm and bearing 190 degrees. At this time, a third line is forming between 4.5, 225 degrees, and 6 nm, 205 degrees. Figures 4.22-4.29 show the first and third lines merging and coming within a mile of the base before landing at the same location as the second flock approximately 6.5 nm south of the base.

Figures 4.30a, 4.30b, and 4.30c present the bird activity detected by the AN/GPN-21, the AN/TPN-18A, and the marine radar within 2 seconds of each other. This sequence was selected because the extent of the line from approximately 2 nm to 6 nm clearly demonstrates the relative capabilities of the three sensors. On the AN/GPN-21 display (Figure 4.30a), the birds show up as very bright targets out to 6 nm. A strong return is also received from the birds located 3 nm to within 2 nm northwest of the radar. Figure 4.30b presents the 10 nm PPI display of the AN/TPN-18A. The range rings are spaced 1 nm apart with an enhanced ring at 5 nm. While weaker, the system does detect the flock between 3 and 7 nm of the radar. (The AN/TPN-18A is located approximately .5 nm north of the AN/GPN-21, accounting for the range difference.) Within three miles, the flock is masked by ground clutter although the flock to the northwest between 2.5 and 2 nm can just be made out. In the display of the X-Band marine radar (Figure 4.30c), the flocks are not obvious. A faint line can be seen just within 2 nm to the west-northwest and some of the detections out to three nm to south may be portions of the same flock, but a long clear line of birds is not

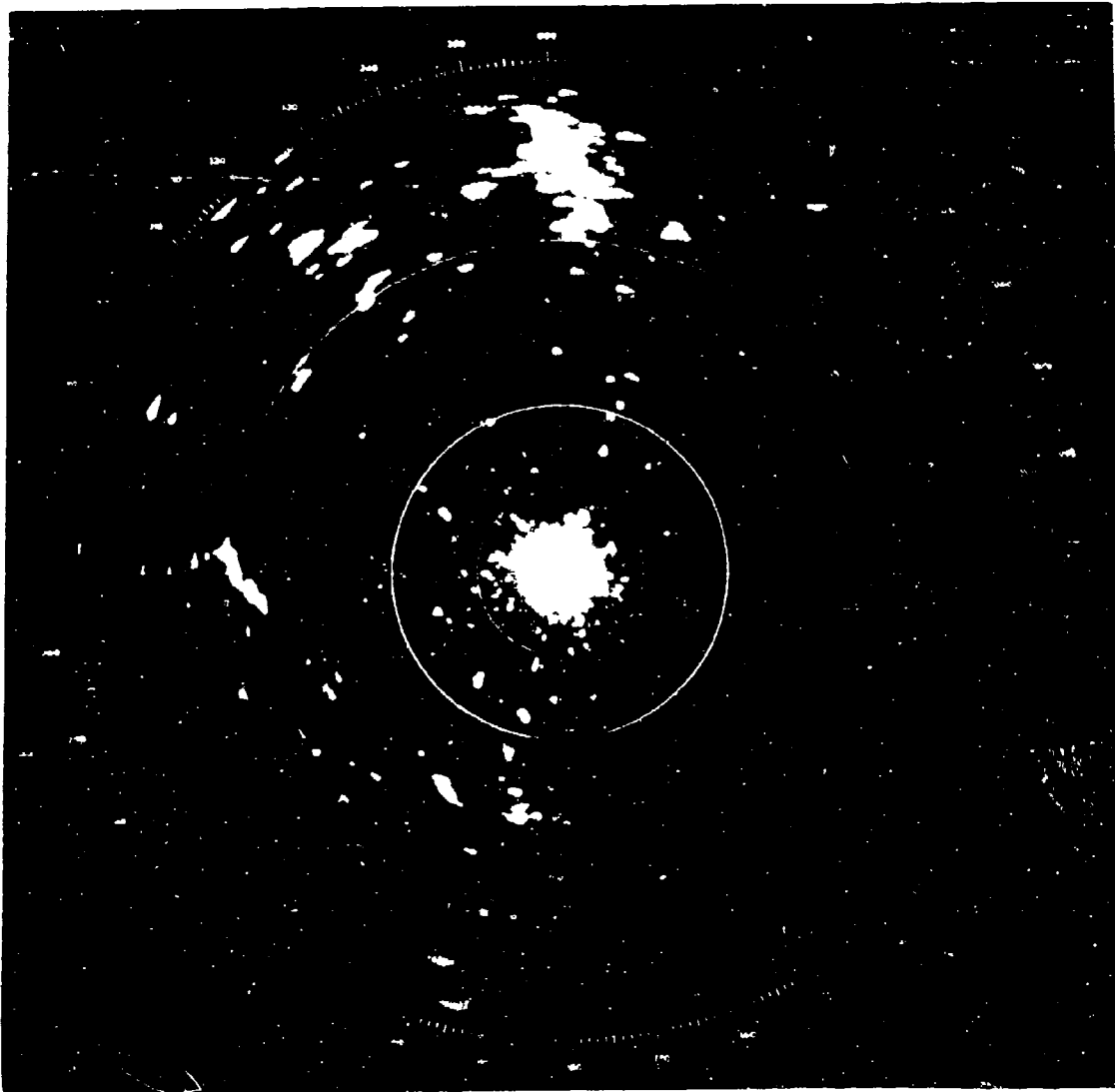


Figure 4.19 Time 1720, 2nm Range Rings, 24nm Total
Diameter AN/GPN-21 Radar, October 25, 1983

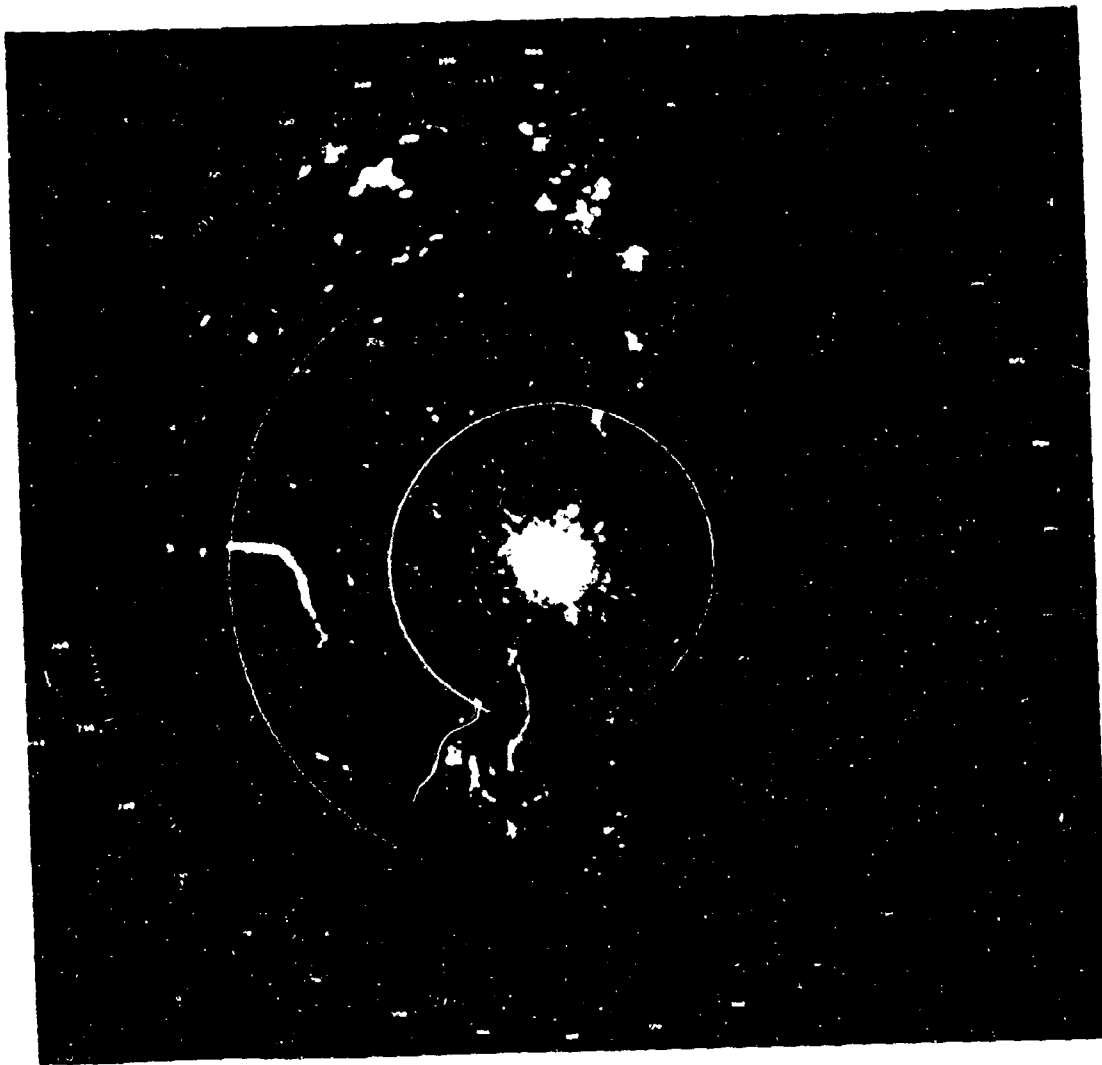


Figure 4.20 Time 1725, 2nm Range Rings, 24nm Total
Diameter AN/GPN-21 Radar, October 25, 1983

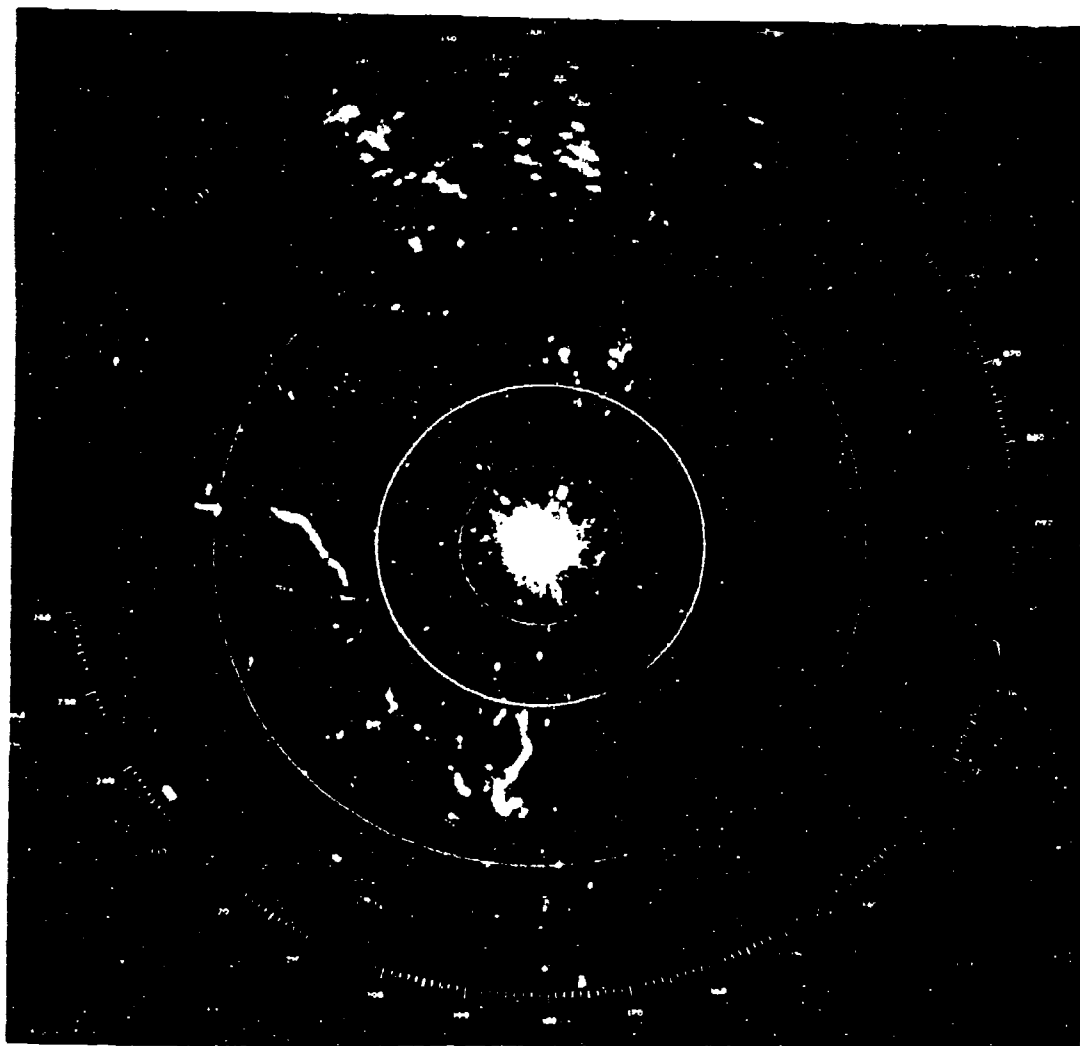


Figure 4.21 Time 1730, 2nm Range Rings, 24nm Total
Diameter AN/GPN-21 Radar, October 25, 1983

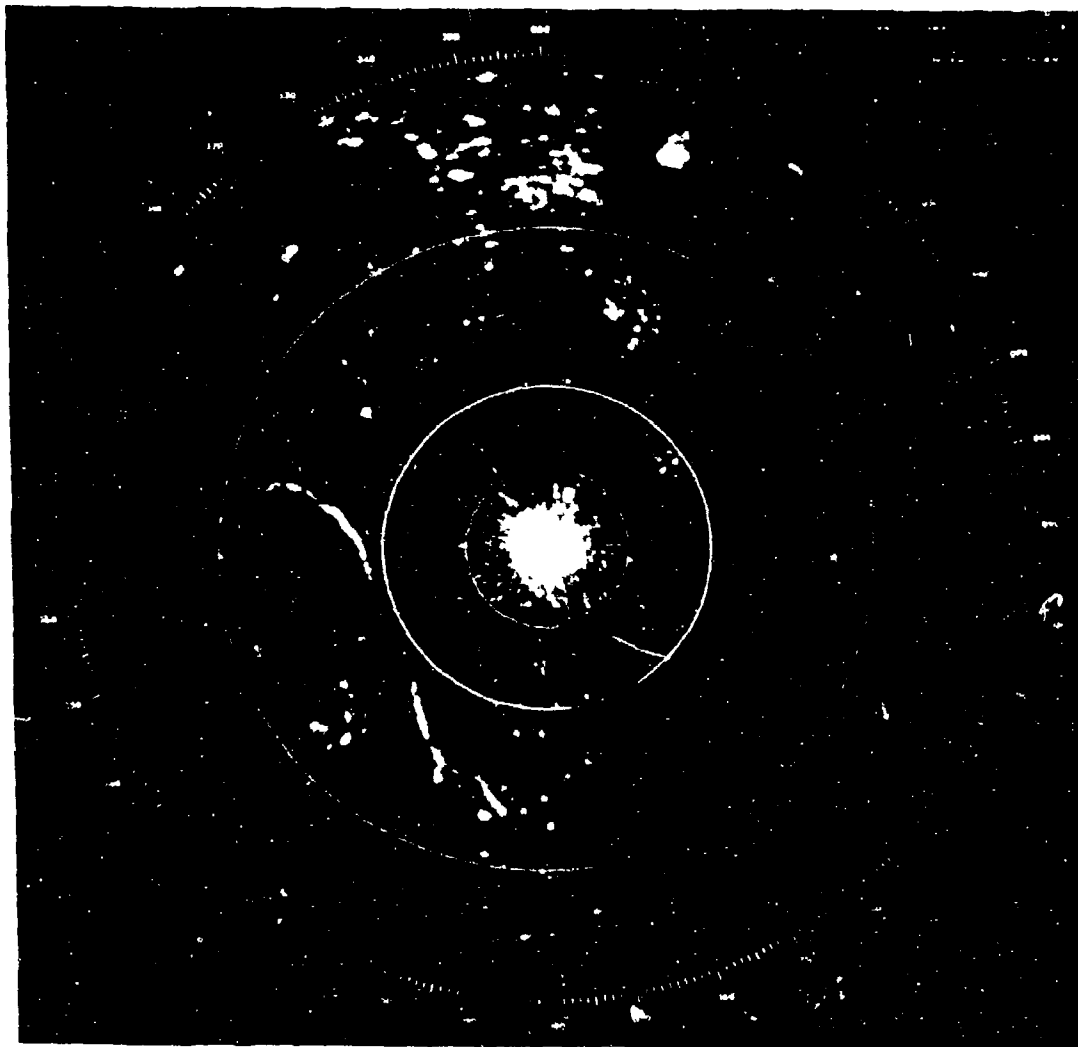


Figure 4.22 Time 1735, 2nm Range Rings, 24nm Total
Diameter AN/GPN-21 Radar, October 25, 1983

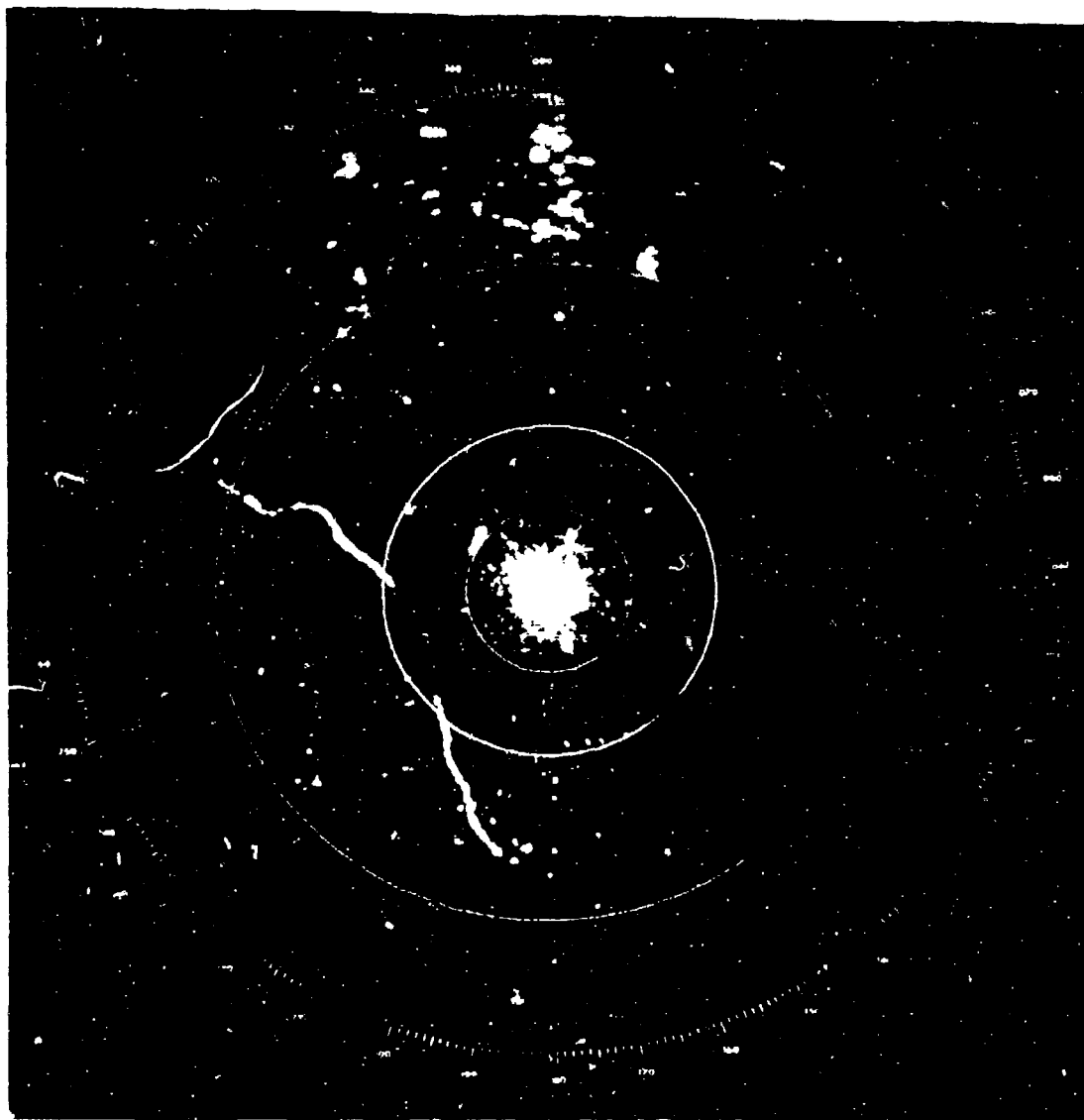


Figure 4.23 Time 1740, 2nm Range Rings, 24nm Total
Diameter AN/GPN-21 Radar, October 25, 1983

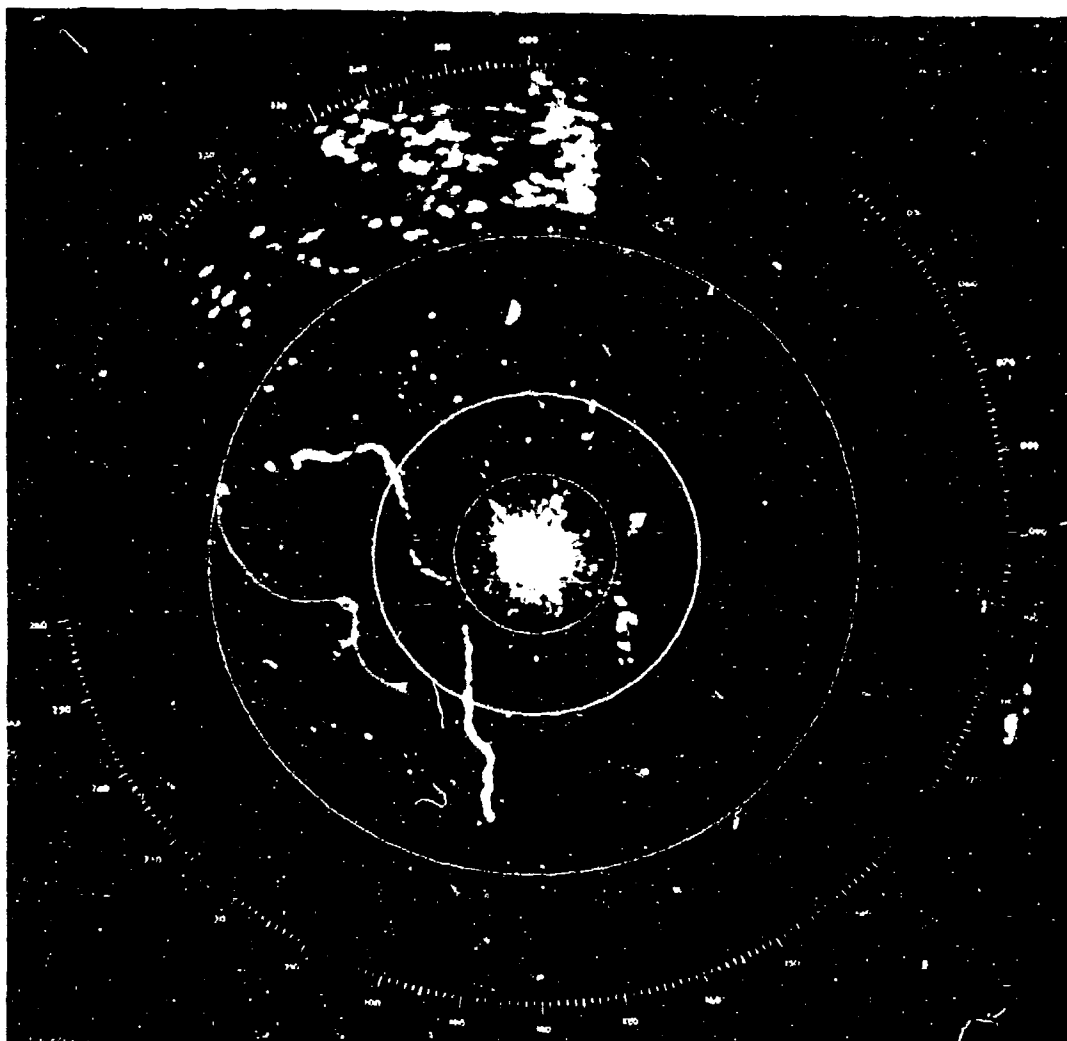


Figure 4.24 Time 1750, 2nm Range Rings, 24nm Total
Diameter AN/GPN-21 Radar, October 25, 1983



Figure 4.25 Time 1755, 2nm Range Rings, 24nm Total
Diameter AN/GPN-21 Radar, October 25, 1983

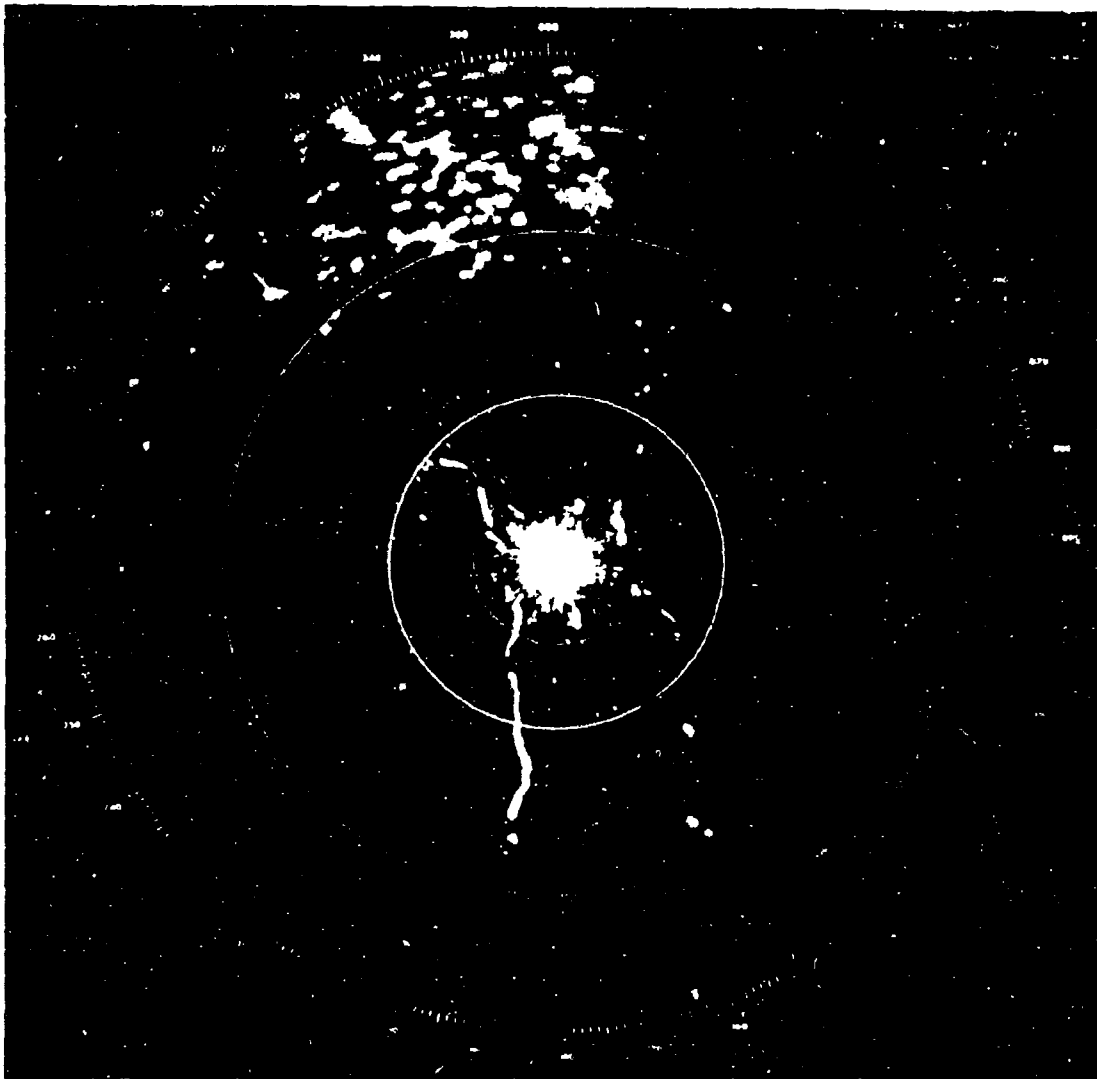


Figure 4.26 Time 1800, 2nm Range Rings, 24nm Total
Diameter AN/GPN-21 Radar, October 25, 1983

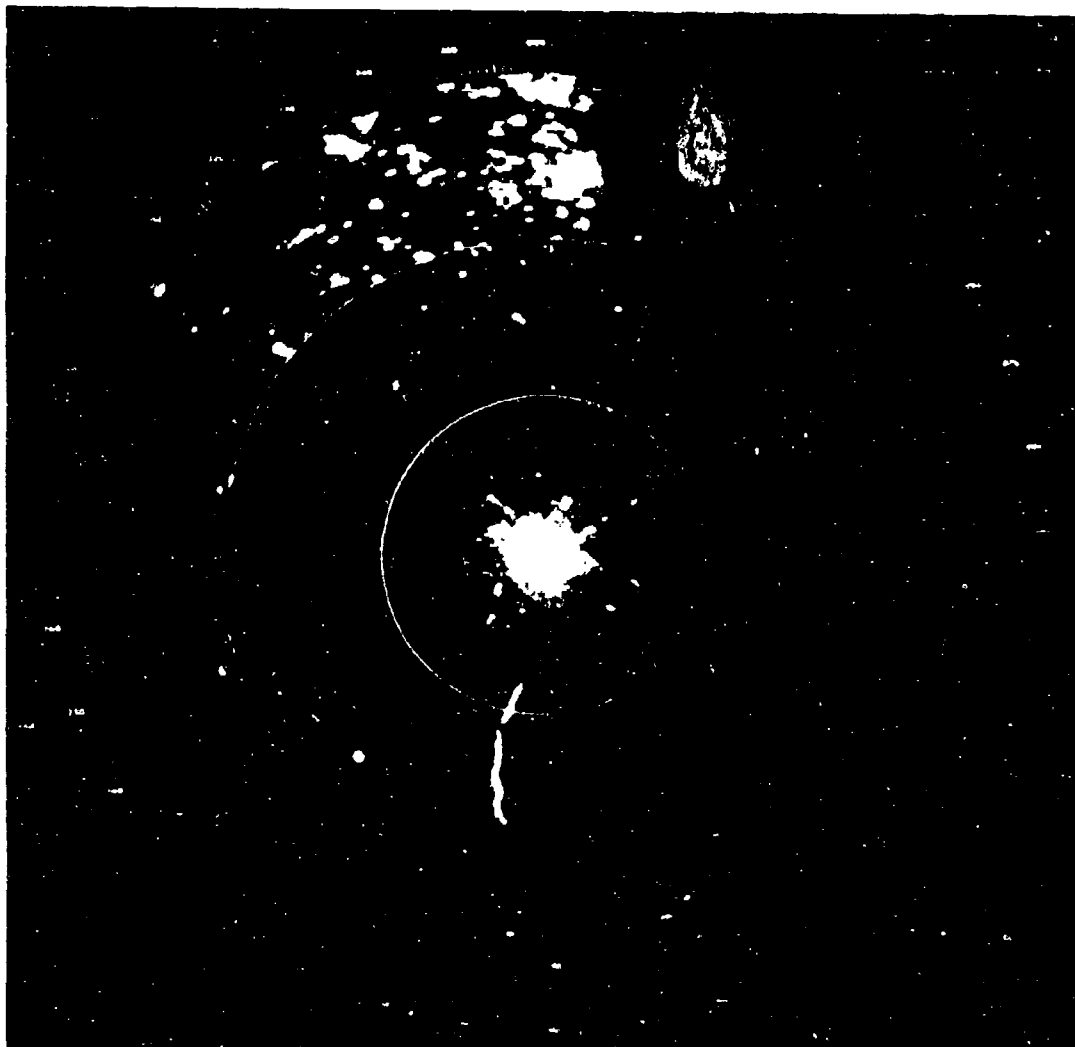


Figure 4.27 Time 1805, 2nm Range Rings, 24nm Total
Diameter AN/GPN-2J Radar, October 25, 1983

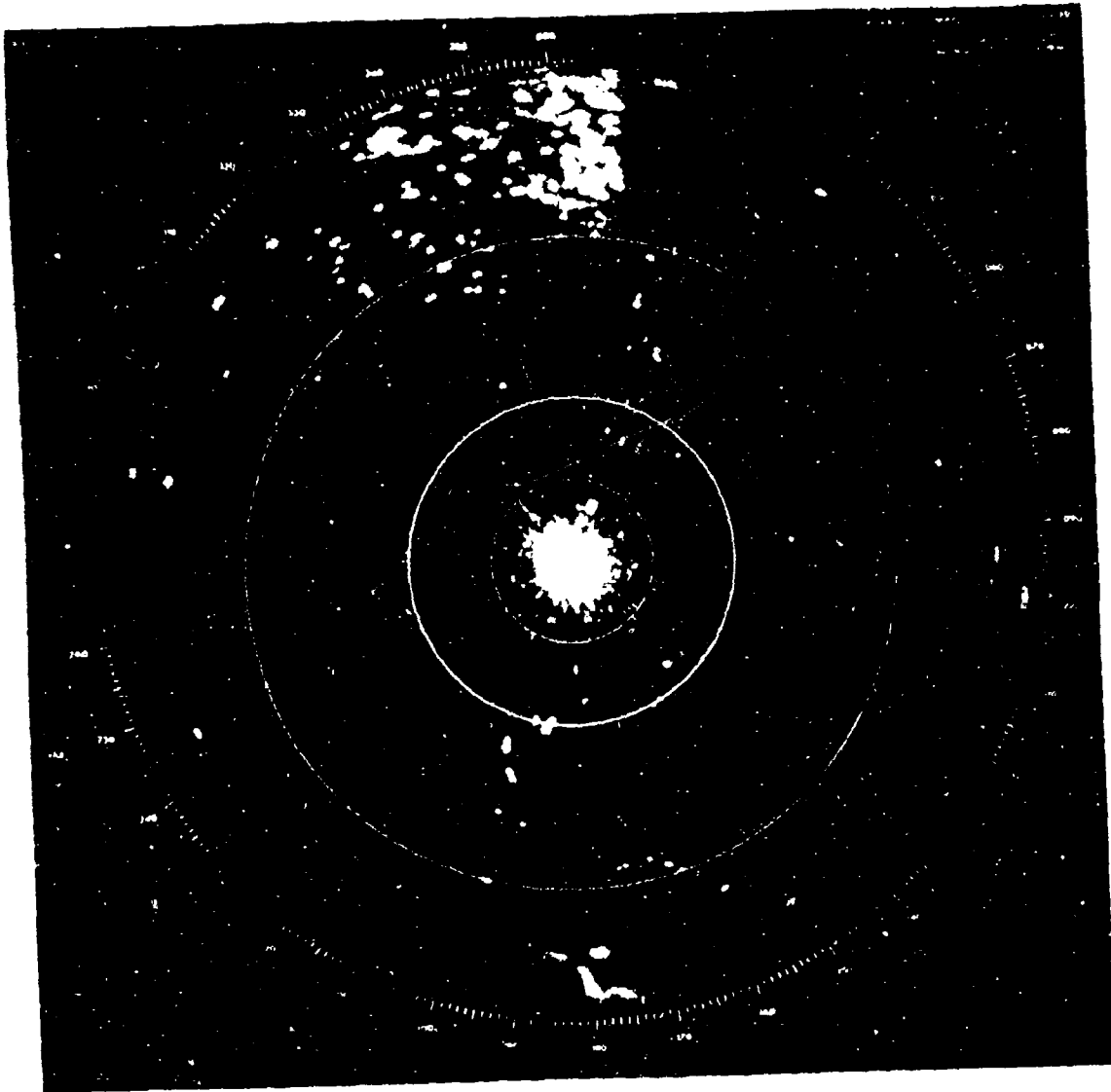


Figure 4.28 Time 1810, 2nm Range Rings, 24nm Total
Diameter AN/GPN-21 Radar, October 25, 1983

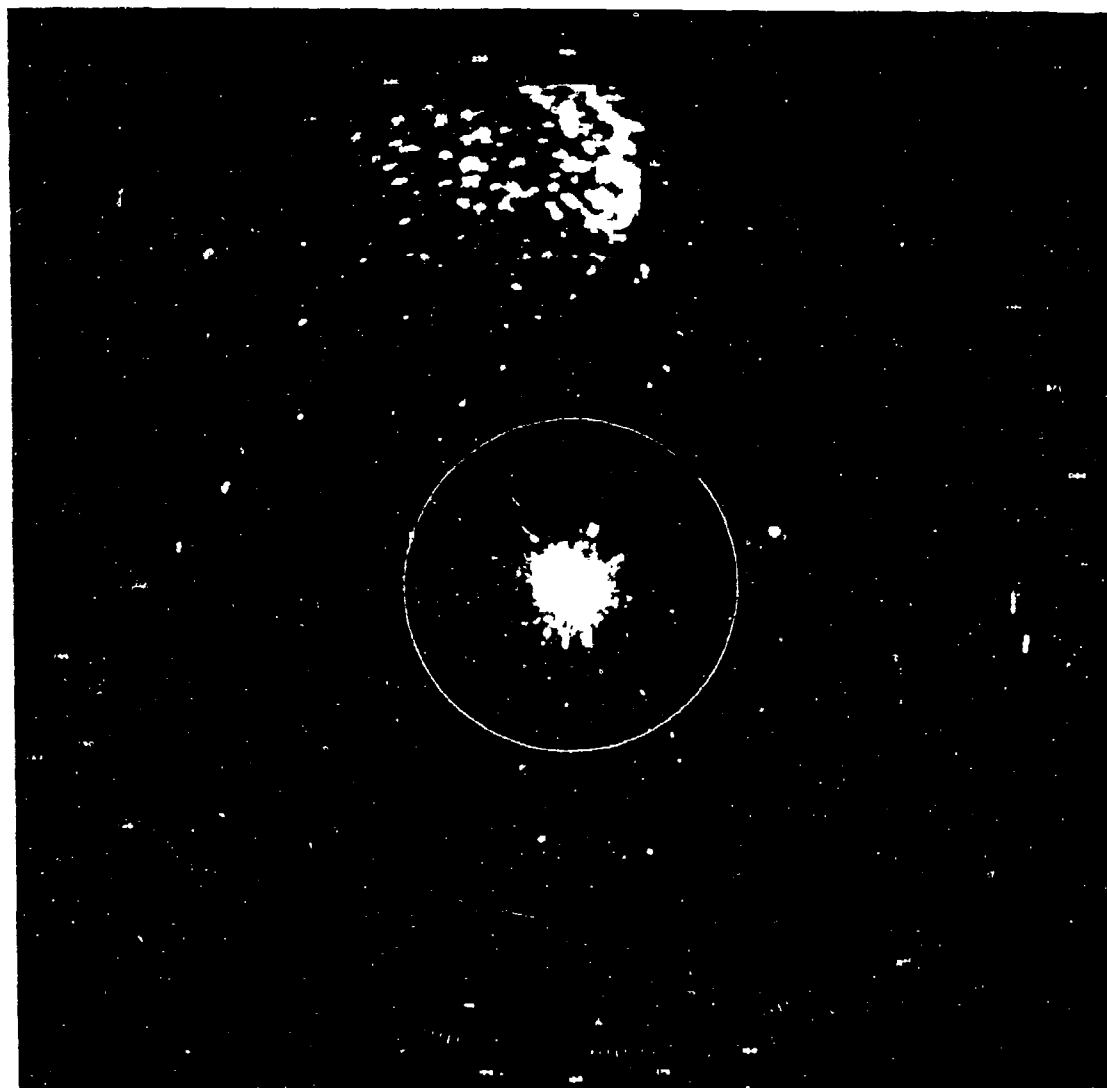


Figure 4.29 Time 1815, 2nm Range Rings, 24nm Total
Diameter AN/GPN-21 Radar, October 25, 1983

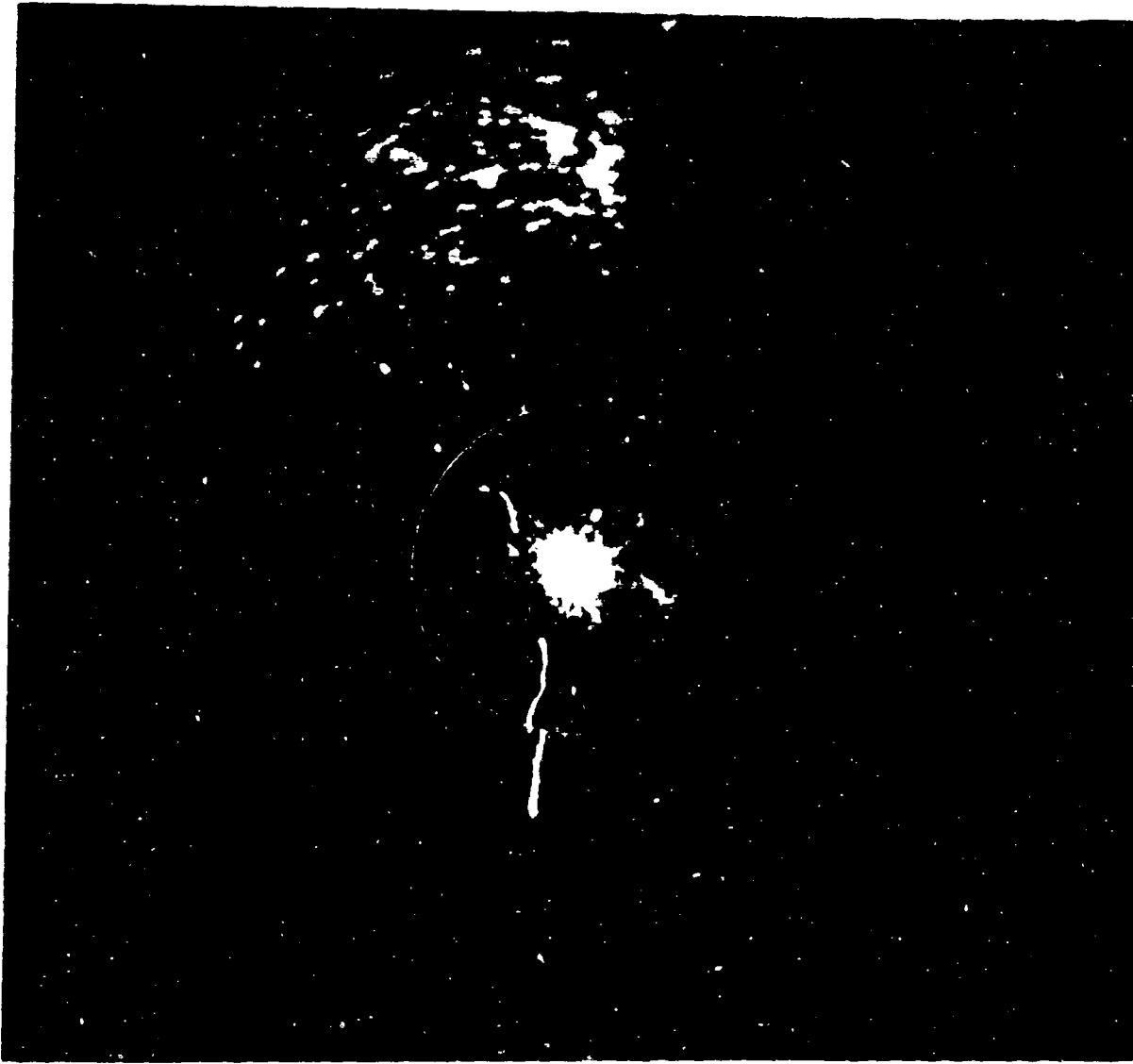


Figure 4.30a AN/GPN-21 Radar PPI Taken At The Same Time As Figures 4.30b and 4.30c. 2nm Range Rings, 24nm Total Diameter

detected.

Although Figure 4.30a shows two separate lines of birds to the south and northwest, time-lapse photography clearly infers that these two lines are really the ends of one continuous line. The birds due west of the radar are south bound and have no radial velocity component toward the radar. As described in section 4.4.2, the MTI attenuates target returns with little or no radial velocity, such as returns from buildings, tree, etc. Therefore, it also inhibits the detection of birds flying tangential to the propagation of the radar energy. This is a limitation inherent in an MTI processor and, consequently, of the AN/GPN-21 for the BIRDWATCH application.

Figures 4.31-4.40 document the bird activity as displayed on the PPI (MTI channel) of the AN/GPN-21 on 3 November 1983. The range rings are spaced 2 nm apart with every other range ring enhanced. The maximum displayed range from the radar is approximately 13 nm. The photos show the display in 5 minute intervals between 1620 and 1705. Extensive activity can be noted in the vicinity of Bombay Hook National Refuge approximately 7 to 10 nm to the north, the Little Creek Refuge located 2-4 nm to the east and northeast, and over the marshlands around Frederica located 3-7 nm to the south. The most notable activity in this series is the intense activity south of the base and the development of the V-shaped formation extending from 7 to 10 nm between azimuths 180 and 220.

Figures 4.41a, 4.41b, and 4.41c present the displays of the AN/GPN-21, AN/TPN-18A, and a version of a modified S-band marine radar, respectively, within 30 seconds of the same instant. The modified

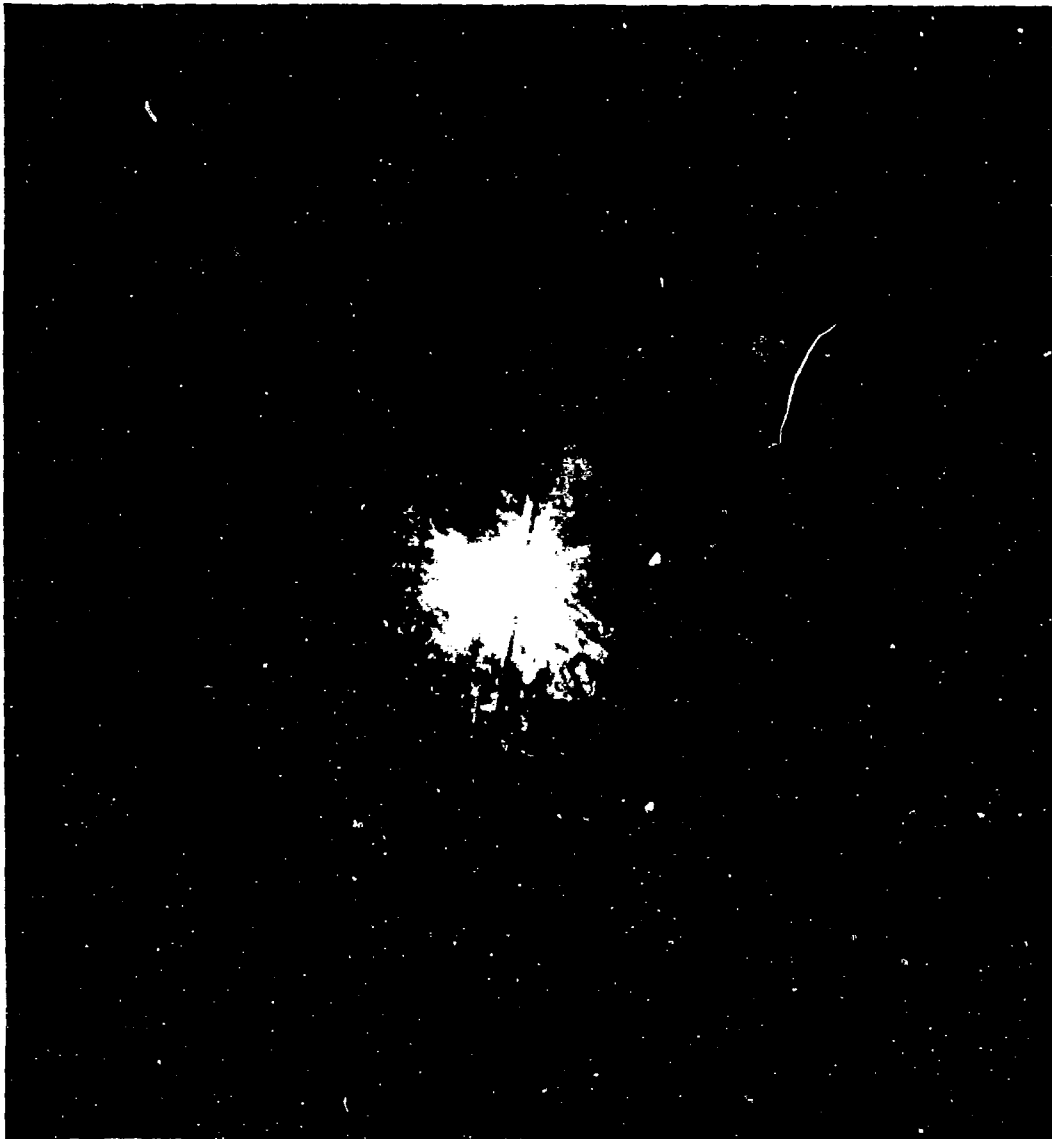


Figure 4.30b AN/TPN-18A Radar PPI Taken At The Same
Time As Figures 4.30a and 4.30c. 1nm
Range Rings, 20nm Total Diameter

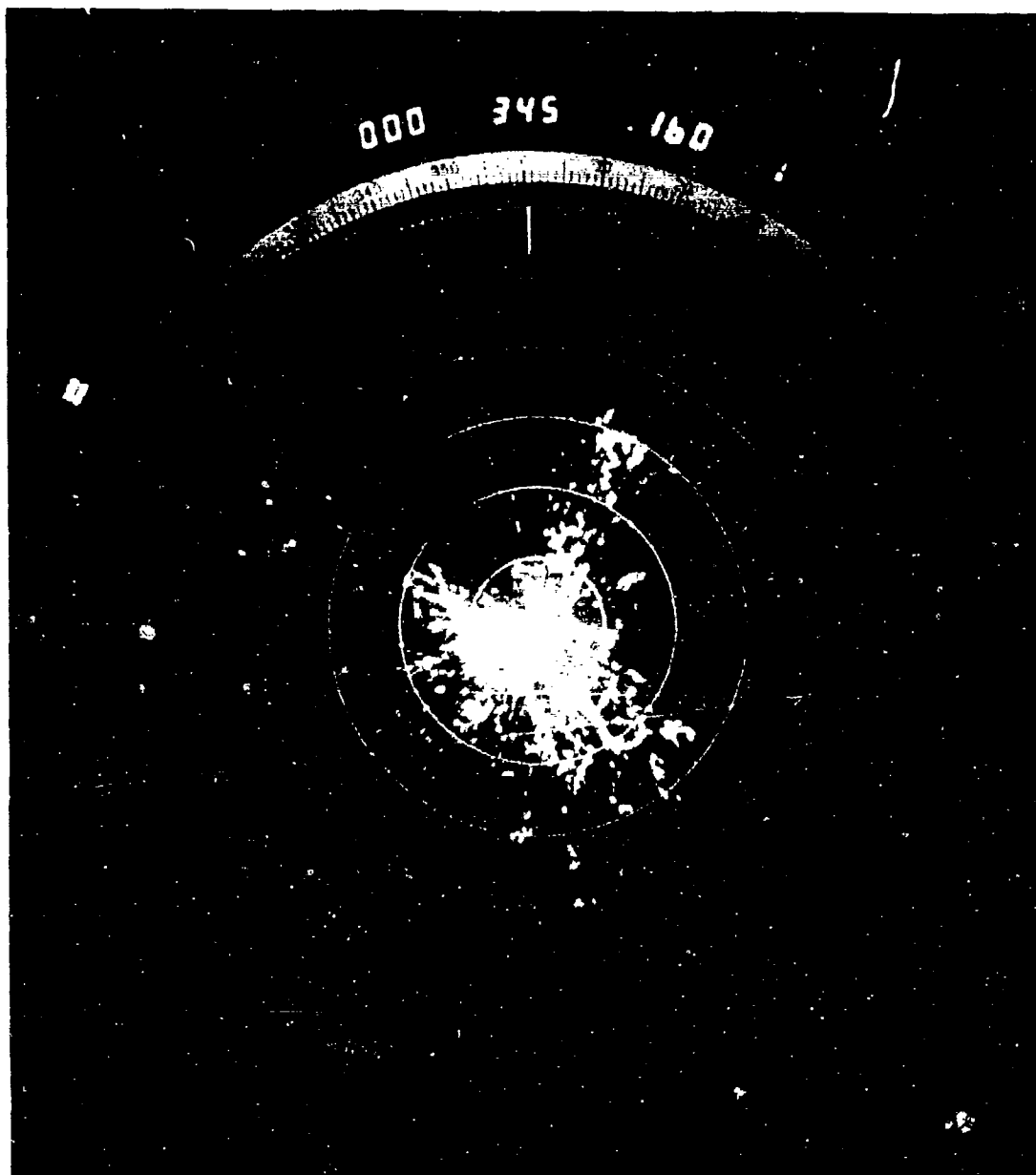


Figure 4.30c X-Band Marine Radar PPI Taken At The Same
Time As Figures 4.30a and 4.30b. 1nm
Range Rings, 12nm Total Diameter

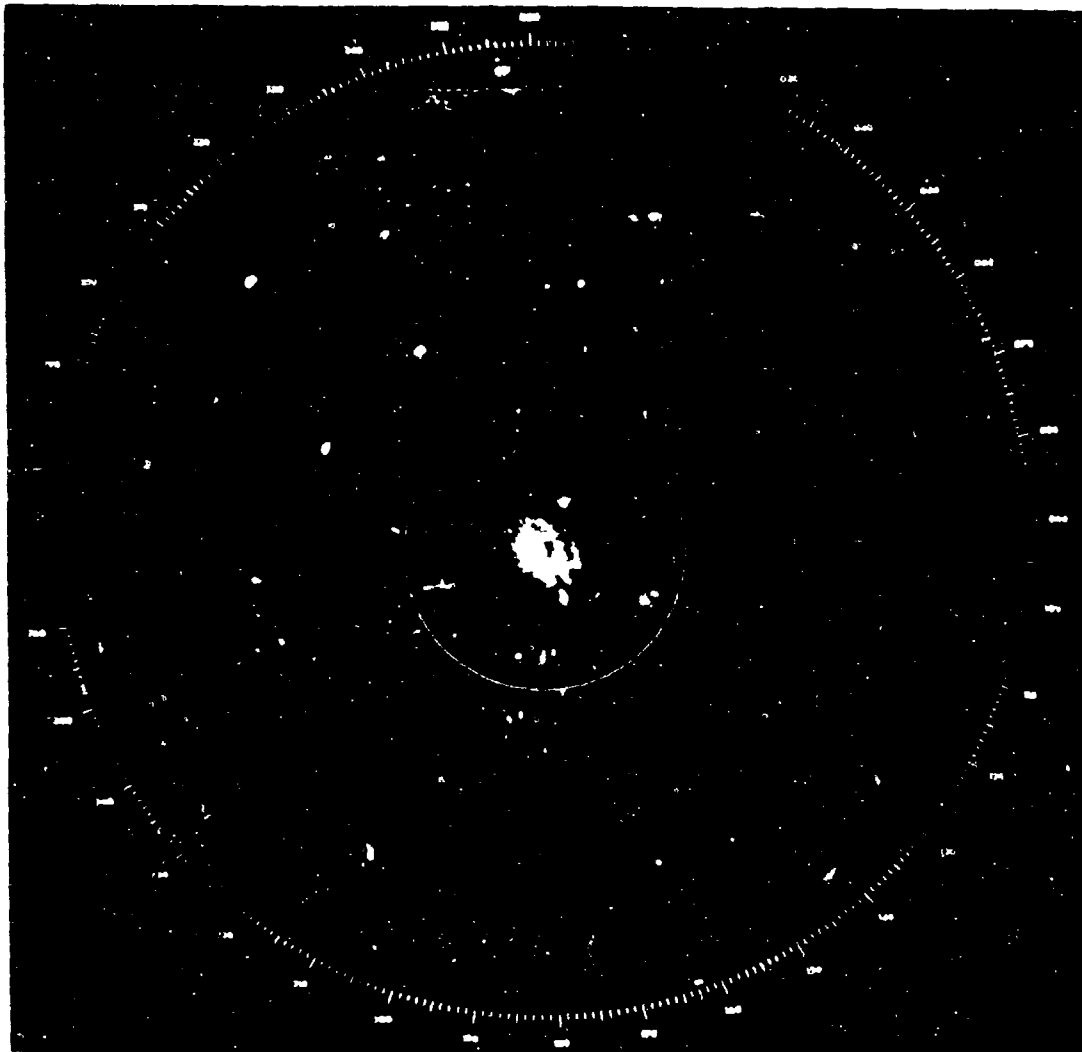


Figure 4.31 Time 1620 AN/GPN-21 Radar PPI, 2nm Range
Rings, 24nm Total Diameter, 3 November, 1983

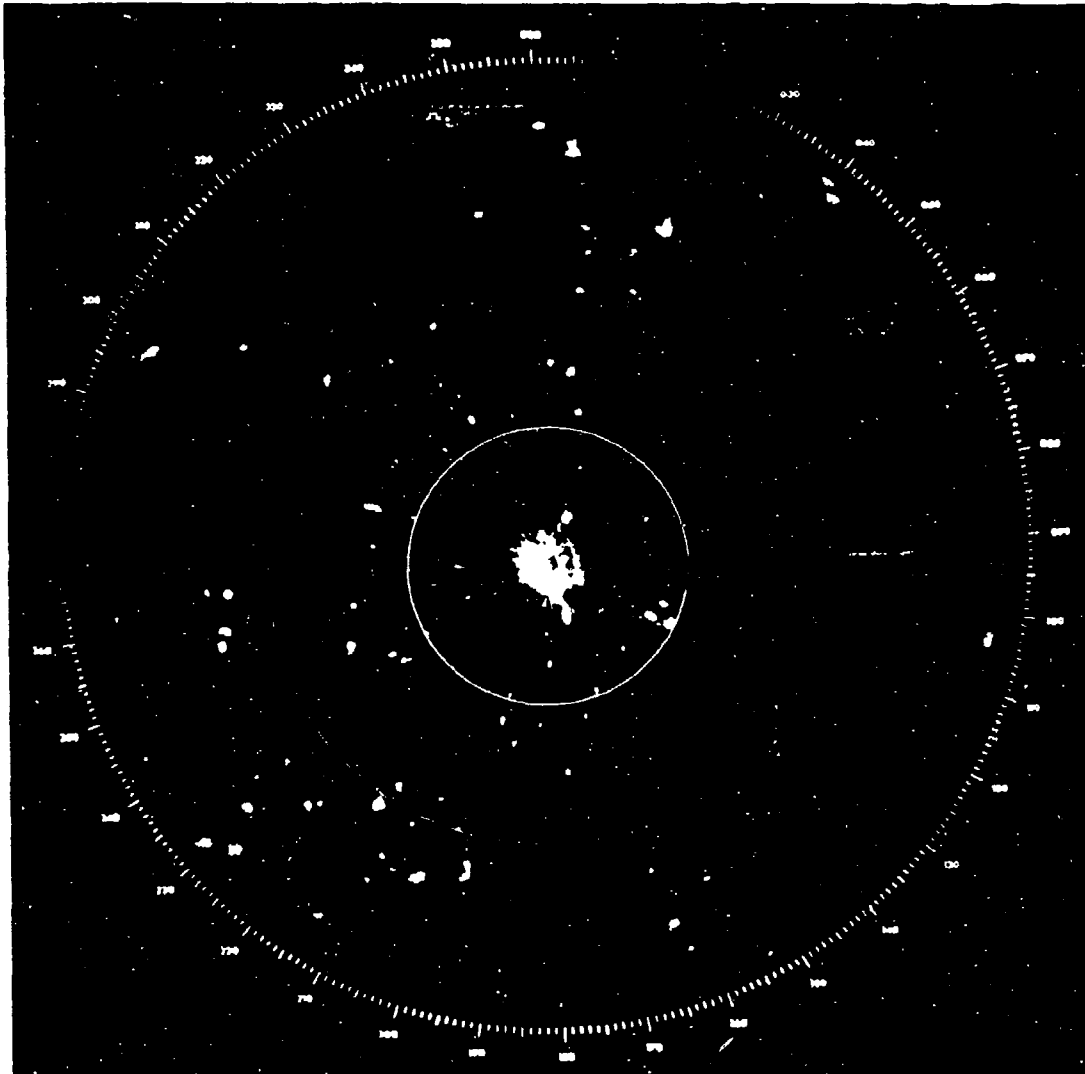


Figure 4.32 Time 1625 AN/GPN-21 Radar PPI, 2nm Range
Rings, 24nm Total Diameter, 3 November, 1983

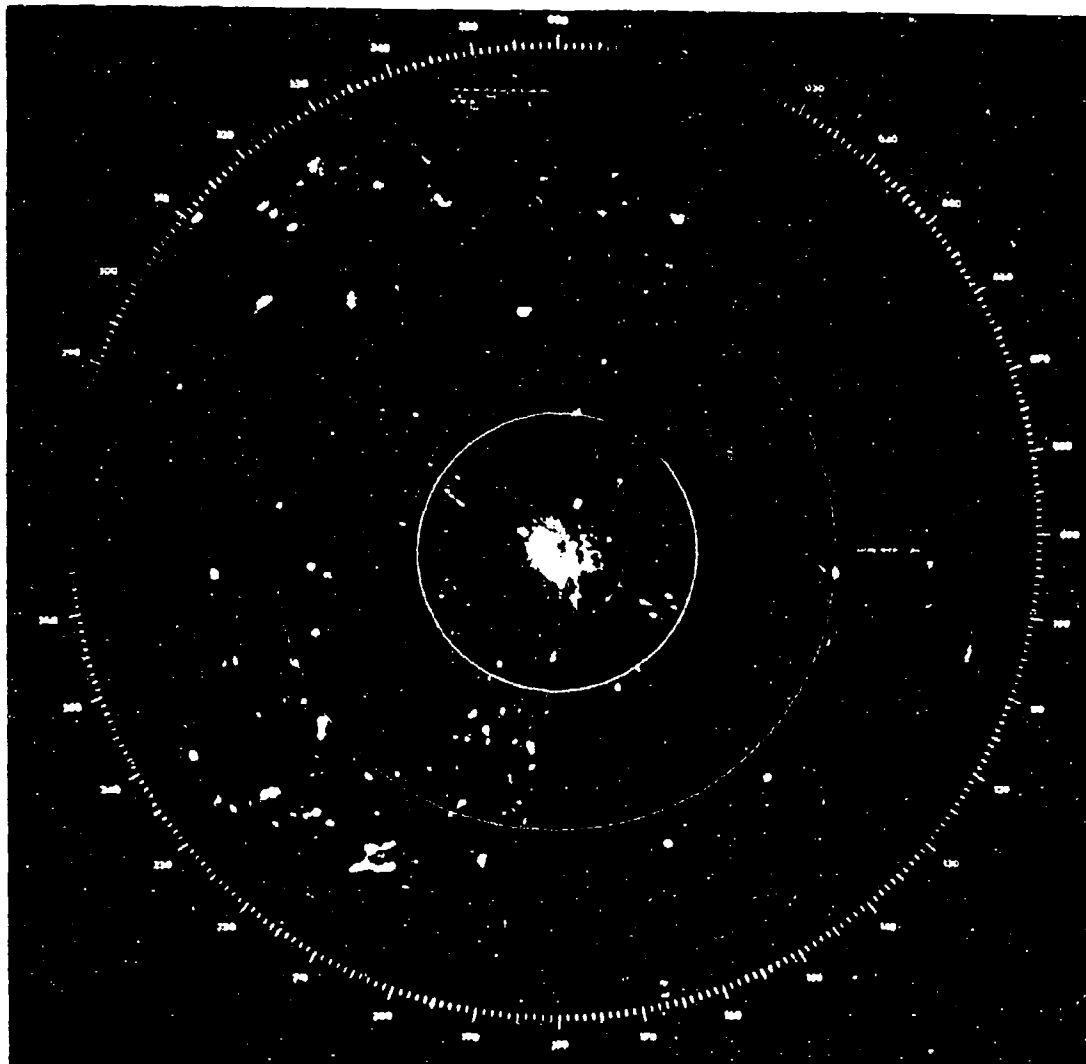


Figure 4.33 Time 1630 AN/GPN-21 Radar PPI, 2nm Range
Rings, 24nm Total Diameter, 3 November, 1983

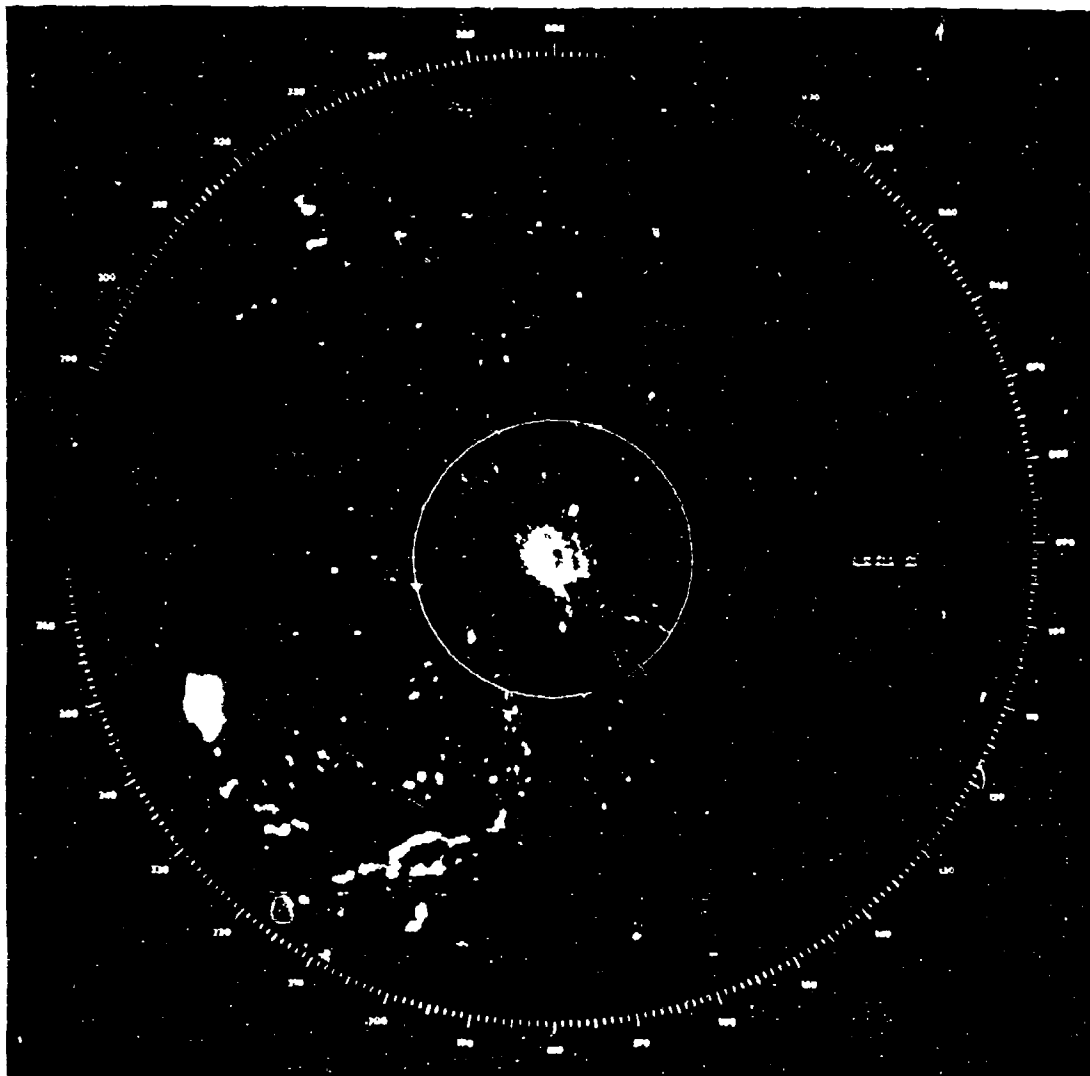


Figure 4.34 Time 1635 AN/GPN-21 Radar PPI, 2nm Range
Rings, 24nm Total Diameter, 3 November, 1983

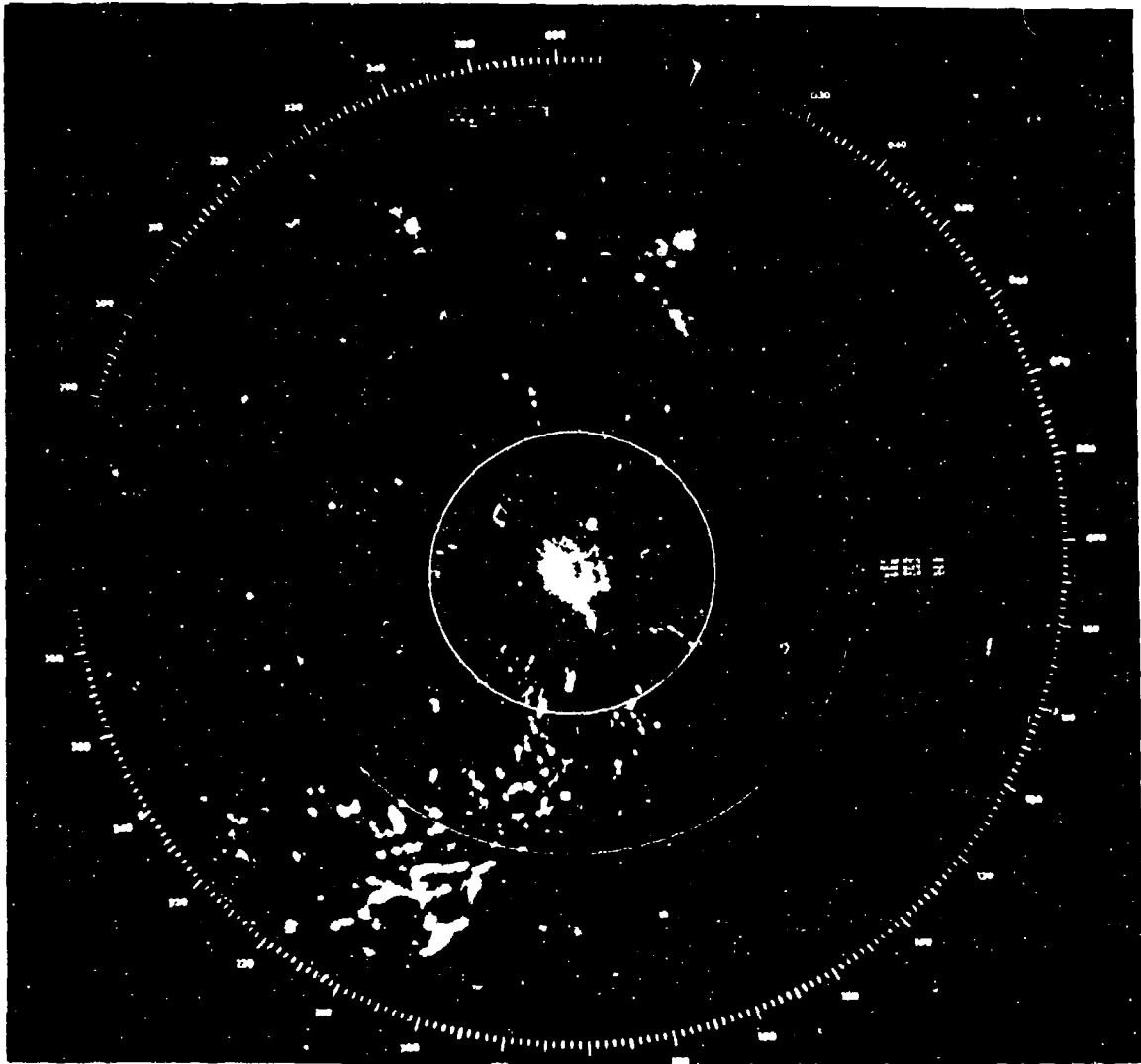


Figure 4.35 Time 1640 AN/GPN-21 Radar PPI, 2nm Range
Rings, 24nm Total Diameter, 3 November, 1983

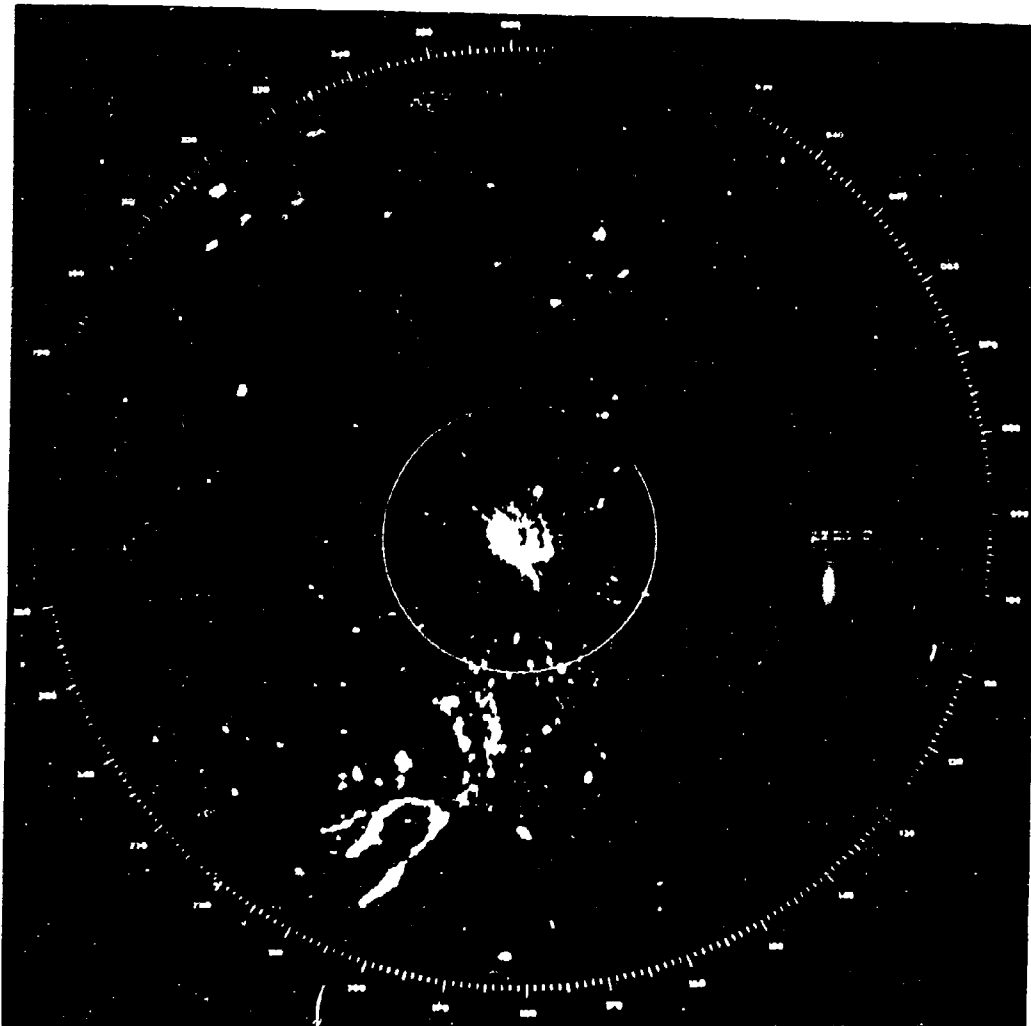


Figure 4.36 Time 1645 AN/GPN-21 Radar PPI, 2nm Range
Rings, 24nm Total Diameter, November 3, 1983

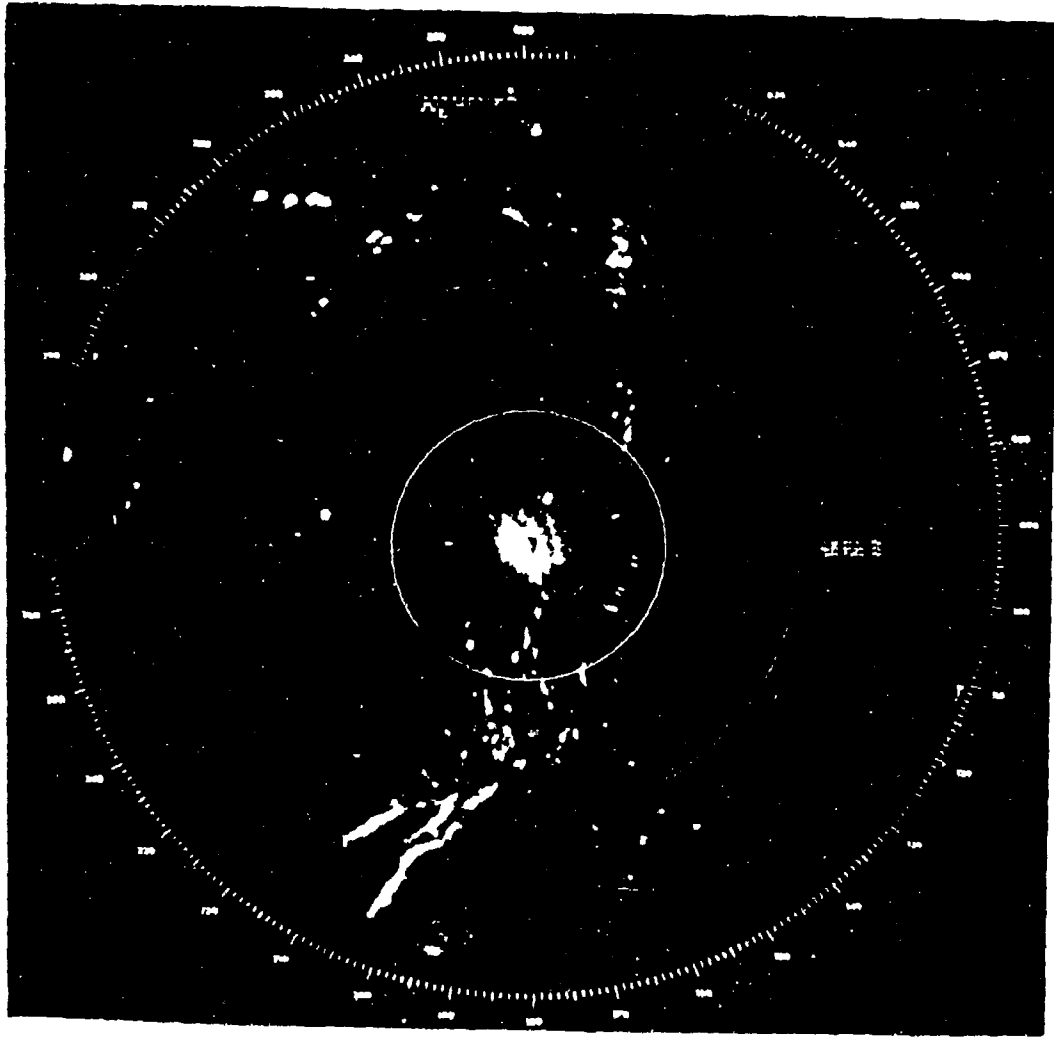


Figure 4.37 Time 1650 AN/GPN-21 Radar PPI, 2nm Range
Rings, 24nm Total Diameter, 3 November, 1983

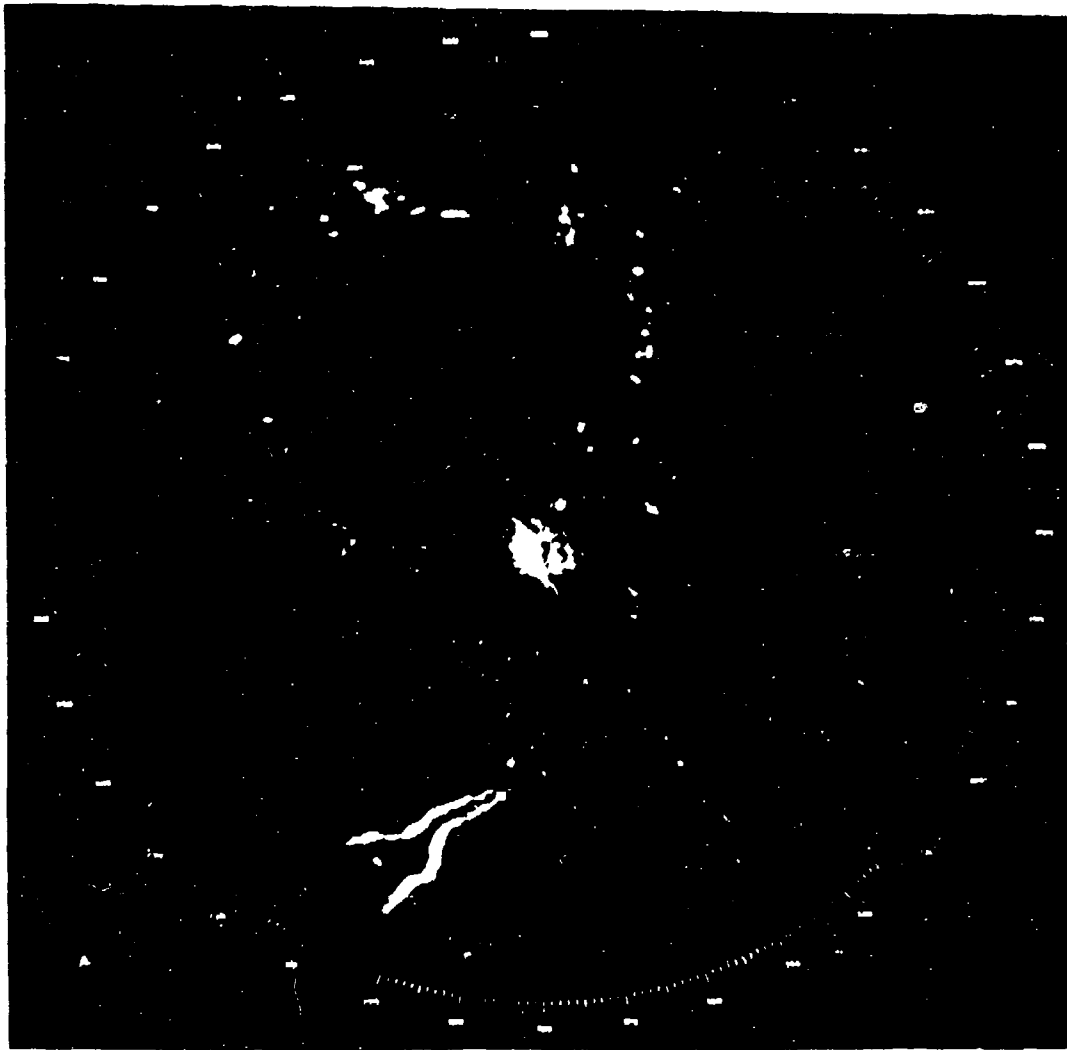


Figure 4.38 Time 1655 AN/GPN-21 Radar PPI, 2nm Range
Rings, 24nm Total Diameter, 3 November, 1983

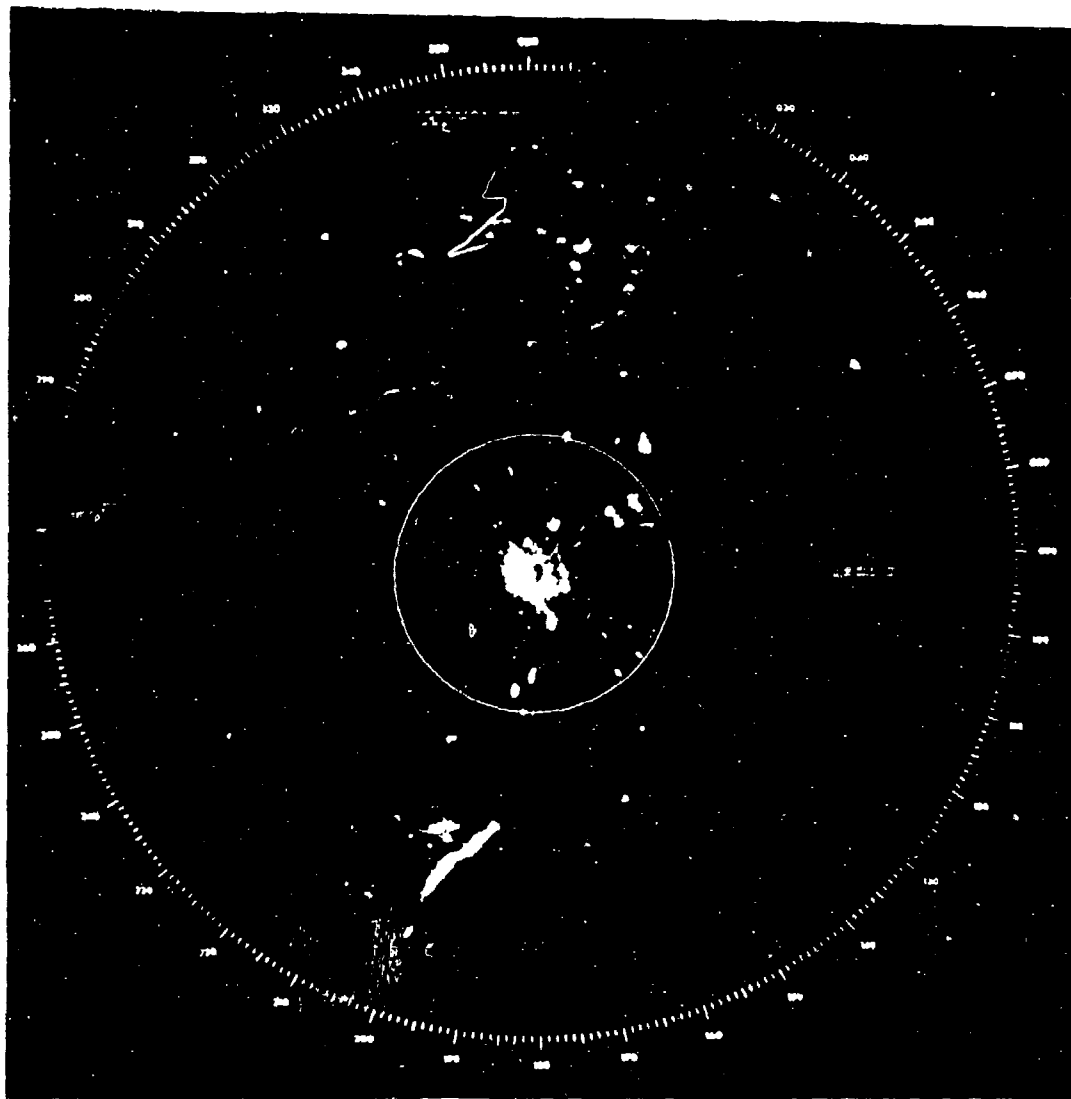


Figure 4.39 Time 1700 AN/GPN-21 Radar PPI, 2nm Range
Rings, 24nm Total Diameter, 3 November, 1983

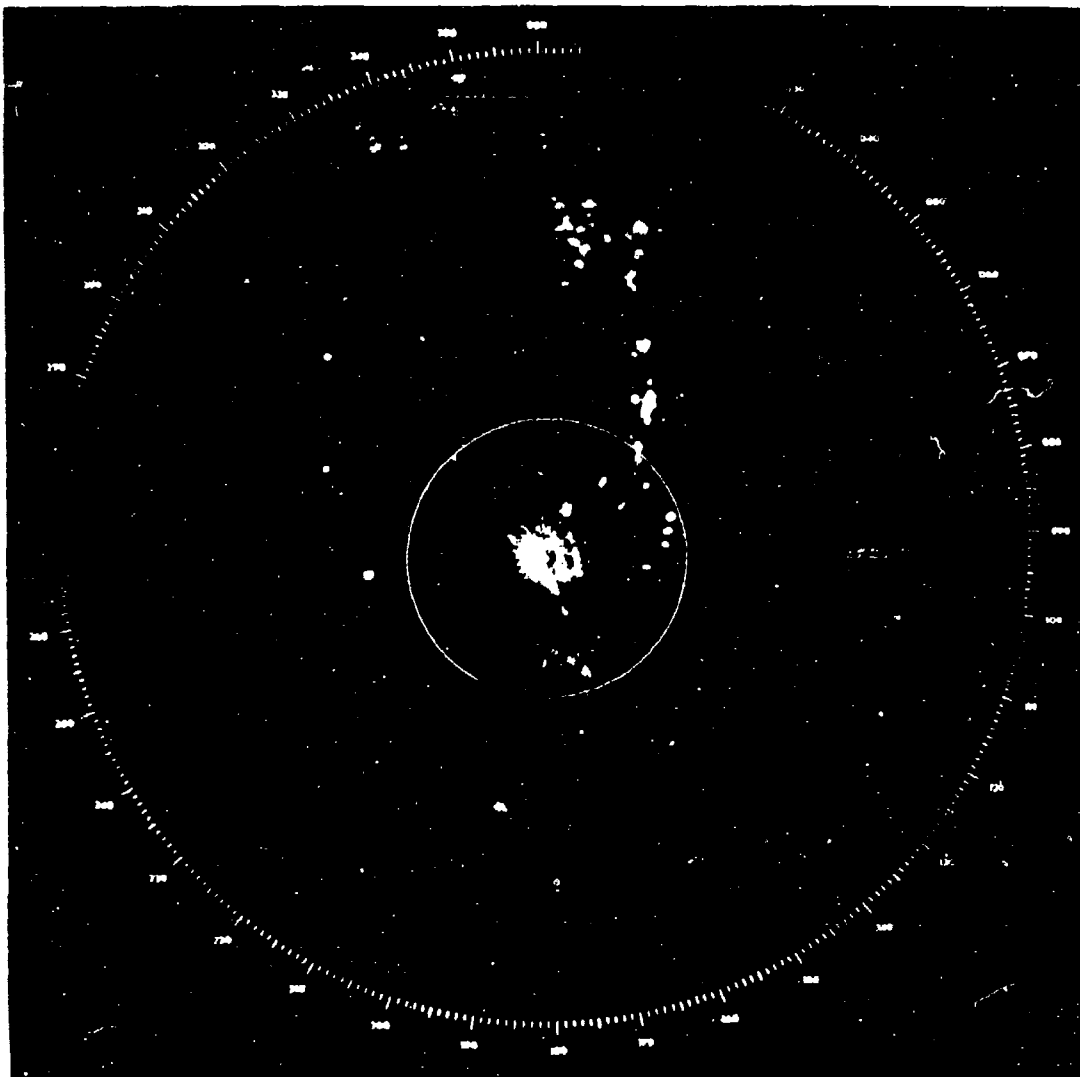


Figure 4.40 Time 1705 AN/GPN-21 Radar PPI, 2nm Range
Rings, 24nm Total Diameter, 3 November, 1983

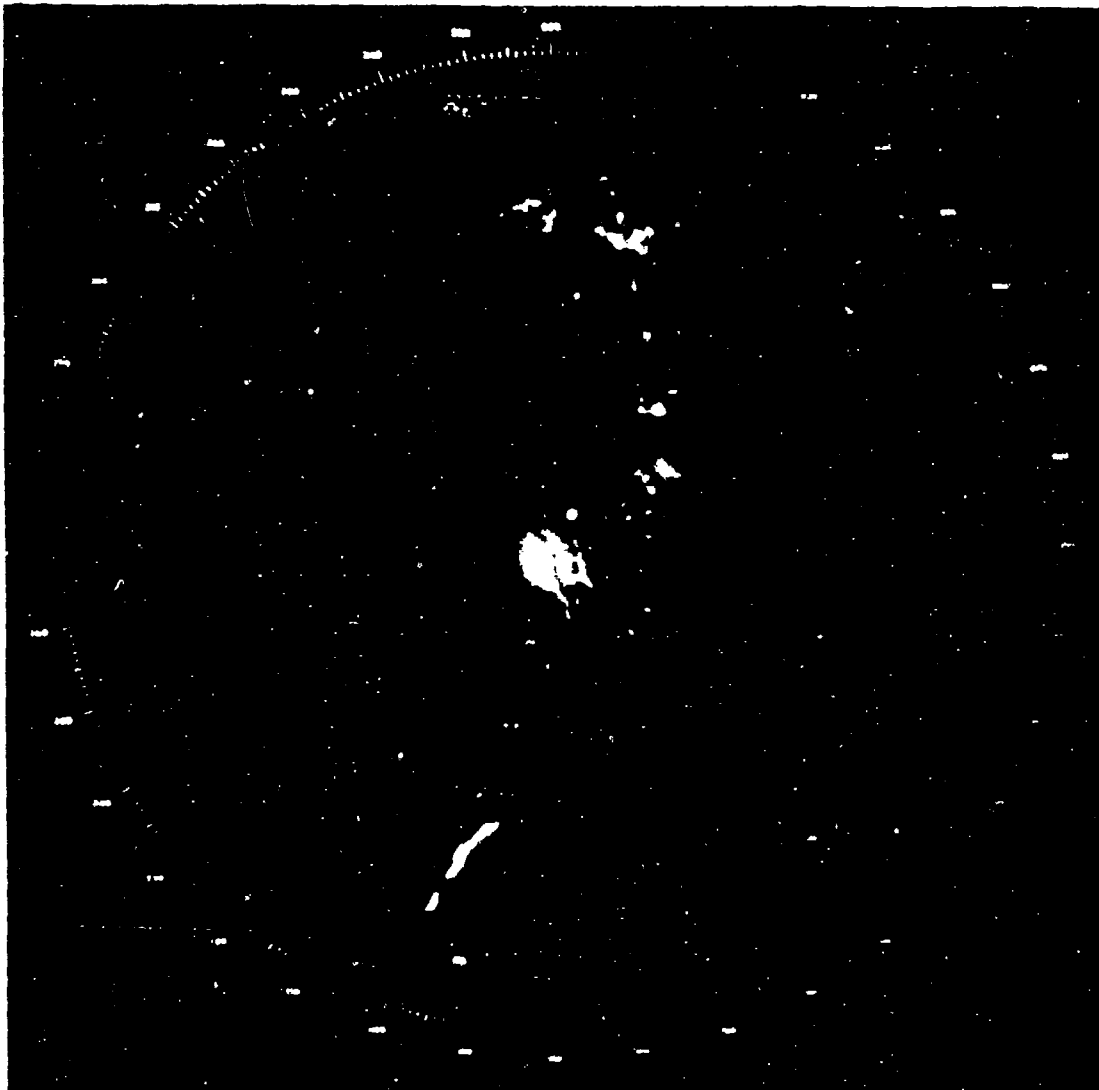


Figure 4.41a AN/GPN-21 Radar PPI Taken At The Same
Time As Figures 4.41b and 4.41c. 2nm
Range Rings, 20nm Total Diameter

S-Band system, shown in Figure 4.42, consisted of an AN/MPN-13 antenna and feed combined with the electronics from an S-band marine radar. It was made temporarily operational by HQ/MAC and Raytheon personnel for the duration of the one-on-one tests to document its performance and potential in a BIRDWATCH application. Returns detected on the AN/GPN-21 that are also detected on the other two radars are a plane at 10.5 nm, 50 degrees (just within 10 nm, 60 degrees on the other radar displays), two bird flocks at 5 nm, 190 degrees (5.5 nm, 190 degree on the others), and assorted bird activity at between 4nm and 5.5 nm (3.5nm and 5 nm on the others) to the northeast. The large line of birds, detected by the AN/GPN-21 south of the base between 7.5 nm and 10 nm is not detected by the other two systems. However, the approaching aircraft at 11.5 nm on the AN/GPN-21 is detected by the modified marine radar inferring that the birds may be flying too low to be detected due to screening.

Again, the limitations of the AN/GPN-21's MTI can be seen in these photographs. An aircraft detected by the AN/TPN-18A and the modified marine radar at a range of about 5.75 nm and bearing 310 degrees is not detected on the AN/GPN-21 scope. At this moment, the aircraft is not flying toward or away from the radar and is attenuated by the MTI filter.

The results of the test demonstrated that the AN/GPN-21 performance far exceeds the capability of the other radars tested. Therefore, despite of its limitations, the AN/GPN-21 was chosen as the interim BIRDWATCH sensor for the immediate future.

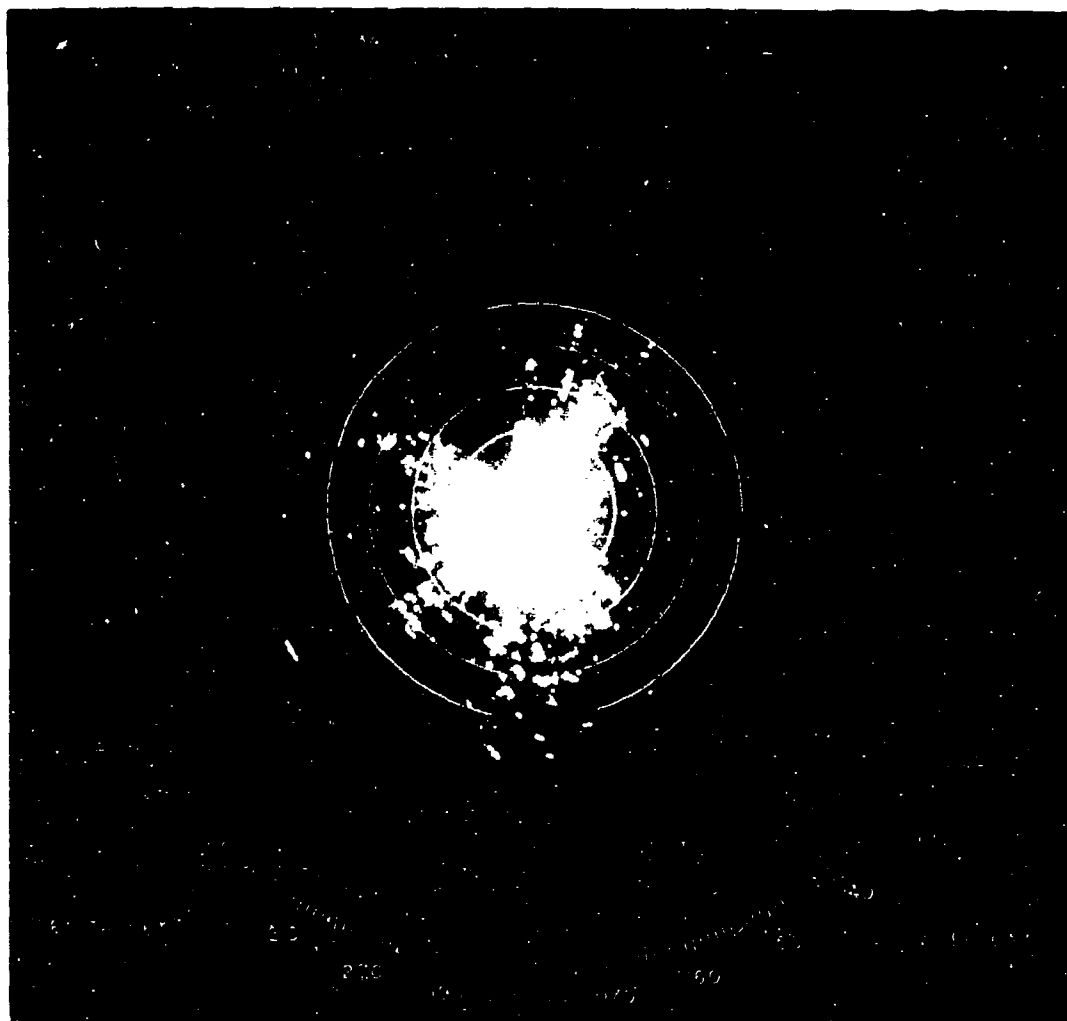


Figure 4.41b AN/TPN-18A Radar Taken At The Same Time
As Figures 4.41a and 4.41c. 1nm Range
Rings, 20nm Total Diameter

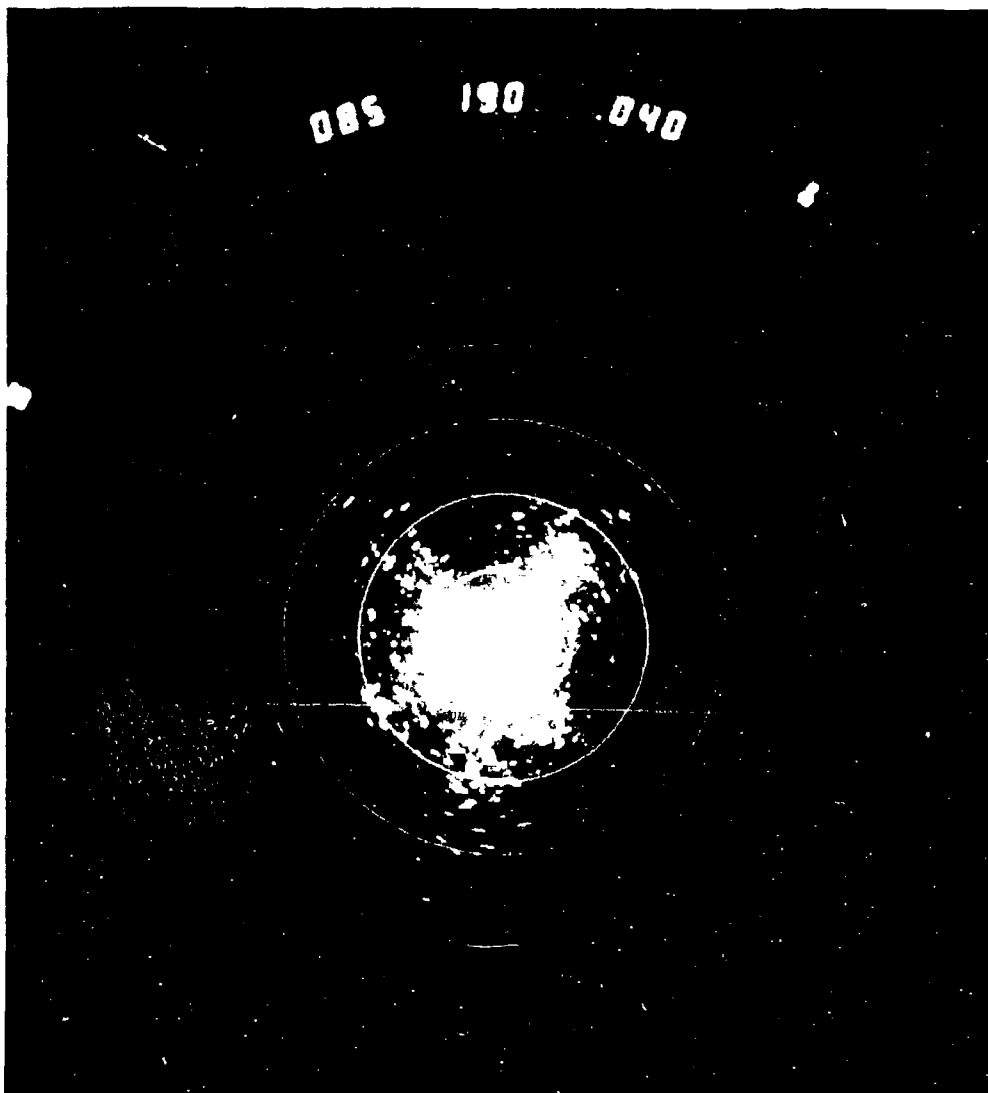


Figure 4.41c S-Band Marine Radar PPI Taken At The Same
Time As Figures 4.41a and 4.41b. 2nm
Range Rings, 24nm Total Diameter

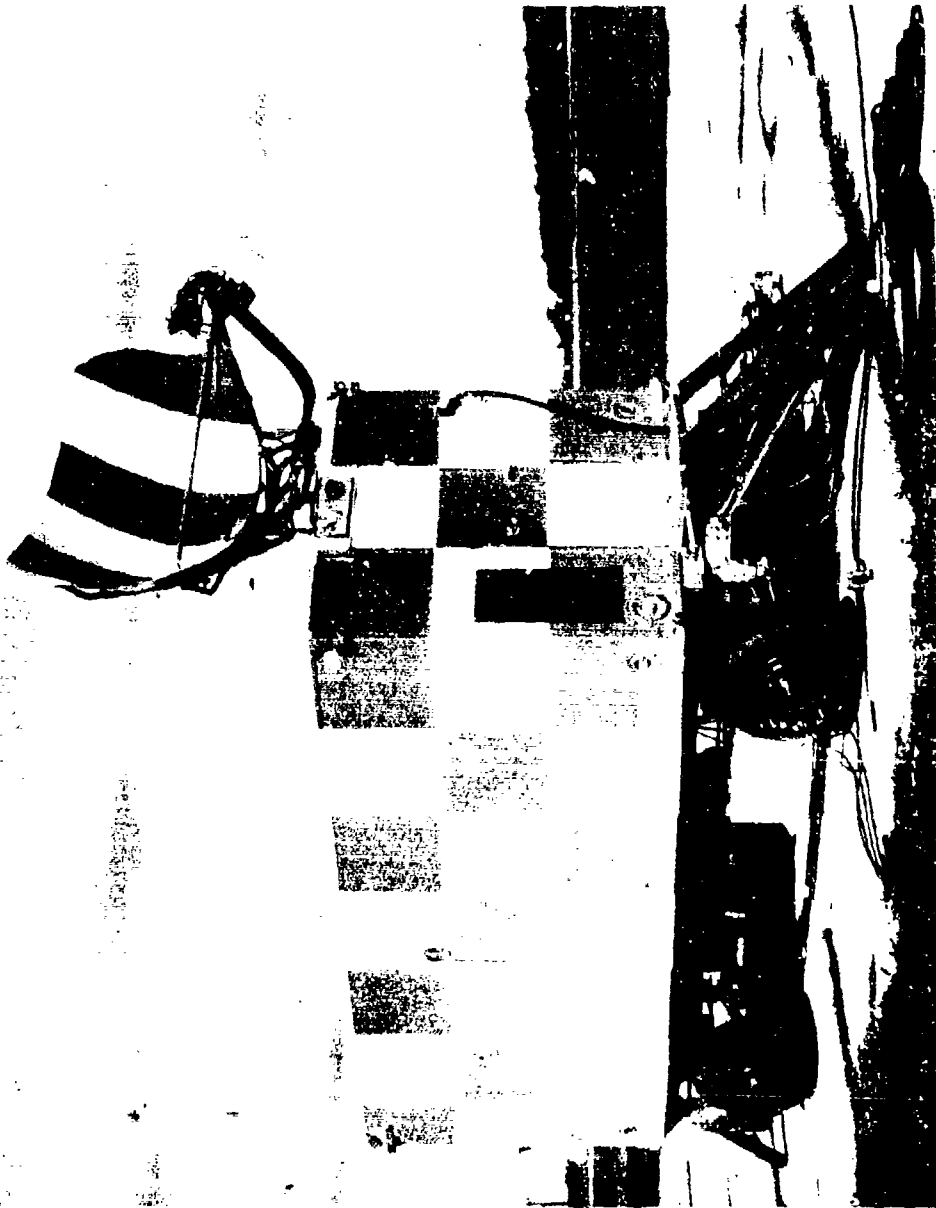


Figure 4.42 Modified S-Band Marine Radar (Raytheon S-Band Electronics With MPN-13 Antenna and Van)

5.0 THE INTERIM BIRDWATCH SYSTEM: AN OVERVIEW AND RECOMMENDATIONS

An interim BIRDWATCH system currently exists at Dover AFB, DE. The procedures required to implement the system have been jointly developed by HQMAC/DC, AFCC, the 2016 CS, and the 436 MAW. The current operation of the BIRDWATCH system is based on an ATC/BIRDWATCH operational concept developed by the 2016 CS and a BASH plan formulated by the 436 MAW. These plans define the close cooperation that exists between the aircrews, the ATC controllers, the control tower personnel, and the BIRDWATCH monitors in the attempt to reduce the hazard caused by bird activity.

As of the middle of November, 1983, the AN/GPN-21 GCA radar has been performing both the ATC and BIRDWATCH functions. During the end of 1983, the BIRDWATCH system used the PPI scope normally used for ATC training and maintenance. However, with the installation of an extra PPI scope by the 485th EIG stationed at Griffiss AFB, NY, the impact of using the AN/GPN-21 radar for BIRDWATCH has been minimized. In adverse weather or propagation conditions when the radar parameters required to provide the best display for the ATC function inhibit or reduce the system's BIRDWATCH capability, a "quick lock" procedure has been developed by the 2016 CS which allows adequate monitoring of bird activity to be maintained. Upon receipt of a request for an advisory, the radar parameters can be momentarily switched to a more sensitive setting for improved monitoring of the bird activity. After a few scans, the BIRDWATCH monitor can assess the level of bird activity and respond to the request. The radar parameters can then be switched back to the original settings for normal ATC operation. It

should be noted that this "quick look" procedure is controlled by the ATC personnel and is performed only if air traffic safety conditions are not compromised. While the BIRDWATCH system uses ATC operators for monitors, the BIRDWATCH personnel are not authorized to control aircraft.

The control tower and aircrews contact BIRDWATCH for recommendations on runway selection and confirmation of bird activity before approval for takeoff or landing. A simple color-coded warning system, developed during March 1983 by the 436 MAW, is used to indicate the relative levels of bird activity. A green condition indicates very low or no activity, a condition that exists primarily between the months of May and September when migratory waterfowl are not present. A yellow condition indicates that low to moderate bird activity exists in the vicinity of the base and that the BIRDWATCH system should be contacted for advisories. The red condition indicates that heavy activity exists within 10 nm of the base. During this condition, all local missions are terminated or sent to other locations. Aircraft are not authorized to take off, land or fly in the Dover AFB area without contacting BIRDWATCH for advisories. Information to this effect has been widely distributed through various flight publications and information manuals.

It is important to note that, while the current interim system has reduced the hazard to aircraft landing or taking off at Dover AFB, it has not eliminated the threat. For example, the interim BIRDWATCH system has no capability of providing an adequate warning against birds that feed and rest on or near the runway or in the fields at the end of

the runways. Once the birds are allowed to exist in these areas, they can fly up in front of an approaching aircraft too quickly to allow warning by the BIRDWATCH system or avoidance by the aircraft. The only way to reduce this hazard is to deter the birds from inhabiting these area.

The risk of a catastrophic incident can be further reduced by increasing the capabilities of the system's sensor. For instance, most bird activity occurs below 1500 feet and is no threat to aircraft except when taking off or landing. Therefore, in order to distinguish a threatening flock from the other detections, the BIRDWATCH monitor must be able to determine the height of the detected activity. Since the AN/GPN-21 can only provide range and azimuth information on detected bird activity, a monitor in the current system cannot make this distinction and issues many "false" hazard reports to the pilots. This high "false" report rate is causing the pilots to become "desensitized" and they take the advisories less seriously. The implementation of a three dimensional (3-D) radar capability would greatly improve the credibility of the BIRDWATCH advisories. The primary areas around the base where height information is most important are the takeoff and landing corridors. The AN/GPN-22 PAR system can provide this information down the one corridor used for landing. However, a system to provide correlated height, range, and azimuth information down each landing and takeoff corridor before use by the aircraft would be a big improvement to the current system. Three dimensional coverage of local aircraft traffic for 360 degrees and out to 10 nm will further reduce the bird strike hazard.

However, since the probability of a bird strike is significantly reduced above 2000 feet, this secondary coverage is less important.

Another current limitation that can be improved is the clutter processing and velocity filtering capability of the BIRDWATCH sensor. Due to the limitations of its clutter filter, the AN/GPN-21 does not detect all of the bird activity around Dover AFB. As shown in section 4, the AN/GPN-21 has three problems. First, the instability of the transmitter limits the radar's subclutter visibility (SCV), a measure of the system's ability to detect small moving targets over large stationary scatters such as the buildings to the north of the base. Second, the shape of the Moving Target Indicator clutter filter used in the AN/GPN-21 allows detection of small flocks of birds only if they are traveling toward the radar at velocities exceeding 10-15 knots. Birds (or aircraft) with little or no velocity vector toward the radar, i.e. birds that are flying tangentially to the radar beam, will not be reliably detected. Finally, critical operating parameters of the current BIRDWATCH such as the STC and RAG attenuation, the use of circular polarization, and the use of the lower gain passive receive beam of the antenna, are determined by the requirements of the ATC function. The first two limitations can be reduced significantly through the use of a coherent klystron or TWT transmitter and Doppler filter processing as exists in the AN/GPN-25. The third limitation requires that the BIRDWATCH system have an independent receiver and processor.

The final limitations of the current BIRDWATCH system concern its important man-machine interfaces and communication channels.

Currently, when heavy bird activity exists at Dover AFB, hundreds of flocks can be detected on the AN/GPN-21 PPI display during each 4 second scan, overloading the processing capability of a human operator. It is estimated however that, due to the aforementioned limitations of the AN/GPN-21, a significant fraction of the activity is not detected on each scan. If these limitations are reduced thru the use of a coherent Doppler processing system, the number of flocks detected per scan could be well over a thousand in peak periods. The addition of height information for each detection would simply add to the overload. Therefore, some form of automated processing is needed to take full advantage of the additional improvements. For example, an ideal automated system would track both aircraft and bird detections, integrate height information with the established tracks, test the 3-D bird and aircraft tracks for possible intercepts, and flag potential intercepts to the BIRDWATCH monitor and/or the ATC controller. However, such a system does not exist at this time and acquisition of a future system would require a considerable development.

6.0 SUMMARY AND CONCLUSION

In conclusion, this report has documented the efforts that were performed by the RADC team to define, analyze, and provide a radar-based bird hazard warning system. The basic parameters of a warning system have been defined including an important analysis that determined the sizing requirements of a BIRDWATCH radar sensor and provided important guidelines for the development of an operational concept. Advantages and limitations of existing radars were analyzed and one-on-one performance tests were performed between selected systems.

An interim system is currently operating at Dover AFB using the AN/GPN-21 radar. This system significantly reduces the hazard to aircraft landing and taking off at Dover AFB but does not eliminate the threat. The limitations of the current system have been identified and recommendations have been proposed to improve the effectiveness of a far term BIRDWATCH system. These recommendations include the automation of bird and aircraft tracking and intercept calculations, the installation of a three dimensional capability to allow estimates of the height of the bird activity, especially in the landing and takeoff corridors, and improvements in the clutter cancellation and Doppler filtering capability of the BIRDWATCH sensor.

PPI photos and audio/video recordings demonstrating the bird hazard problem at Dover AFB have been sent upon request to HQ MAC, for use in briefing CINCMAC on the problem and in planning future BIRDWATCH surveillance efforts and procurements; to USAFALCENT for use in evaluating operational procedures in hazardous bird environments;



to Dover AFB for use in local safety programs and reviews; and to the BASH squadron at Tyndall AFB, the Air Force focal point for bird strike problems.

APPENDIX A CLUTTER PROFILE OF THE AN/TPN-18A RADAR

Major sources of undesired radar returns that degrade the detection and tracking of targets are backscatter from trees, buildings, ground terrain, raindrops, and other environmental scatterers illuminated by the radar. These unwanted returns clutter the PPI scope or other radar indicators, hence the term clutter, and often conceals targets of interest. These clutter phenomena are usually distributed in nature. Clutter returns are classified as resulting from discrete or distributed objects. Discrete clutter returns are from isolated scatterers, which are no larger than a radar resolution cell.* Distributed clutter consists of many point scatterers and extends over many radar resolution cells in both range and azimuth. Large patches of distributed ground clutter can severely limit radar performance since the total energy received from the clutter echo is generally much greater than that received from the targets of interest.

Ground clutter returns are highly correlated from pulse to pulse (narrow spectrum around zero doppler shift). One important method of reducing the clutter return displayed on the radar indicator depends upon this correlation, and is the basis of the MTI (Moving Target Indicator) Radar.[24] Another less sophisticated method of reducing the clutter return (as well as the return signal from targets of interest) is by the simple technique of reducing the system gain at close range.

* The radar resolution cell is that volume bounded by the antenna beam in azimuth and elevation. The length of the volume in range is determined by the transmit pulse width. To receive less backscatter from clutter objects such as rain, a smaller resolution cell is required. This can be achieved by using a small antenna beam width and a short transmitted pulse.

This method is known as Sensitivity Time Control (STC). High pass filtering of the video signal in the receiver will also reduce interference, and this is referred to as Fast Time Constant (FTC). These techniques are implemented in the AN/TPN-18A using a programmable attenuator in the receiver which reduces the system gain at short range where the clutter is strong, and a differentiating circuit in the receiver before the first video stage. Clutter returns are primarily from fixed permanent objects in ground based radar systems.

The amount of clutter the radar will see depends upon the height of the radar antenna above the ground. The clutter return increases with antenna height and is due to the screening effect of near-in clutter. The returns from buildings and other manmade structures at Dover AFB are more intense than the returns from trees and vegetation because these structures are composed of smooth metallic surfaces, which are excellent reflectors. Radar returns from these manmade structures and natural ground clutter are usually much larger than the reflections from desired targets (bird hazards in this case) and these clutter returns can severely limit the performance of a radar which does not employ MTI filtering. Because of this limitation, an experienced Army Air Traffic Control Team operated the radar at Dover AFB and determined the severity of the bird hazard conditions when aircraft were landing and taking off. Even the detection capability of an MTI Radar will be degraded by very large clutter returns, since no MTI filter provides complete cancellation.

A Clutter Profile was obtained using the AN/TPN 18A Radar to characterize the Dover terrain for use in future evaluations. To

obtain the Ground Clutter Profile, the radar system parameters were adjusted to the following conditions: 200 kilowatts peak power, 0.2 microseconds pulse duration, 1200 pulses per second transmitted, 9125 megahertz center frequency, linear polarization, sensitivity time control off, fast time constant off, +1/2 degree mechanical tilt and full receiver gain. To develop an accurate clutter profile, the PPI gain is adjusted so that receiver noise is barely visible across the PPI display. Figure A1 is a photograph of this setting. Attenuation is inserted before the receiver front end in steps of 12 dB and the PPI display is photographed after each step. Figure A2 is a photograph of the PPI display after 12dB of attenuation is placed before the receiver front end, there is considerable reduction in the distributed clutter return, but a minimal reduction in the discrete clutter return. Figure A3 is a photograph of the PPI display after 24 dB of attenuation is placed before the receiver front end. Notice that only returns from discrete clutter remain. The AN/GPN-20 Radar MTI filter will cancel up to 25 dB of ground clutter return. From this photograph we see that some of the returns from the hangar buildings and the parked C5A aircraft will not be eliminated by the MTI canceller. However STC will reduce the return from the near in clutter enough to clean up the PPI display. From the clutter profiles in Figures A1 through A6 it is apparent that the performance of any radar will be degraded due to the strong clutter return over the sector 170 to 280 degrees, however, a coherent radar with MTI and Doppler filter processing will give the most accurate indication of a bird hazard over this sector, all other factors being equal in the radar evaluation.

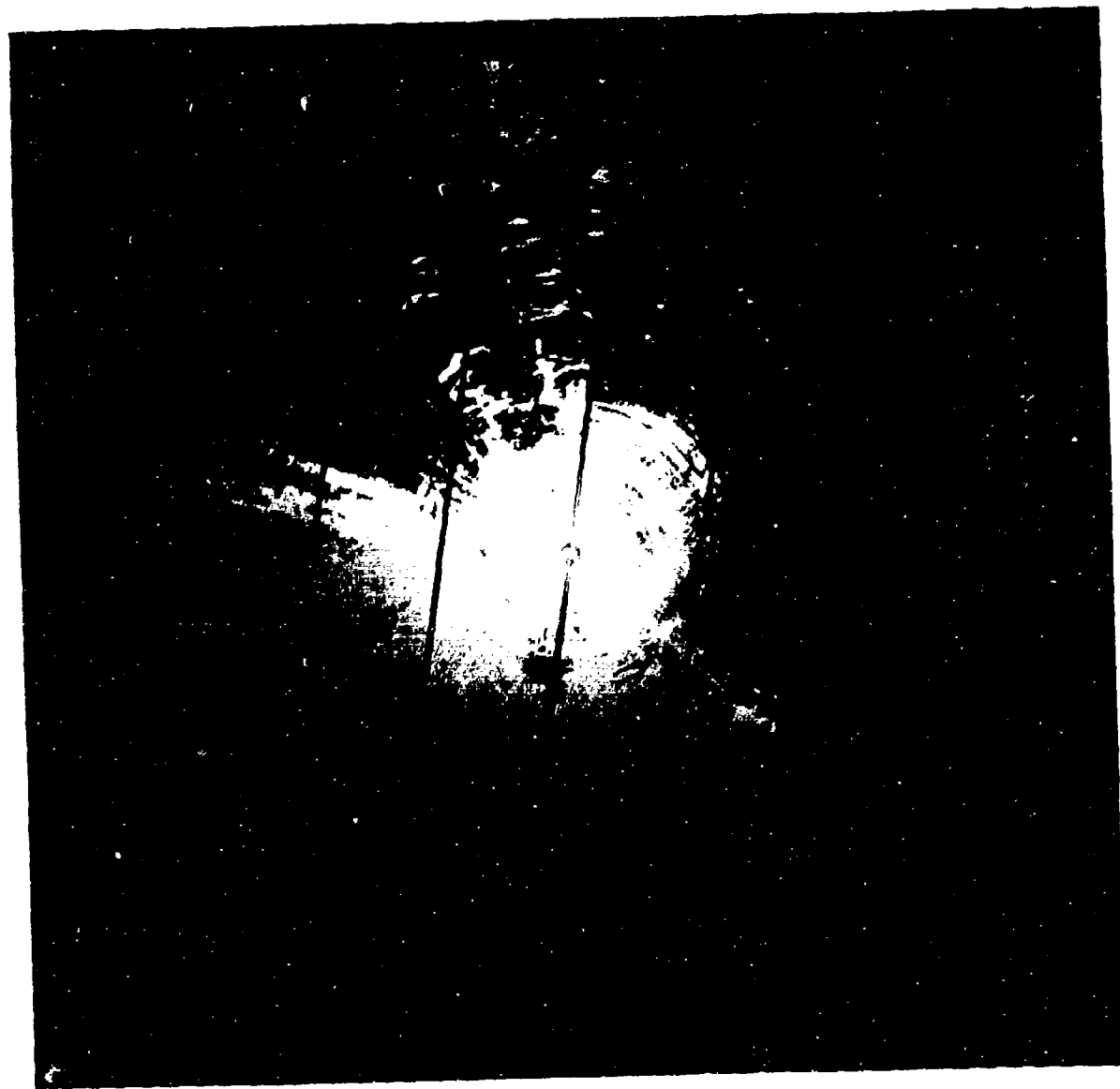


Figure A1 PPI Display, 0dB Attenuation - 10nm Total
Diameter (Clutter Map)

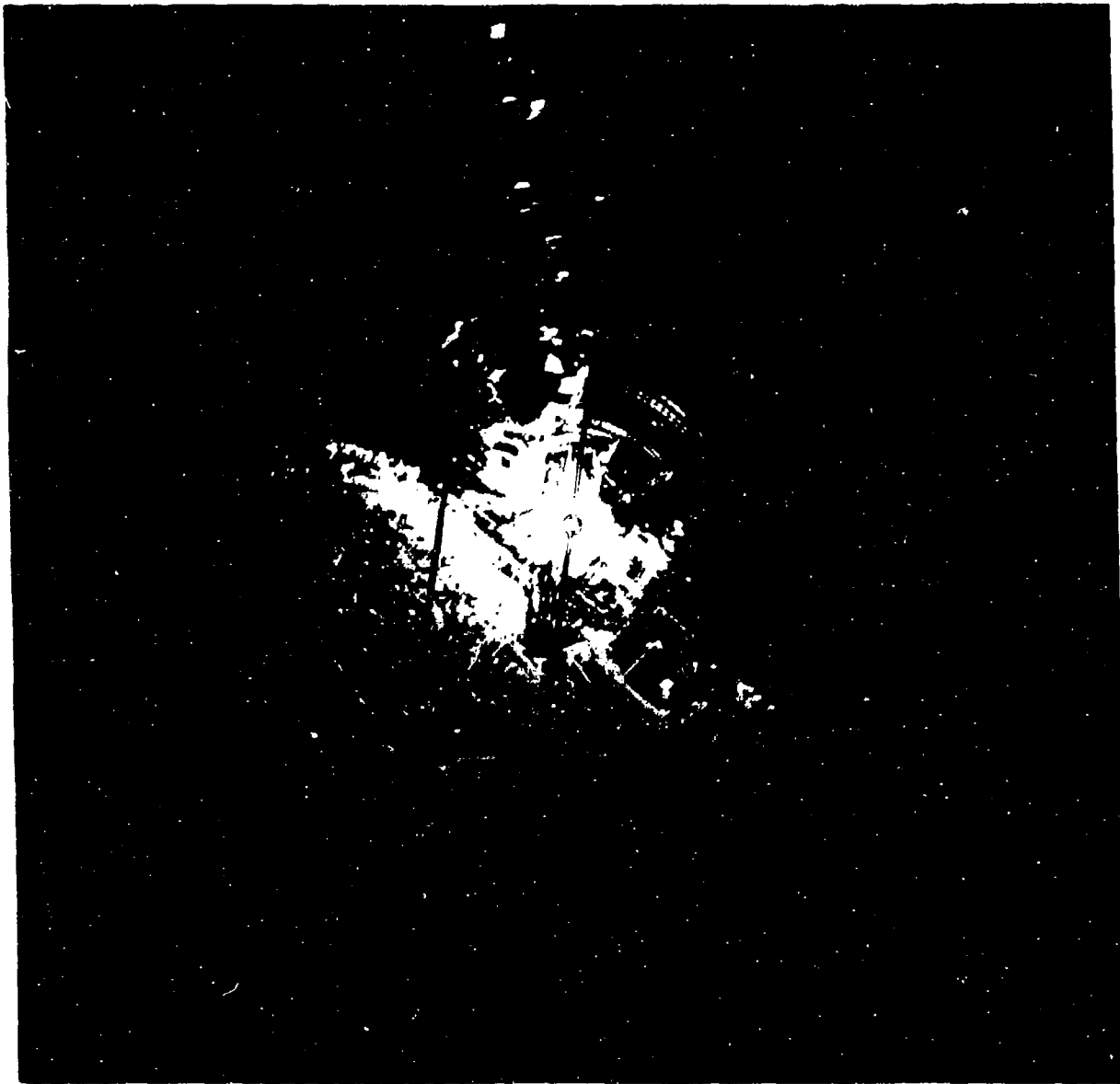


Figure A2 PPI Display, 12dB Attenuation - 10nm Total
Diameter (Clutter Map)

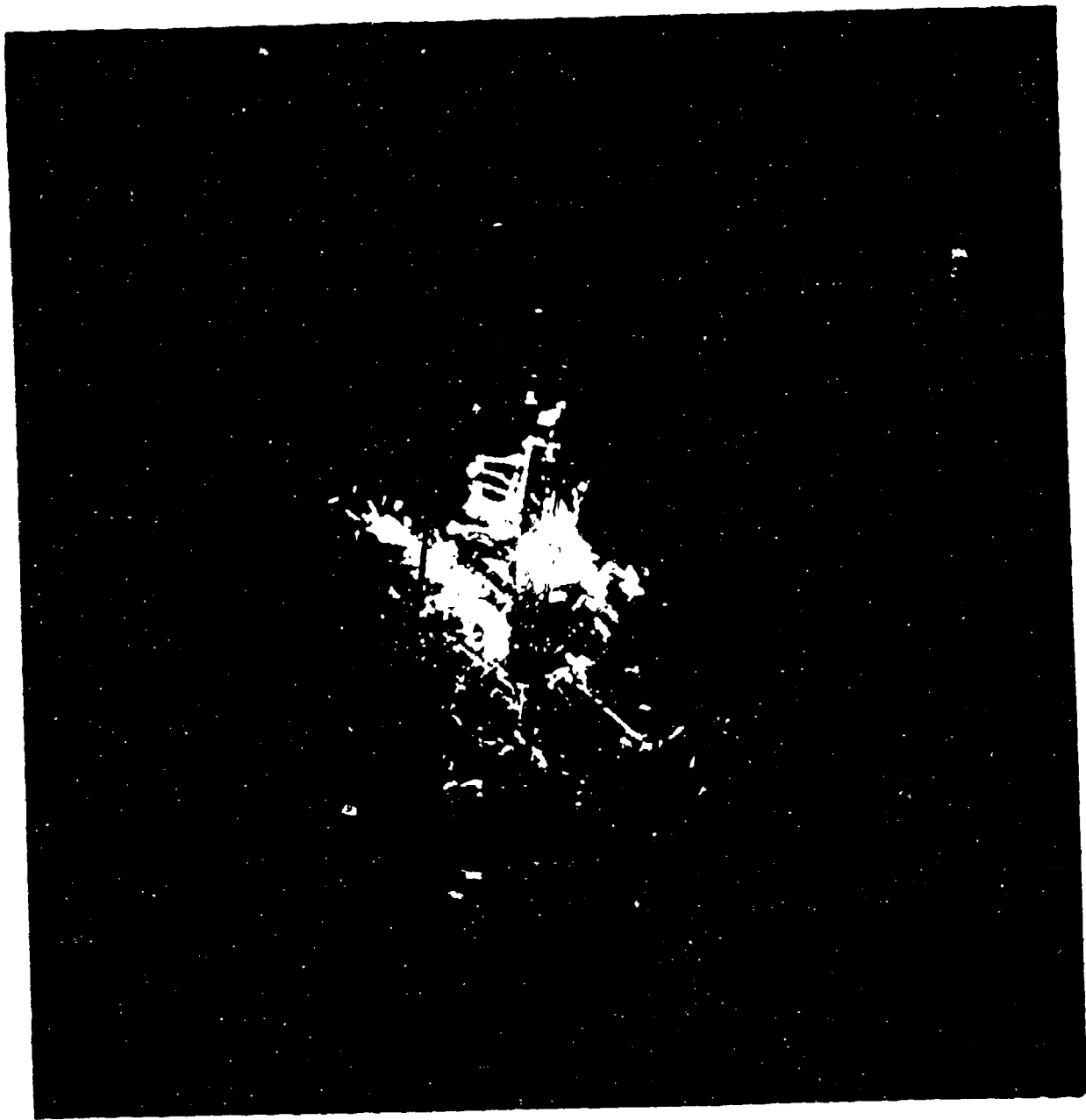


Figure A3 PPI Display, 24dB Attenuation - 10nm Total Diameter (Clutter Map)

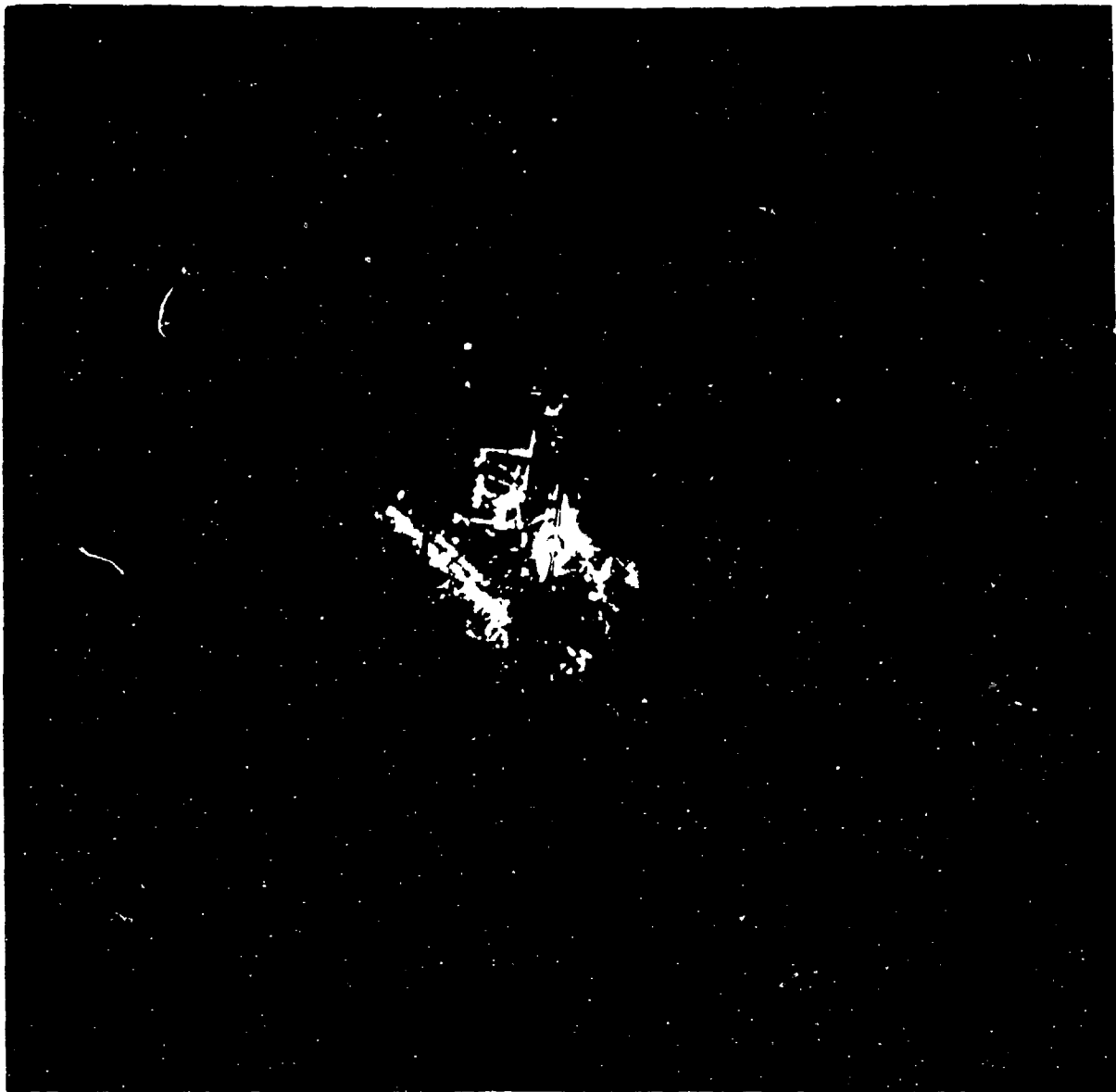


Figure A4 PPI Display, 36dB Attenuation - 10nm Total Diameter (Clutter Map)

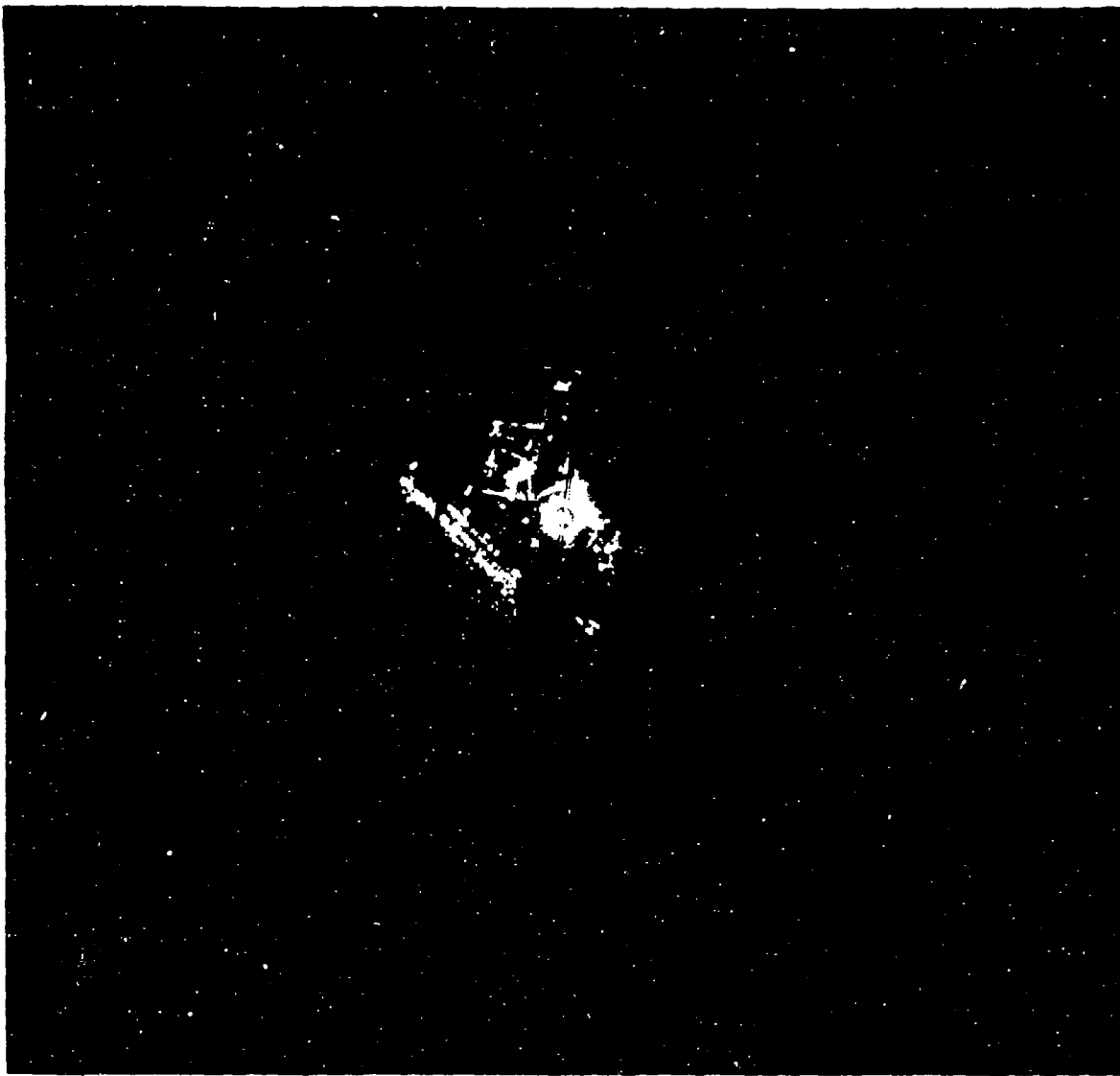


Figure A5 PPI Display, 48dB Attenuation - 10nm Total Diameter (Clutter Map)

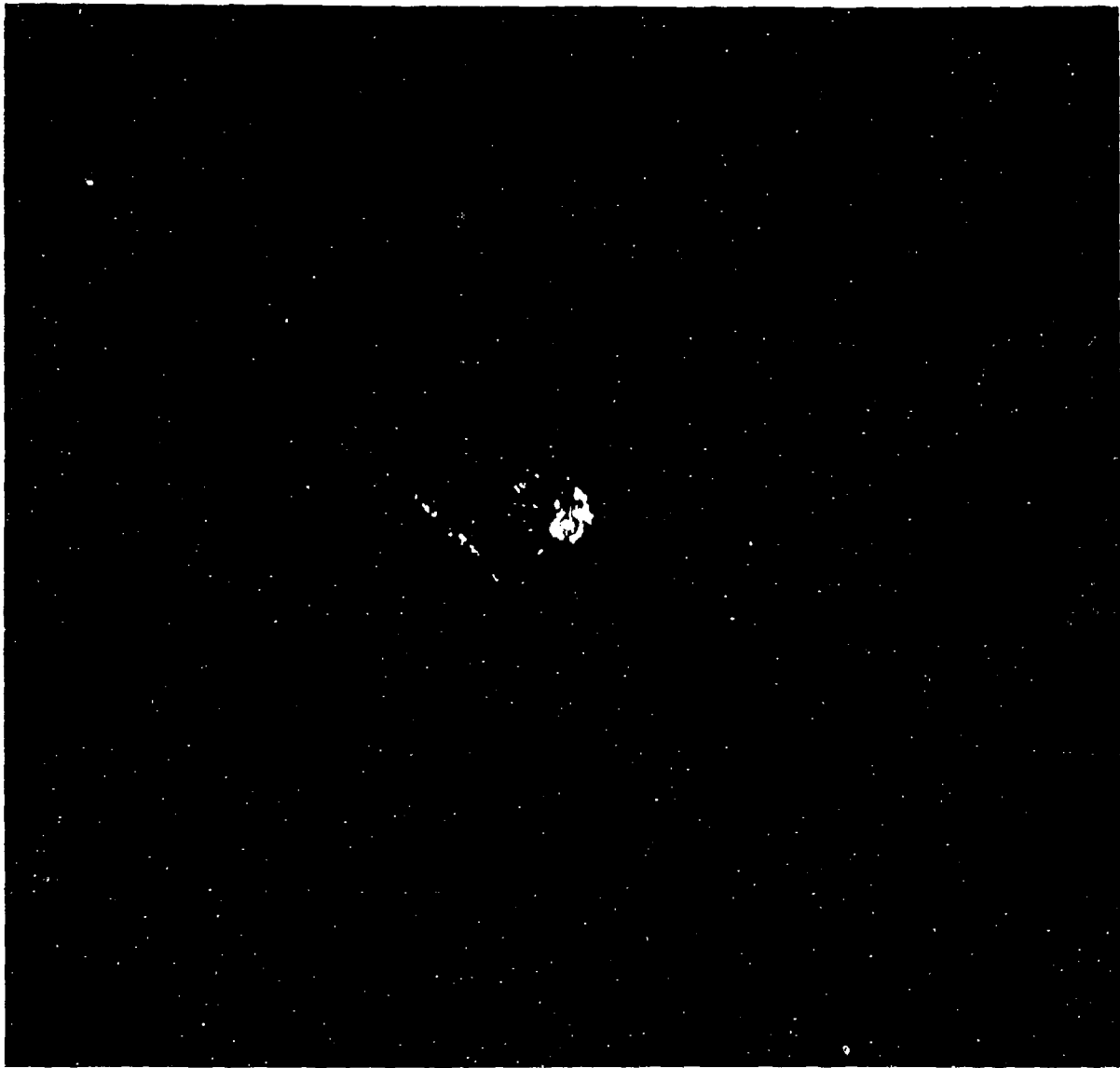


Figure A6 PPI Display, 66dB Attenuation - 10nm Total Diameter (Clutter Map)

APPENDIX B CLUTTER FENCE MEASUREMENTS

Conducting shields can be useful in reducing the ground clutter return received by a radar. The design of a clutter fence for an X-Band Air Traffic Control Radar was verified by measurements taken using the AN/TPN-18A radar at Dover Air Force Base (see Figure B1). A clutter fence at a distance of several hundred wavelengths from the radar antenna will give a nominal reduction in the ground clutter return of about 10 to 20 dB. Additional reduction of the clutter return can be achieved by cutting rectangular slots in the top edge of the fence. While 10 to 20 dB is a significant reduction in the ground clutter return, it is not sufficient in areas where the maximum distributed clutter to receiver noise ratio ranges from 25 to 30 dB or more over the region of interest. Also, a clutter fence is considered to be of more practical use where the radar return from high flying targets is to be enhanced. For low flying targets (as in the Dover AFB application) an improperly constructed fence may shield the low flying targets from the radar as well as the ground clutter, and in fact degrades the sensor performance.

A radar system designed and configured to perform the Air Traffic Control function at Dover AFB may be limited by its ability to track birds. In addition, large returns from the environment, such as parked C5A aircraft and hanger buildings will degrade the sensor capability. In this application, doppler filtering, range gating and MTI filtering offer partial solutions if available, but a properly designed clutter shield would reduce the strict requirements placed on this type of signal processing equipment.



The electromagnetic field behind a clutter fence can be calculated using diffraction theory as developed by Sommerfield in the late 19th century. For the clutter fence described in Figure B2, the electric field in the optical shadow region is given by equation B1, and Figure B3 shows the resulting knife edge diffraction pattern.

Due to the presence of the clutter fence, a cylindrical wave front emanating from the top edge of the fence and proportional in magnitude to the function plotted in Figure B3 is propagated in the optical shadow region. In the unobstructed region, the original field plus a disturbing field emanating from the top edge of the fence propagates. At a distance of several hundred wavelengths from the clutter fence the field strength will theoretically be down 6 dB at the edge of the optical shadow region, and the field strength continues to decrease below this region.

To obtain high clutter attenuation and low target detection angles, the clutter fence should be constructed far from the radar antenna and consequently quite high. This would make the fence quite expensive. At best, 10 to 25 dB of clutter rejection can be achieved with a reasonable structure. At Dover Air Force Base, the clutter shield was tilted away from the radar set, to direct the backscatter from the clutter fence away from the radar antenna and prevent overloading of the radar receiver. Many suggestions have appeared in the literature to further reduce the field strength in the optical shadow region. Among them are simple serration of the top edge of the fence at different heights so that cancellation occurs, additional attenuation of up to several dB may be achieved.

Figure B4 best illustrates the ground clutter problem at Dover AFB. In the sector 170 - 280 degrees, large returns from the parked C5A aircraft and the hangars interfere with the bird watch mission. A clutter fence was constructed over this region at a distance of 35 feet from the radar. The fence was 13' 11" high, and tilted 15 degrees away from the radar. The antenna was tilted 0.5 degrees above horizontal to illustrate the worst case clutter environment at Dover AFB. In Figure B5, the clutter return is reduced over the sector 180 - 270 degrees covered by the clutter field. This result is not sufficient, because hazardous bird activity in the optical shadow region will go undetected. Therefore the noncoherent radar with clutter shielding is not considered a viable long term solution to the Dover Bird Strike Hazard Problem.

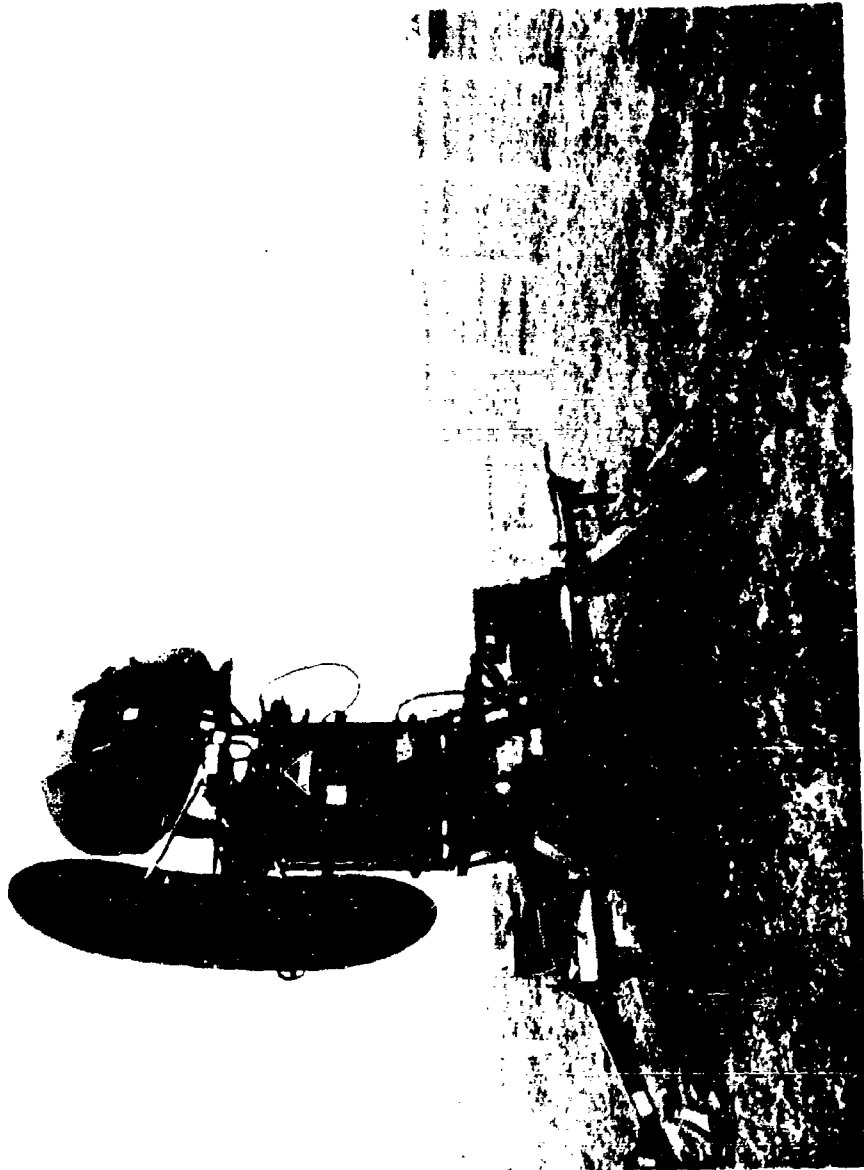


Figure B1 AN/TPN-18A Radar With Clutter Fence 35 Feet
Behind The Radar

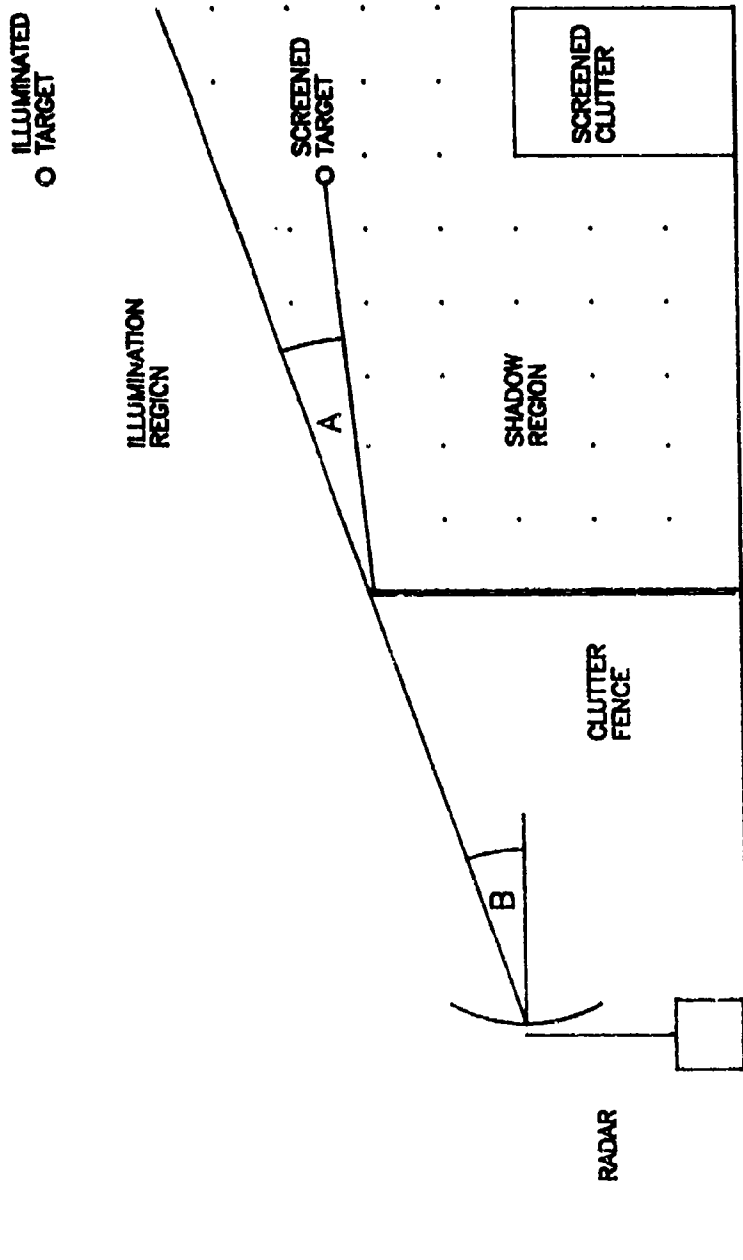


Fig B2 Clutter Fence Geometry

(B1) $E(A) \sim E_0 \exp(jkr \cos(A)) (.5 - C(W) + j(.5 - S(W)))$

Where $C(W)$ and $S(W)$ are Fresnel Integrals

And $W = 2 \sqrt{2r/c} \sin(A/2)$

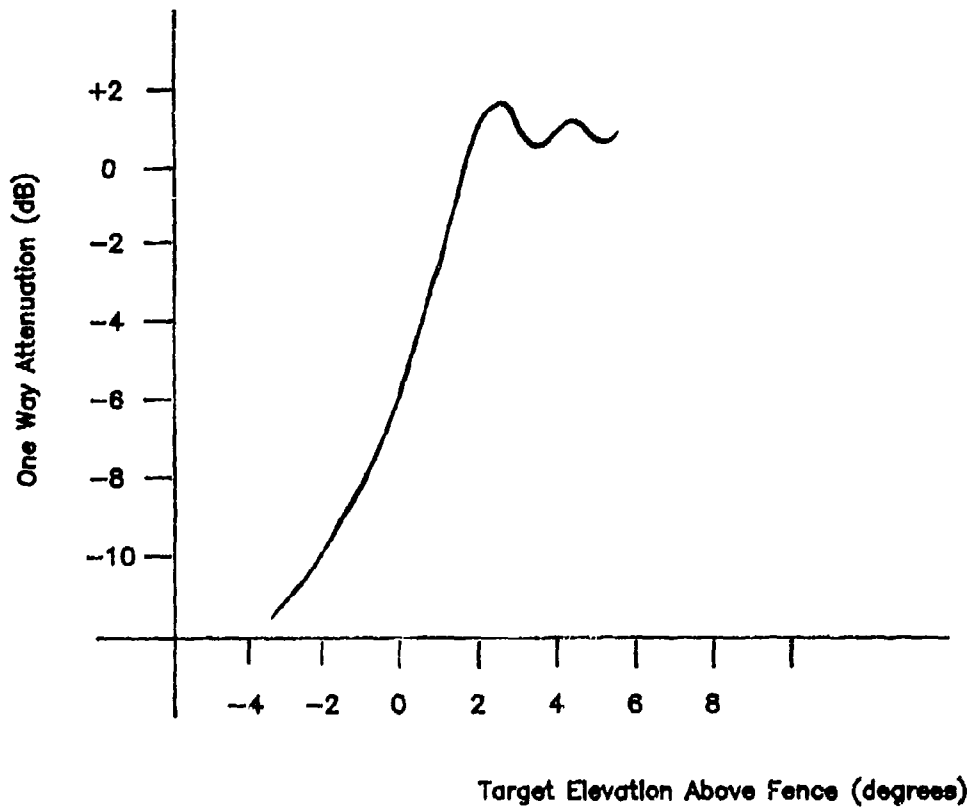


Fig B3 Calculated Knife-Edge Diffraction Pattern

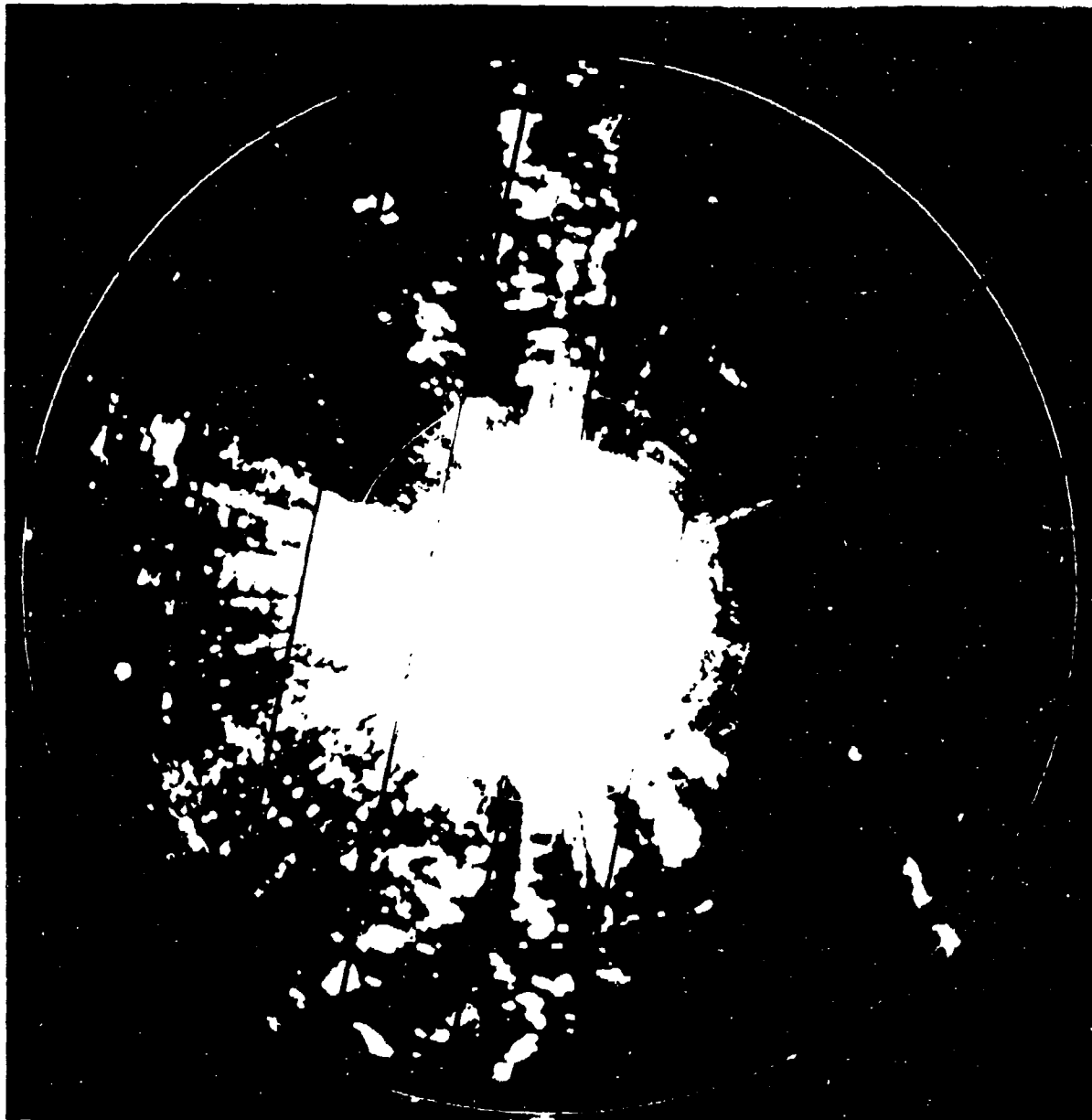


Figure B4 AN/TPN-18A Radar PPI Display of Clutter,
Without Clutter Fence

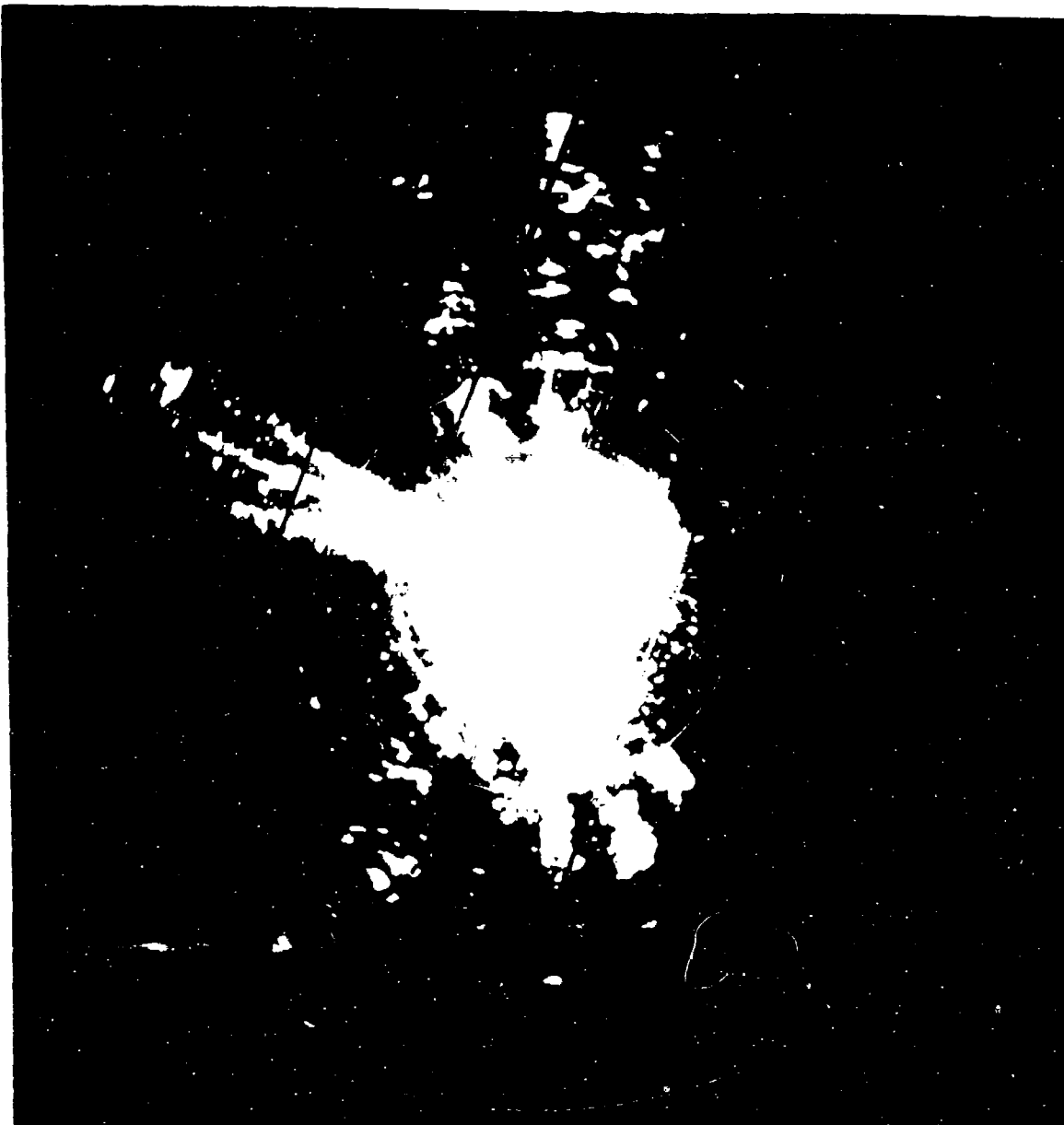


Figure B5 AN/TPN-18A Radar PPI Display of Clutter, With
Clutter Fence 35 Feet Behind The Radar

APPENDIX C INFORMATION ON HAZARDOUS BIRD SPECIES

This appendix presents additional information on the habits and characteristics of the hazardous bird species in the Dover AFB area. The waterfowl present the greatest hazard from October through April when they migrate through or winter in the area. Since DAFB lies in the Atlantic Flyway and is located so close to the Bombay Hook National Wildlife Refuge and Little Creek Wildlife Area, the base is exposed to several hundred thousand waterfowl each year. The waterfowl that present the primary hazard are the Canada Goose, the Mallard, the Black Duck, Whistling Swans and, during recent years, the Snow Goose. Hawks and various pest birds such as blackbirds, starlings, and various gull species represent a year-round hazard.

C.1 CANADA GOOSE (*Branta canadensis canadensis*)

The Canada Geese begin to arrive in the area during the beginning of October and peak in the area by the end of the month. In the 1977-78 season, the Bombay Hook National Wildlife Refuge reported a peak of 70,000 Canada geese at the end of October with a wintering population of 25-30,000 [1]. During migration, the Canadians often fly to and from the staging areas along the St. Lawrence to the Dover area in large numbers. Geese are primarily nocturnal migrators but can and do fly during all hours of the day and night. [2]

While wintering in the Dover area, the flying activity is most intense within a couple of hours after sunrise and plus or minus one hour around sunset. In the morning, large numbers of geese will leave the refuge in flocks that easily exceed 20 or 30 birds as they pass near the base. From late morning thru the afternoon, the Canadians fly

in smaller family groups of 4 to 10 birds [25]. Single birds are also often noted during this time. In the evening, the Canadians fly back to the resting grounds in various size groups ranging from the small family groups of less than ten to occasional large groups exceeding forty or more birds.

However, the flying hours of unpredictable Canadians do not strictly follow these general trends. In particular, intense activity and deviations from the above pattern have often been noted preceding a storm front. The Canadians may stay in the feeding ground well into the night and next morning feeding heavy in anticipation of several days of bad weather. Flights back to the resting grounds can then occur at all hours of the day or night and in the presence of all but the heaviest rain [25]. Another source causing deviations in the general pattern is the hunting activity which begins at the end of October.

The altitudes flown by migrating Canada Geese vary with weather condition and distance to be flown. The most likely altitudes range from about 700 feet to 4000 feet [2]. However, in overcast weather, geese will fly only a few hundred feet above the ground and, in fair weather, migrating flocks of Canadas have been visually sighted by aircraft pilots at altitudes exceeding 30,000 feet [2]. However, the Canadas wintering in the Dover area usually fly less than 1500 feet in their flights to and from the feeding grounds, with a large number of flights less than 500 feet. The typical flying speeds range from 20 to 45 knots although when chased or frightened, the Canadians can exceed 50 knots. When frightened, Canadians are also capable of gaining

altitude at a rate exceeding 500 feet/min (a vertical component of approx. 5 nm/hr).

The Canada goose represents a severe bird strike hazard at Dover AFB primarily due to their large size (8 lbs avg.) and the large numbers that winter in the area. Reports by local observers indicate that the birds, which are indigenous to the area, do seem to be more wary of the base traffic than the Snow Goose and will tend to go toward the ground if threatened by an approaching plane.

C.2 SNOW GOOSE (*Anser caerulescens atlantica*)

The Snow Goose migrates to the Dover area at roughly the same time as the Canadians, arriving in strength by the end of October. The snow geese stage along the St. Lawrence River and like the Canadians, fly into the Dover area in large numbers during all hours of the day and night. The average wintering populations of the Snow Goose have increased sharply in recent years. (See Section 2.) During the spring migration, the population around Dover AFB peaks at over 50,000 birds in February and March as birds from North Carolina and Virginia enter the area. These large flocks remain until April when they proceed northward to the St. Lawrence staging areas.

Like the Canadians, their most intense flying activity occurs within a couple of hours of sunrise and sunset. However, unlike the more independent Canadians, the snow geese tend to be a more gregarious bird, leaving from and returning to their wintering or migrating areas within a smaller interval of time. Thus snow geese are often seen flying in larger denser flocks ranging from 40 to several hundred birds [2][26]. These denser flocks are especially predominant during the

morning when the snows leave the refuge wintering areas for the various feeding grounds in Delaware and Maryland. A descriptive analogy given was that they leave the refuge " like a thundercloud and return like a string of rainshowers." [26]

Like the Canadians, the morning/evening pattern is a general trend rather than a rule. Weather fronts, hunting activity, and feeding conditions can cause high flying activity at other hours. The migrating altitudes and speeds are also similar to Canadians. Due to their large size, their tendency to fly in large flocks, and their increasing population in the Dover area, the snow geese presents a severe birdstrike hazard as was evidenced by the C5A birdstrike incident that initiated this study.

C.3 WHISTLING SWANS

Whistling Swans arrive in the Chesapeake Bay area in December and January with few wintering in the Dover area. In 1978, 700 whistling swans were estimated to winter in the Little Creek Wildlife Area [1] and, while swans may feed in the fields a few miles west of Dover, no large numbers winter or migrate near the base [5]. Thus, while the size of the whistling swan (16 lbs avg for a large male [2]) makes it a threat to aircraft, the small number in the vicinity of Dover AFB makes the whistling swan a minor birdstrike hazard.

C.4 DUCKS

The predominant duck species in the Dover area are the Mallard, Black Duck, Pintail, and Green-Winged Teal [3][25]. While the Dover area is a year-round habitat for the Black Duck, the others winter in the area, arriving in late November or December as they are driven

south by the lack of food in the snow covered north. In 1978, the Bombay Hook National Wildlife Refuge reported an average wintering population of 30,000 ducks with peaks over 40000 occurring in December [1]. The ducks stay no farther south than necessary for food. Consequently, they begin their northerly trek in late January or early February during which time the duck population in the local refuges reaches their primary peak of about 50000 [2].

During migration, the ducks usually fly below 2000 feet with most of the flights occurring at night. While wintering in the Dover area, most of the flights to and from the feeding and wintering areas take place at treetop levels within 200 feet from the ground. Due to the large number of ducks in the area and fly directly over or near the base, they are considered a threat to planes taking off and landing at Dover AFB. However, due to their smaller size (which if injected will cause less damage to an engine) and their speed and maneuverability in flight, they are judged to be a moderate birdstrike hazard.

C.5 RAPTORS

Marsh Hawks (*Circus cyaneus*), Ospreys (*Pandion haliaetus*), and various owls species are the most common raptors hunting on or near the DAFB airfield. Of the 8 bird strikes reported in 1978, raptors were involved in the four incidents in which bird species were identified. An Osprey was involved in a bird strike with a C-5 during 1977. Therefore, raptors do represent a significant threat to local aircraft. However, since raptors usually hunt alone or in pairs, they pose a minor hazard compared to the Canadian and snow geese.

C.6 GULLS

The gulls that represent hazards include the Herring Gull, the Ring-billed Gull and the Laughing Gull. These birds inhabit the area year round and represent the major threat from April to October. During periods of rain, low ceilings, and low visibility, gulls land on the airfield in large numbers, feeding on earthworms that crawl onto the runways and taxiways, or the insects exposed by grasscutting mowers, or just loafing in the relative security of the airfield [1]. When the gulls are frightened by an approaching aircraft or loud unexpected noises, the birds fly up to within 25 to 100 feet of the ground and circle overhead directly in front of approaching aircraft. Since the gulls tend to react slowly, they are not able to avoid approaching aircraft and consequently are a major source of birdstrike incidents. The only way to reduce this hazard is to transform the areas around the runways into undesirable resting or feeding grounds. Suggestions on how this may be performed can be found in an analysis of the DAFB bird problem performed by the EASH squadron out of Tyndall AFB, FL [1].

C.7 BLACKBIRDS AND STARLINGS

Although small groups of these birds do not present a major hazard, large trailing blackbird flocks that exist in the spring and fall represent a major bird strike threat. Often these birds feed in grain fields near the base and fly up in the air when frightened by approaching aircraft. This hazard can be reduced only if the fields located off the end of the runways are made inhospitable to these pests.

APPENDIX D LOG OF DETECTED BIRD TRAFFIC

During the Spring 1983 Project BIRDWATCH mission at Dover Air Force Base, the Army Air Traffic Control Team compiled a log of all bird hazard sightings which were reported to the Dover AFB Control Tower. A sample of the Bird Siting Log appears in Table D-1. Table D-2 presents a summary of the bird detections logged for each 20 degree azimuth sector between 15 and 21 March 1983. The analysis of such logs along with visual observations of bird activity by pilots, RADC personnel, and the ARMY operators allowed a rapid assessment of the bird hazard, the AN/TPN-18A's capability and limitations, and the impact of siting on the radar's performance. It is recommended that the monitors keep a similar log of their BIRDWATCH detections, pilot verifications and any problems noted in using the AN/GPN-21. This documentation will assist HQ/MAC and AFCC in drafting the specifications of a future automated system.

Local Time	Range (nm)	Bearing (degrees)	Flock Size*	Flock Heading	Antenna Tilt	Operator Initials
1241	1-2	030-100	1x1	hold	3	DW
1248	3.25	010	1/8x1/8	NW	3	DW
1252	3.25	020	3x1/8	NW	3	DW
1734	4	300	1/8x1/2	hold	2	DW
1740	1.50	180	1/8x1/8	S	1	DW
1804	1.5-2	355	1(line)	SE	2	VL
1807	3.5	330	1/8x1/8	SE	1.5	VL
1810	1.5	355	1x1/10	SE	2	VL
1812	3.5	350	3/4x1/8	SE	2	VL

* The flock size was measured in terms of its North-South dimension and its East-West dimension in nautical miles. The shapes of the flocks ranged from lines to v-shapes to shapeless blobs and rarely completely filled the rectangular areas implied by the dimensions given above.

TABLE D-1 SAMPLE OF BIRD DETECTION LOG FOR 15 MARCH 1983

Sector (Degrees)	Number of Detections	Range of Detections	Footnotes
1 to 20	26	1 nm to 4 nm	(2)
21 to 40	24	1 nm to 4 nm	(2)
41 to 60	4	1 nm to 2 nm	(1)
61 to 80	6	1 nm to 2 nm	(1)
81 to 100	43	1 nm to 4 nm	(5)
101 to 120	22	1 nm to 4 nm	(5)
121 to 140	14	1 nm to 4 nm	(5)
141 to 160	17	1 nm to 5 nm	(2), (4)
161 to 180	29	1 nm to 5 nm	(2), (4)
181 to 200	20	1 nm to 5 nm	(2), (4)
201 to 220	12	1.5 nm to 5 nm	(2), (4)
221 to 240	14	1.5 nm to 5 nm	(2), (4)
241 to 260	6	1.5 nm to 5 nm	(2), (4)
261 to 280	17	2 nm to 5 nm	(3), (4)
281 to 300	18	2 nm to 5 nm	(3), (4)
301 to 320	13	2 nm to 5 nm	(3), (4)
321 to 340	31	1 nm to 5 nm	(2)
341 to 360	26	1 nm to 5 nm	(2)

(1) Screening by 50 foot trees located within 2000 ft severely limited the detection performance at these azimuths.

(2) Detections within 2 nm were obtained between clutter patches.

(3) Screening by the hangers limited detections to high flying flocks beyond 2 nm.

(4) Clutter patches from buildings and trees limited detection performance within 2.5 nm.

(5) Low angle screening and low clutter return from Delaware Bay allowed good detection beyond 1 nm.

TABLE D-2 SUMMARY OF BIRD DETECTIONS, 15 TO 21 MARCH 1983

APPENDIX E SUPPORTING ORGANIZATIONS

Several organizations were directly involved or provided valuable assistance at various times during the BIRDWATCH effort. Figure E-1 provides a brief history of the effort from its conception in January, 1983 thru the evaluation of the performance tests in November, 1983 and documents the time frame when the various organizations were contacted or were significantly involved in the effort.

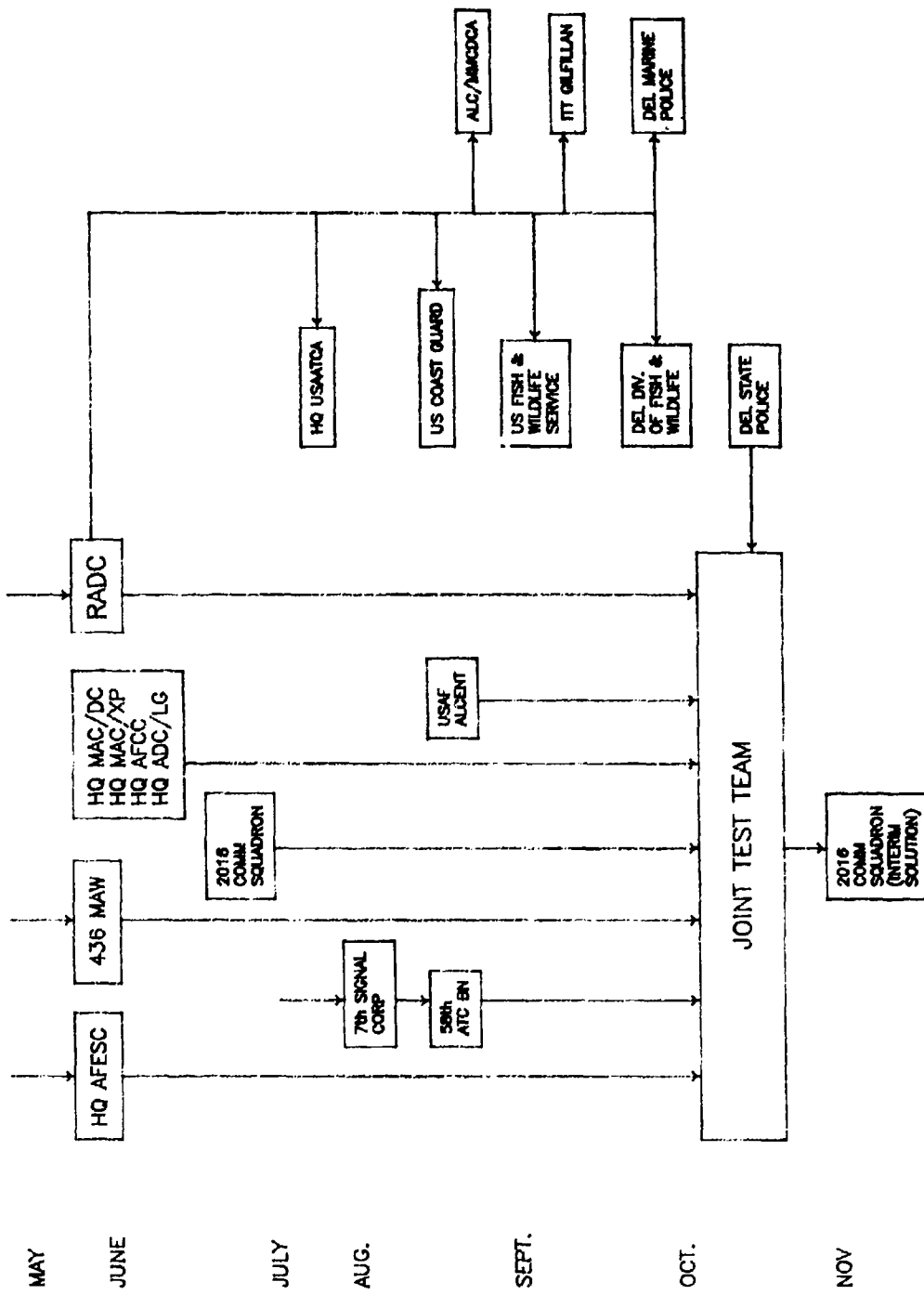


FIG E.1 ROADMAP OF SUPPORT FROM CONTRIBUTING ORGANIZATIONS (CONT)

P_t	= average transmitter power (watts)
t_s	= time taken to perform one volume scan (seconds)
RPM	= revolutions per minute
A_e	= effective aperture (square meters) = $\frac{G_r \lambda^2}{4\pi}$
G_r	= power gain of the receiving antenna
λ	= wavelength (meters)
σ	= radar cross section of target (square meters)
ψ	= angular volume searched (steradians) = $2\pi\theta_e$
θ_e	= one-way 3 dB elevation beamwidth (radians) = $\frac{\lambda}{L_e h}$
h	= height of antenna aperture (meters)
L_e	= inefficiency of antenna due to weighting
(S/N)	= minimum integrated signal-to-noise ratio at threshold detector $\Delta 17.7$ dB (sw I, $P_d = .8$, $P_{fa} = 10^{-6}$)
K	= Boltmann's constant = 1.37×10^{-23} w-s/ K = -228.6 dBw-s/ K
T_s	= system noise temperature (degrees Kelvin) $\Delta T_a + T_{tr} + L_{tr} T_o$ (NF-1)
NF	= noise figure of the receiver
T_a	= antenna noise temperature (degrees Kelvin) $\Delta 100$ K
T_r	= noise temperature of transmission line and passive components connecting the antenna and the receiver (degrees Kelvin) = $T_o(L_{tr}-1)$
L_a	= transmitter power loss of antenna due to azimuth weighting
$F^4(\theta, \phi, R)$	= propagation factors = 1 for free space
L_b	= mismatch loss of receiver bandpass filter = $B_n T$
B_n	= noise bandwidth of the receiver (Hz) = 3 dB bandwidth
τ	= pulse width (seconds)
L_i	= non-coherent integration inefficiency of equal amplitude pulses ($2.4 \log N_p$ ($5 < N_p < 30$); $3 \log N$ ($30 < N_p < 100$))
N_p	= number of pulses per one-way antenna beamwidth = $\frac{T_a \phi a PRF}{360}$
ϕ_a	= one-way azimuthal beamwidth (degrees)
PRF	= pulse repetition rate (pulses per second)
L_p	= pattern loss = 1.6 dB
L_t	= plumbing loss in transmitter
L_r	= non-ohmic loss and ohmic loss not included in noise temperature or receiving antenna gain
L_{atm}	= loss in atmosphere (2 way)
L_{rain}	= loss in absorption by rain = $.0011 (3.2/f)^{-2.8_r}$ (dB/Km)
f_r	= radar operating frequency (GHz)
r	= rain rate (mm/hr)
L_{log}	= additional loss in non-coherent integration when a logarithmic detector is used $\sim .5 \log N_p$
L_{ftc}	= loss in S/N by FTC -3dB
R	= range (meters)

TABLE F.1 DEFINITION OF TERMS FOR RADAR RANGE EQUATION

APPENDIX F RADAR RANGE EQUATIONS

The purpose of this appendix is to present the derivations of the various forms of the radar range equation used in the text. A more complete discussion of the radar range equation and its parameters can be found in the standard radar texts [24][27][28][29].

For a monostatic radar system, the signal power S in a single pulse received from a target at the output of the antenna terminals can be given as

$$(F.1) \quad S = \frac{\hat{P}_t G_t \sigma A_e F^4(\theta, \phi, R) L_{atm} L_{rain}}{(4\pi)^2 R^4}$$

where

P_t = the peak power of the transmitter at the transmitting antenna terminals,

G_t = power gain of the transmit antenna,

and the other parameters are defined in Table F.1.

The noise N in the receiving system can be given by

$$(F.2) \quad N = K T_s B_n$$

where B_n is assumed to be the matched filter of the waveform prior to the detection threshold. Therefore, the single pulse signal-to-noise ratio $(S/N)_1$ can be given as

$$(F.3) \quad (S/N)_1 = \frac{\hat{P}_t G_t \sigma A_e F^4(\theta, \phi, R) L_{atm} L_{rain}}{(4\pi)^2 R^4 K T_s B_n}$$

This is often called the "track" form of the range equation because the search volume and the timing required to search that volume are not explicitly present in the equation. Since the radar required in the BIRDWATCH system is a search radar which integrates many returns prior to detection, the form of the equation must now be changed thru appropriate substitution of parameters.

The transmit gain G_t of the antenna can be related to the volume illuminated by the transmit energy.

$$(F.4) \quad G_t = \frac{4\pi L_e L_a}{\Omega}$$

where Ω is the volume of the antenna beam and L_e and L_a are the elevation and azimuth weighting losses of the transmit antenna.

The limited amount of energy or average power P_t available to the radar can be related to the peak power P_t through the pulse width τ , the time required to scan the volume of one beamwidth t_0 , and the number of target returns N_p received within this time.

$$(F.5) \quad \hat{P}_t = \frac{P_t t_0}{\tau N_p}$$

In radars using a PPI display, the multiple target returns are superimposed on the display, resulting in a noncoherent integration gain I_g

$$(F.6) \quad I_g = N_p \cdot L_i \cdot L_p$$

This integration gain can be interpreted by the increase in signal-to-noise obtain by the equivalent reduction in bandwidth of the matched filter.

$$(F.7) \quad B_n = \frac{1}{\tau \cdot I_g \cdot L_b}$$

Substituting these equalities into equation (F.3), the integrated signal-to-noise ratio at the detection threshold can be given as

$$(F.8) \quad S/N = \frac{P_t \sigma A_e L_e L_a L_b L_i L_o t_o L_{atm} L_{rain} F^4 (\theta, \phi, R)}{(4\pi) R^4 K T_s \Omega}$$

Recognizing that

$$t_o / \Omega \text{ (the volume of 1 beamwidth)} = t_s / \Psi \text{ (the search volume)}$$

the "search" form of the radar range equation can be obtained. Furthermore, in many systems, the power of the transmitter is not measured at the antenna terminals; the advertised antenna power gain does not include waveguide loss, and the signal processing contains additional losses that may not be addressed by the manufacturer. By including these additional losses, the form presented in equation (F.9) and equation (4.2) can be obtained.

$$(F.9) \quad (S/N) = \frac{P_t \sigma A_e L_e L_a L_b L_i L_o L_t L_r L_{atm} L_{rain} F^4 (\theta, \phi, R) t_s}{(4\pi) R^4 K T_s \Psi}$$

By segregating the parameters unique to a sensor from those that define the surveillance requirement and assuming a typical value for

the losses, the figure-of-merit or FOM presented in equation (4.1) can be defined.

$$(F.10) \quad FOM = \frac{P_t A_e t_s}{K T_s} = \frac{(4\pi) \psi R^4 (S/N)}{\sigma (\Sigma \text{ losses})}$$

The above equation applies when the signal return from the target is competing with noise. When the backscatter from other scatterers such as the surface of the earth, buildings and trees, or raindrops, exceed the noise level, the detection of the target is depends on the (S/C+N). Since the power return from these clutter sources depend on the same parameters as the target, the radar range equation can be given as

$$(F.11) \quad (S/N) = \frac{z F^4 (\theta, \phi, R) \sigma L_p}{R^4}$$

where

$$(F.12) \quad z = \frac{P_t A_t L_e L_a L_b L_i L_t L_r L_{atm} L_{rain} t_s}{(4\pi) K T_s \psi}$$

Replacing σ the target radar cross section with σ_c , the radar cross section of the clutter, the volume clutter-to-noise ratio can be given as

$$(F.13) \quad (C/N) = \frac{z F_c^4 (\theta, \phi, R) \sigma_c}{R^4}$$

$$(F.14) \quad \sigma_c = N_v \left(\frac{\pi}{4}\right) \frac{c^2}{2} \phi_a \theta_e R^2 = K_C R^2$$

where $L_p = 1$ (because the clutter is assumed to be distributed uniformly across the beam),

N_v = the volume reflectivity of the rain

$$= (6.12 \times 10^{-14}) (r^{1.6} / \lambda^4) (\text{meters})^2 / (\text{meters})^3,$$

r = rainrate in millimeters/hour.

The $(C+N/N)$ can now be given as

$$(F.15) \quad \frac{C+N}{N} = \frac{C}{N} + \frac{N}{N} = \frac{K_C \Sigma F^4(\theta, \phi, R)}{R^2} + 1$$

and the equation for $(S/C+N)$ follows directly.

$$(F.16) \quad (S/C+N) = (S/N) \cdot (N/C+N) = \frac{\Sigma \sigma L_p F^4(\theta, \phi, R)}{R^2 [\Sigma K_C F_C^4(\theta, \phi, R) + R^2]}$$

If the propagation factors $F_t = F_c = 1$, then the form presented in Equation 4.3 is obtained.

For the case where $C \gg N$, ($ZK_C F^4(r, \theta, \phi) \gg R^2$) and the $(C+N/N)$ is approximately equal to (C/N) . $(S/C+N)$ is then inversely proportional to the square of the range to the target and clutter.

$$(F.17) \quad (S/C+N) = (S/N) \cdot (N/C+N) = \frac{\sigma L_p F^4(\theta, \phi, R)}{K_C R^2 F_C^4(\theta, \phi, R)}$$

For the case where $C \ll N$, then $R \gg ZK_C F^4(R, \theta, \phi)$ and equation (F.16) reduces to equation (F.11).

BIBLIOGRAPHY

- [1] Clark, L.T., Lavey, J.M., Kent, J.S., An Evaluation of the Bird/Aircraft Strike Hazard, Dover Air Force Base, Delaware, April 1978, (AD A061297)
- [2] Bellrose, Frank C., "Ducks, Geese, Swans of North America", Stackpole Books, Harrisburg, Pa., 1976
- [3] Sprunt, A. and Zim, H.S., "Gamebirds", Golden Press, New York, 1961
- [4] Alexander, H. Lloyd, Delaware Dept. of Natural Resources and Environmental Control, Division of Fish and Wildlife, private communication, Feb 1983. (Data taken from aerial survey photographs over Unit 5, located north of the city of Dover and containing the Bombay Hook Refuge, and Unit 6 which is located south of Dover and contains the Little Creek Refuge, and area now known as the Logan Lane Tract, and the marshlands, fields and smaller refuges between Dover and Milford, Delaware.)
- [5] Alexander, H. Lloyd, *ibid*, private communication, Nov. 1983
- [6] Green, J.L., Balsey, B.B., Development of a Doppler Radar Technique for the Detection of Bird Hazards to Aircraft, AFCEC-TR-76-17, Dec. 1975 (AD A030410)
- [7] Hershkovitz, D. and Antonucci, J., RADC/EEC, private communication, April 1983
- [8] Luckenbach, Micheal Major USAF, 436 MAW/SE, Wing Safety Office, Dover AFB, DE, private conversation, July 1983
- [9] Kull, Robert Capt. USAF, Bird/Aircraft Strike Hazard (BASH) Team, AFSEC/DEVN, Tyndall AFB, FL, private conversation, February, 1983
- [10] May, Michael Major USAF, 436 MAW/SE, Wing Safety Office, Dover AFB, DE, private conversation, February, 1983
- [11] Houle, John R. Major USAF, Analysis and Prevention of Bird Strikes by Jet Aircraft, May 1977, (AD B019713)
- [12] Compton, Dennis E., Nemerlut, John P., and Newsom, Keith R., Potential Bird Hazards during the Oversea Phase of the B-1 Flight Test Program, AFWL-TR-75-160, Air Force Weapons Laboratory, Kirkland AFB, New Mexico, July 1975
- [13] Kull, Robert, Capt, USAF, Air Force Bird Strike Report 1980-1982, USAF Safety Journal, July 1983, pp. 4-7
- [14] AFSC NEWSREVIEW, Effort being performed at AEDC and is sponsored by AFWAL, August 5, 1983

- [15] Frings, Gary, A Study of Bird Ingestions into Large High Bypass Ratio Turbine Aircraft Engines, DOT/FAA/CY-82/144, March 1983, (AD A128640)
- [16] Houghton, E.W., Radar Echoing Areas of Birds, R.R.E. Memorandum No. 2557, United Kingdom, 1969
- [17] Pollon, G.E., Distribution of Radar Angels, IEEE Trans. on Aerospace and Electronic Systems, Volume AES-8, No. 6, November 1972, pp 721-727
- [18] Antonucci, J.D., Radar Bird Clutter at the Dew Line, RADC-TR-81-177, June 1981
- [19] Kull, Robert Capt., USAF, BASH Team Member, AFSEC, Tyndall AFB, FL, private conversation, August 1983
- [20] Southern, W.E., Development of Computer-Generated Pheonograms to Forecast Regional Conditions HAZardous to Low-flying Aircraft, Report AFOSR-TR-79-0611, November 1978, (AD A068812)
- [21] Raytheon literature on 3 and 10 cm Mariners Pathfinder Radars, 1982
- [22] Presentation given by the authors at HQ AFSC, Andrews AFB, MD, Aug 10, 1983. Attendees included personnel from HQ AFSC/XR, HQ MAC/XP/DC, RADC/OCT, 436 MAW/DOX, HQ AFESC/DEV, 2016CS/AT, and USAF ALCENT/LG.
- [23] Presentation given by the authors at HQ MAC, Scott AFB, IL, October 5 1983. Attendees included personnel from HQ AFSC/XRK, HQ MAC/XPQ/ACB/DCF/DOV/IGF/LGX, HQ AFCC/ATT/LGM, and 436MAW/DOX.
- [24] Skolnik, "Introduction to Radar Systems", McGraw-Hill, Inc., 1970
- [25] Alexander, H. Lloyd, *ibid*, private communication, Sept 1983
- [26] Goldsberry, Jim, U.S. Fish and Wildlife Service, private communication, September 1983
- [27] Nathanson. F.E., "Radar Design Principles", McGraw-Hill Book Company, 1969
- [28] Barton, D.K., "Radar Systems Analysis", Prentice-Hall, Inc., 1964
- [29] Berkowitz, R.S. (ed.), "Modern Radar - Analysis, Evaluation, and System Design", John Wiley Sons, Inc., 1965



*MISSION
of
Rome Air Development Center*

RADC plans and executes research, development, test and selected acquisition programs in support of Command, Control Communications and Intelligence (C³I) activities. Technical and engineering support within areas of technical competence is provided to ESD Program Offices (POs) and other ESD elements. The principal technical mission areas are communications, electromagnetic guidance and control, surveillance of ground and aerospace objects, intelligence data collection and handling, information system technology, ionospheric propagation, solid state sciences, microwave physics and electronic reliability, maintainability and compatibility.

SUPPLEMENTARY

INFORMATION

AD-8084 552 L

UNCLASSIFIED

ERRATA

12 July 1985

RADC-TR-84-7

Title: PROJECT BIRDWATCH AT DOVER AFB

DATED: MAY 1984

Please make the following corrections:

- Page 12 Figure 2.7 Delete "(Air Corridor Obtained from Ref [7])"
- Page 13 Line 4 Change "...snow geese..." to "...average snow geese..."
- Page 25 Line 10 Change "...specific various altitudes..." to "...specific altitudes..."
- Page 27 Line 5 Change "...damaging strikes," to "...strikes"
- Page 27 Line 7 Change "...120 of these 131 strikes (91.6%)..." to "...119 of the 130 strikes plotted (91.5%)..."
- Page 29 Line 14 Change "...and pulse..." to "..., the pulse..."
- Page 33 Bottom Line Change "...low-level operation." to "...low-level phases of flight."
- Page 39 Line 2 Delete "... (dashed line)..."
- Page 42 Figure 3.7 Change "Required Birdwatch Coverage For Landing Aircraft" to "Required Birdwatch Coverage For Takeoff"

INFORMATION SUBJECT TO EXPORT CONTROL LAWS

This document may contain information subject to the International Traffic in Arms Regulation (ITAR) or the Export Administration Regulation (EAR) of 1979 which may not be exported, released, or disclosed to foreign nationals inside or outside the United States without first obtaining an export license. A violation of the ITAR or EAR may be subject to a penalty of up to 10 years imprisonment and a fine of \$100,000 under 22 U.S.C. 2778 or Section 2410 of the Export Administration Act of 1979. Include this notice with any reproduced portion of this document.

**ROME AIR DEVELOPMENT CENTER
Air Force Systems Command
Griffiss Air Force Base, NY 13441-5700**

Page 43 equation 4.1
and page 158, Eq. F.10

Change " $(\sum \text{losses})$ " to " $(\prod_{i=1}^{i=N} \text{loss}_i)$ " where

$$\prod_{i=1}^{i=N} Y_i \triangleq Y_1 \times Y_2 \times \dots \times Y_{n-1} \times Y_n$$

Page 44 TABLE 4.1 and
Page 154 TABLE F.1

- *Change in Line 11 "...due to weighting" to "due to elevation weighting"
- *Change in Line 14 "w-s/ K" to "w-s/ °K" and
"dBw-s/ K" to "dBw-s/ °K"
- *Change in Line 17 "100 K" to "100 °K"

NOTE: In the equations and calculations of TABLE 4.1 and F.1, the losses are defined to be quantities equal to or less than unity (decibel values less to zero). Therefore, to be consistent, the following changes should be made.

- *Change in Line 22 " $\approx B_n \tau$ " to " $\approx 1/B_n \tau$ for $B_n \tau > 1$ "
- *Replace Line 26 "-2.4 log N_p (dB) ($5 < N_p < 100$)"
"-3 log N_p (dB) ($30 < N_p < 100$)"
- *Change in Line 30 "1.6 dB" to "-1.6 dB"
- *Change in Line 35 "...rain = .0011 (3.2/f)^{-2.8} r (dB/km)" to
"...rain in dB = -.00007 f_r^{2.36} r (dB/km)"
- *Change in Line 39 "... .5 log N_p " to "... -.5 log N_p (dB)"
- *Change in Line 40 "... 3 dB" to "... -3 dB"

Page 48 Line 5

Replace first sentence in paragraph with the following:
 "Inserting these values into equation (4.1) and assuming the total losses to be -10dB, the figure of merit required for the candidate sensors is +221.5 dB watt-seconds/degree Kelvin or 1.41×10^{22} w-s/ °K."

Page 64 Equation 4.2

Replace equation (4.2) with the following:

$$(S/N) = \frac{P_t \sigma A_e L_e L_a L_b L_f L_p L_t L_r L_{atm} L_{rain} L_x t_s}{(4\pi)^4 R^4 K T_s \psi}$$

- Page 64 Line 20 Change "...the calculation. In..." to "...the calculation, i.e. $F(\theta, \phi, R) = 1$. Also, L_x denotes the signal processing losses in the system. In..."
- Page 65 Line 1 Change "...ranges at..." to "...ranges in the absence of rain ($L_{rain} = 1$) at..."
- Page 68 TABLE 4.3 Replace the term given as L_a with $L_a L_e$
- Page 73 Line 3 Change "...performance are 30 dB..." to "...performance on the bird are 30 dB..."
- Page 73 Line 15 Change "...the 0 dB point..." to "...the unity gain point..."
- Page 156 Line 10 Change "...where n is the volume..." to "...where is the volume..."
- Page 157 Line 14 Change "...additional losses that..." to "...additional losses L_x that..."
- Page 157 Line 16 Change "...and equation (4.2)..." to "...and, with $F(\theta, \phi, R) = 1$, equation..."
- Page 157 Equation F.9 Replace equation (F.9) with the following

$$(S/N) = \frac{P_t \sigma A_e L_e L_a L_b L_i L_p L_t L_r L_{atm} L_{rain} L_x t_s F^4(\theta, \phi, R)}{(4\pi)^4 R^4 K T_s \psi}$$

- Page 158 Equation F.12 Replace equation (F.9) with the following:
- $$Z = \frac{P_t A_e L_e L_a L_b L_i L_p L_t L_r L_{atm} L_{rain} L_x t_s}{(4\pi)^4 K T_s \psi}$$
- Page 159 Equation F.15 Change "... $F(\theta, \phi, R)$..." to "... $F(\theta, \phi, R)$..."
- Page 159 Line 13 Change "... $F(r, \theta, \phi)$..." to "... $F(\theta, \phi, R)$..."
- Page 159 Line 17 Change "... $F(R, \theta, \phi)$..." to "... $F(\theta, \phi, R)$..."



DEPARTMENT OF THE AIR FORCE
AIR FORCE RESEARCH LABORATORY (AFRL)

1 Jun 04

MEMORANDUM FOR DTIC-OCQ

ATTN: Larry Downing
Ft. Belvoir, VA 22060-6218

FROM: AFRL/IFOIP

SUBJECT: Distribution Statement Change

1. The following documents have been reviewed and have been approved for Public Release; Distribution Unlimited:

ADB084552, "Project Birdwatch at Dover AFB", RADC-TR-84-7

ADB191869, "Acousto-Optic Beam Steering Study", RL-TR-94-121

AD0800669, "Use of Commercial Broadcast Facilities for Emergency DoD Communications", RADC-TR-66-392

ADB058979, "Multi-Rate Secure Processor Terminal Architecture Study", RADC-TR-81-77, Vol 1.

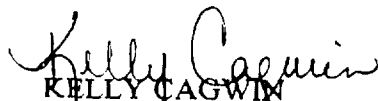
ADB053656, "16 KB/S Modem (AN/GCS-38) CONUS Test", RADC-TR-80-89

ADB055136, "VINSON/AUTOVON Interface Applique for the Modem, Digital Data, AN/GCS-8", RADC-TR-80-341

ADB043556, "16 KB/S Data Modem Partitioning", RADC-TR-79-278

ADB029131, "16 Kilobit Modem Evaluation", RADC-TR-78-127.

2. Please contact the undersigned should you have any questions regarding this document. Thank you very much for your time and attention to this matter.


KELLY CAGWIN
STINFO Officer
Information Directorate
315-330-7094/DSN 587-7094